




This is to certify that the
dissertation entitled

KINETIC STUDIES OF CHARGE RECOMBINATION REACTIONS
IN PHOTOSYSTEM II BY TRANSIENT ABSORPTION SPECTROSCOPY
presented by

Xingmin Liu

has been accepted towards fulfillment
of the requirements for

Ph.D. degree in Chemistry


Major professor

Date 6/29/90.

LIBRARY
Michigan State
University

**PLACE IN RETURN BOX to remove this checkout from your record.
TO AVOID FINES return on or before date due.**

[illegible]

MSU Is An Affirmative Action/Equal Opportunity Institution

C:\circ\datedus.pm3-p.1

**KINETIC STUDIES OF CHARGE RECOMBINATION REACTIONS
IN PHOTOSYSTEM II BY TRANSIENT ABSORPTION SPECTROSCOPY**

By

Xingmin Liu

A DISSERTATION

Submitted to
Michigan State University
in partial fulfillment of the requirements
for the degree of

DOCTOR OF PHILOSOPHY

Department of Chemistry

1990

1977-1978

ABSTRACT

KINETIC STUDIES OF CHARGE RECOMBINATION REACTIONS IN PHOTOSYSTEM II BY TRANSIENT ABSORPTION SPECTROSCOPY

By

Xingmin Liu

The rates of charge recombination reactions of Q_A^- and P^+680 in tris, NaCl, and NH_2OH treated PSII membrane fragments have been measured under repetitive flash excitation by monitoring the time course of optical absorption changes that occur in the ultraviolet and near infrared spectral regions. In tris-inhibited membranes, the recombination reaction was stimulated by increasing the flash repetition rate; following NH_2OH addition to these membranes and a preillumination regime, Q_A^-/P^+680 recombination was the major decay pathway for all flash repetition rate employed (0.2-10 Hz). In both preparations, however, the halftime of the charge recombination reaction between Q_A^- and P^+680 is approximately 230 μs . In NaCl washed PSII, on the other hand, the recombination is faster, with a halftime of $\sim 130 \mu s$. This difference confirms earlier EPR results and indicates that the presence of the manganese ensemble involved in water oxidation and the 33 KDa peripheral polypeptide influence the rate of the Q_A^-/P^+680 recombination reaction. Secondary electron transfer from Q_A^- to Q_B does not compete effectively with

Q_A^-/P^+680 recombination in the inhibited, PSII membrane fragments used in this study. This behavior may result from release of plastoquinone during preparation of the membranes or from a Coulombic effect in which the positive charge on P^+680 retards the Q_A^- to Q_B electron transfer. The $P^+680/P680$ absorption difference spectrum measured in tris-washed PSII and NH_2OH treated tris-PSII have nearly identical features. This suggests that NH_2OH has no direct interactions with the reaction center $P680$; the inhibition site of NH_2OH is probably located at Y_2 , at an auxiliary chlorophyll or, in the PSII reaction center polypeptides.

To my parents, my wife, my teachers, and all friends of mine
who have given me love, encouragement, and placed great hopes
on me.

ACKNOWLEDGMENTS

I would like to thank Dr. Gerald T. Babcock for the independence and guidance he offered through this project. I would also like to thank Marty Rabb for his great assistance on the electronics, Dr. Tom Atkinson for his help on the critical points of programming, Dr. Dwight Lillie and Dr. Curtis Hoganson for their patience and time spent teaching and helping me with the computer interfacing. Finally, I would like to thank all my fellow colleagues in the laboratory for their friendship and assistance.

TABLE OF CONTENTS

	Page
LIST OF TABLES	ix
LIST OF FIGURES	x
LIST OF SYMBOLS	xv
CHAPTER I - INTRODUCTION	
Photosynthesis in Higher Plants	3
Electron Transfer in Photosystem II	7
The Structure of Photosystem II	12
Transient Absorption Spectroscopy in the Studies of Photosystem II	17
Reaction Center P680	18
Acceptor Side	19
Donor Side	22
Description of Work to be Presented	24
References	28
CHAPTER II - TRANSIENT ABSORPTION SPECTROSCOPY	
System Design	36

Optical Subsystem	38
Detecting and Signal Processing	42
Computer Interface	48
Data Acquisition	49
Timing control	55
Software Design	57
Program TASCII	58
Program DTDSP	60
References	63

CHAPTER III - THE CHARGE RECOMBINATION REACTIONS OF THE CHARGE SEPARATION STATE Q_A^-/P^+680

Introduction	64
Materials and Methods	69
Photosystem II Membrane Preparation	69
Tris Treatment	71
NaCl Treatment	72
Hydroxylamine Treatment	73
Measurement Conditions	73
Results	75
Excitation Saturation Profile	75
Q_A^-/P^+680 Recombination in Tris-PSII	77
Q_A^-/P^+680 Recombination in NaCl Washed PSII ...	83
Q_A^-/P^+680 Recombination in NH_2OH Treated Tris-PSII	85
C-550 Bandshift	88
Discussion	91
Conclusion	96

References	98
CHAPTER IV - CHARACTERIZATION OF P ⁺ 680/P680 AND Y ₂ ⁺ /Y ₂ ABSORPTION DIFFERENCE SPECTRUM	
Introduction	103
Materials and Methods	107
Results	109
P ⁺ 680/P680 Difference Spectrum	109
Y ₂ ⁺ /Y ₂ Difference Spectrum	116
Discussion	121
Conclusion	128
References	130
CHAPTER V - SUMMARY AND FUTURE WORK	
Summary	134
Future Work	137
References	140
APPENDIX A - SOURCE CODES OF PROGRAM TASCI	142
APPENDIX B - SOURCE CODES OF PROGRAM DTDSP	157

LIST OF TABLES

CHAPTER II		Page
Table 1	Command Register	52
Table 2	Status Register	53
CHAPTER III		
Table	Halftimes of the Microsecond Decays	90

LIST OF FIGURES

	Page
Figure 1-1	The electron transfer and proton transfer patterns of photosynthesis in higher plants 5
Figure 1-2	Z-scheme of electron transport in higher plants. P700 and P680 are the photochemical reaction centers of the photosystem I and photosystem II respectively. Pheo is a pheophytin molecule that acts as the primary electron acceptor of the P680. A is the primary electron acceptor of P700 and is presumed to be a Fe-S center 6
Figure 1-3	The kinetics of electron transfer in photosystem II 11
Figure 1-4	A possible structure of photosystem II reaction center 14
Figure 2-1	Instrument setup 37
Figure 2-2	Optical layout of the transient absorption spectrometer used in the studies of the electron transfer in PSII (only relative positions are shown) 40
Figure 2-3	The block diagram of the detecting and signal processing subsystem 43

Figure 2-4	Pre-amplifier circuit. I_{in} comes from the PMT anode, V_{out} goes to the fourth order low pass active filter. The offset is controlled from the instrument panel. The operational amplifiers used are Burr Brown 3551 with 50 MHz GBP 45
Figure 2-5	The sample/hold amplifier. The two outputs, one is normal output (the upper output) for DC level measurement, another is DC subtracted output (the lower output) for the signal digitizer. Two variable resistors are used to balance the inverted signal 47
Figure 2-6	The address map of the WAAG-1000 data acquisition board 50
Figure 3-1	Amplitude of the absorption changes at 325 nm as a function of the excitation flash energy in tris-washed PSII. [Chl]=196 $\mu\text{g/ml}$, optical path=0.14 cm, 2.5 mM $\text{K}_3\text{Fe}(\text{CN})_6$ and $\text{K}_4\text{Fe}(\text{CN})_6$ were added as the electron acceptor system 76
Figure 3-2	Microsecond time courses of the absorption changes at 325 nm (trace A) and 820 nm (trace B) with tris-washed PSII. [Chl]=215.7 $\mu\text{g/ml}$, optical path=0.14 cm, excitation flash repetition rate 5.8 Hz. 2.5 mM $\text{Fe}(\text{CN})_6^{-3}/\text{Fe}(\text{CN})_6^{-2}$ were added as the electron acceptor system. The transient in the first few μs was unreliable because of flash artifacts 78
Figure 3-3	Millisecond time courses of the absorption changes at 325 nm with tris-washed PSII (trace A) and NH_2OH treated tris-PSII (trace B). [Chl]=215.3 $\mu\text{g/ml}$, optical path=0.14 cm, the time between the excitation flashes was 1.98 second. 2.5 mM $\text{Fe}(\text{CN})_6^{-3}/\text{Fe}(\text{CN})_6^{-2}$ were added as

	the electron acceptor system. The transient in the first few μ s was unreliable because of flash artifacts	79
Figure 3-4	The dependence of the absorption changes at 820 nm on the flash repetition rate. Trace A is tris-washed PSII, trace B is NH_2OH treated tris-PSII	81
Figure 3-5	The dependence of the absorption changes at 325 nm on the flash repetition rate in tris-washed PSII	82
Figure 3-6	Microsecond time courses of the absorption changes at 325 nm (trace A) and 820 nm (trace B) in NaCl washed PSII. $[\text{Chl}] = 214.1 \mu\text{g/ml}$, optical path = 0.14 cm, excitation flash repetition rate 5.8 Hz. 2.5 mM $\text{Fe}(\text{CN})_6^{-3}/\text{Fe}(\text{CN})_6^{-2}$ were added as the electron acceptor system. The transient in the first few μ s was unreliable because of flash artifacts	84
Figure 3-7	Microsecond time courses of the absorption changes at 325 nm (trace A) and 820 nm (trace B) with NH_2OH treated tris-PSII. Experiment conditions were same as those in Figure 3-2. The transient in the first few μ s was unreliable because of flash artifacts	86
Figure 3-8	The dependence of the absorption changes at 325 nm on the repetition rate of the excitation flash in NH_2OH treated tris-PSII	87
Figure 3-9	Microsecond time courses of the C550 band shift in tris-washed PSII (trace A) and NH_2OH treated tris-PSII (trace B). $[\text{Chl}] = 315.7 \mu\text{g/ml}$, 2.5 mM $\text{Fe}(\text{CN})_6^{-3}/\text{Fe}(\text{CN})_6^{-2}$ were added as the electron acceptor system	89

Figure 3-10	The scheme of the electron transfer pathways in tris-washed PSII	93
Figure 4-1	Absorption difference spectrum of the initial amplitudes of the total absorption changes after 5 μ s following the flash excitation in tris-washed PSII. [Chl]=215 μ g/ml, optical path=0.14 cm, excitation flash repetition rate 5.8 Hz. 2.5 mM $\text{Fe}(\text{CN})_6^{3-}/\text{Fe}(\text{CN})_6^{4-}$ were added as the electron acceptor system	111
Figure 4-2	Absorption difference spectrum of the 230 μ s decay phase in tris-washed PSII	112
Figure 4-3	Absorption difference spectrum of the reaction center $\text{P}^*\text{680}/\text{P680}$ in tris-washed PSII (open circle, continuous line) and the spectrum of $\text{Chla}^+/\text{Chla}$ in CH_2Cl_2 (dash line)	113
Figure 4-4	Absorption difference spectrum of the reaction center $\text{P}^*\text{680}/\text{P680}$ in tris-washed PSII (open circle) and in NH_2OH treated tris-PSII (open triangle). The NH_2OH treatment was performed with the addition of 2.0 mM NH_2OH and 60 pre-flashes before the measurements were taken in tris-washed PSII. The experiment conditions were the same as in Figure 4-1	115
Figure 4-5	Absorption difference spectrum of the millisecond decay phase in tris-washed PSII (open circle) and in NH_2OH treated tris-PSII (open triangle). [Chl]=215 μ g/ml, the time between excitation flashes was 1.98 second. 2.5 mM $\text{Fe}(\text{CN})_6^{3-}/\text{Fe}(\text{CN})_6^{4-}$ were added as the electron acceptor system	118

Figure 4-6	Absorption difference spectrum of the Y_2^+/Y_2 in tris-washed PSII. The spectrum is obtained by subtracting the Q_A^-/Q_A contributions from the spectrum in Figure 4-5 (open circle). The overlaid spectrum (open triangle) is the absorption difference spectrum of the phenoxy radical $TyrO^\cdot$ in water 119
Figure 4-7	Absorption difference spectrum of the millisecond decay phase in NH_2OH treated tris-PSII after subtracting Q_A^-/Q_A spectrum from the spectrum in figure 4-5 (open triangle) 120
Figure 4-8	The electron transfer and hydrogen shift of the electron donor Y_2 during the electron transfer reactions in PSII. Here B represents an amino acid residue that forms a hydrogen bond with the tyrosine 126
Figure 4-9	The possible chemical reactions of NH_2OH with the phenol group of the tyrosine residue of Y_2 in PSII 127

LIST OF ABBREVIATIONS AND SYMBOLS

ADP	adenosine diphosphate
ATP	adenosine triphosphate
BChl	bacteriochlorophyll
Chl	chlorophyll
CP	chlorophyll protein
Cyt	cytochrome
DCBQ	2,6-dichloro-p-benzoquinone
DCMU	3(3',4'-dichlorophenyl)-1,1-dimethylurea
DTDSP	data treatment and display program
EDTA	ethylene diamine tetraacetate
ENDOR	electron nuclear double resonance
EPR	electron paramagnetic resonance
Hepes	2-hydroxyethyl-1-peperazineethanesulfonicacid
Mes	4-morpholine-ethanosulphonic acid
NADP	nicotidamide adenine dinucleotide phosphate
NMR	nuclear magnetic resonance

OEC	oxygen evolving complex
P680	reaction center chlorophyll in photosystem II
PC	phycocyanin
Pheo	pheophytin
PQ	plastoquinone
PSI	photosystem I
PSII	photosystem II
Q_A	quinone acceptor in photosystem II
Q_B	quinone acceptor in photosystem II
S_n (n=0-4)	states of charge accumulating system associated with the oxygen evolving complex
TASCI	transient absorption spectrometer computer interface program
Tris	tris(hydroxymethyl) amino methane
Y_2	tyrosine residue at 160 position of D1 polypeptide of photosystem II reaction center complex, functions as an electron donor to the reaction center P^+680
Y_0	tyrosine residue at 161 position of D2 polypeptide of photosystem II reaction center complex, it does not participate in electron transfer reactions under physiological conditions

CHAPTER I

INTRODUCTION

Photosynthesis is the process whereby solar radiation is captured and converted into chemical energy. It takes place in plants, algae, and some bacteria. It provides most of the energy we use today. All our foods are direct or indirect products of photosynthesis, and the presence of oxygen in the earth's atmosphere is a direct result of the photosynthetic reactions of higher plants and algae.

Photosynthesis starts with the absorption of a photon by one of the antenna pigment molecules that include species such as chlorophylls, bacteriochlorophylls, carotenoids and phycobilins, which are organized in large, light-harvesting or antenna complexes. The excitation energy is then transferred from one pigment molecule to another by means of long range dipole-dipole interaction [1,2], until it reaches a specialized (bacterio)chlorophyll complex, presumably a dimer [3], called the reaction center. There the photochemical reaction takes place, in which the excited (bacterio)-chlorophyll undergoes charge separation in which an electron

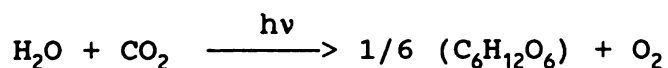
is transferred from the excited (bacterio)chlorophyll to an acceptor molecule. The electron is then quickly transferred to a secondary acceptor and the oxidized chlorophyll is quickly reduced by a donor molecule so that the reducing entity and oxidizing entity are further separated in order to increase the quantum efficiency of the forward electron transfer and reduce the chance of back reaction. The separated charges are subsequently further stabilized by a series of dark electron transport reactions. Eventually the positive charge at the donor side of the photochemical reaction center is neutralized by an electron from an oxidizable substrate H_2A where, in higher plants and algae, A is oxygen and in photosynthetic bacteria A is a highly reduced organic molecule [4]. The negative charge at the reducing side of the photochemical reaction center is ultimately used in the carbon dioxide fixation process in plants, algae and most photosynthetic bacteria, although some photosynthetic bacteria may not fix carbon dioxide [5,6]. The consequences of this process are that solar energy is finally stored in organic compounds as chemical energy and substrate H_2A is oxidized as a by-product.

The electron transfer process in photosynthesis is almost 100% efficient in the sense that for each photon absorbed one electron is transferred from substrate to its acceptor without any significant back reaction during its transport. This

remarkable efficiency of electron transfer is achieved with the highly organized membrane protein complexes of the photosynthetic membrane so that the electronic coupling and reorganization energy of forward electron transfer appear to be optimized. The study of this electron transfer process not only gives us better understanding of the mechanism of photosynthesis but also provides us with very useful clues as to how to store the solar energy more efficiently.

Photosynthesis in Higher Plants

Photosynthesis in higher plants takes place in a special cell organelle, the chloroplast. This contains an intricate lamellar system, composed of flattened membrane sacs (thylakoids), which enclose the so-called lumen. In higher plants, the thylakoids are usually arranged in stacked (grana) and unstacked (stroma) regions [7]. The primary reactions of photosynthesis take place in these membranes. The overall reaction in photosynthesis in plants can be written as:



$$\Delta G = 484 \text{ Kcal/mol}$$

Photosynthesis in plants and algae differs from photosynthesis in photosynthetic bacteria in two aspects (1) Because of the high free energy requirement for photosynthesis

in plants, $\Delta G = 484$ Kcal/mol, a single quantum of visible light has not enough energy to drive the reaction. Thus, in plants there are two photochemical reaction centers working in series so that each electron transfer is driven by two photons. In photosynthetic bacteria, which do not oxidize water, there is only one photochemical reaction center. (2) In plants the main pigments are chlorophylls. In photosynthetic bacteria the main pigments are bacteriochlorophylls.

In plants the two photochemical reactions are performed by photosystem I (PSI) and photosystem II (PSII). The general patterns of electron and proton transfer in these photosystems in higher plants are shown in Figure 1-1. Each photosystem consists of a reaction center, an associated antenna system with one to four hundred pigment molecules (chlorophylls and carotenoids), and several redox active components that serve as electron donors and acceptors. PSII is responsible for the oxidation of water and transfers electrons to PSI through the plastoquinone molecules in the PQ pool, while PSI transfers the electron to its final acceptor NADP^+ , which is used to reduce CO_2 . Coupled with the electron transfer from PSII to PSI, protons are also transferred across the thylakoid membrane from the stroma side to lumen side. The proton gradient generated by this proton transfer is used to synthesize ATP from ADP by the membrane bound ATP synthase. In general, the electron transfer process of photosynthesis in

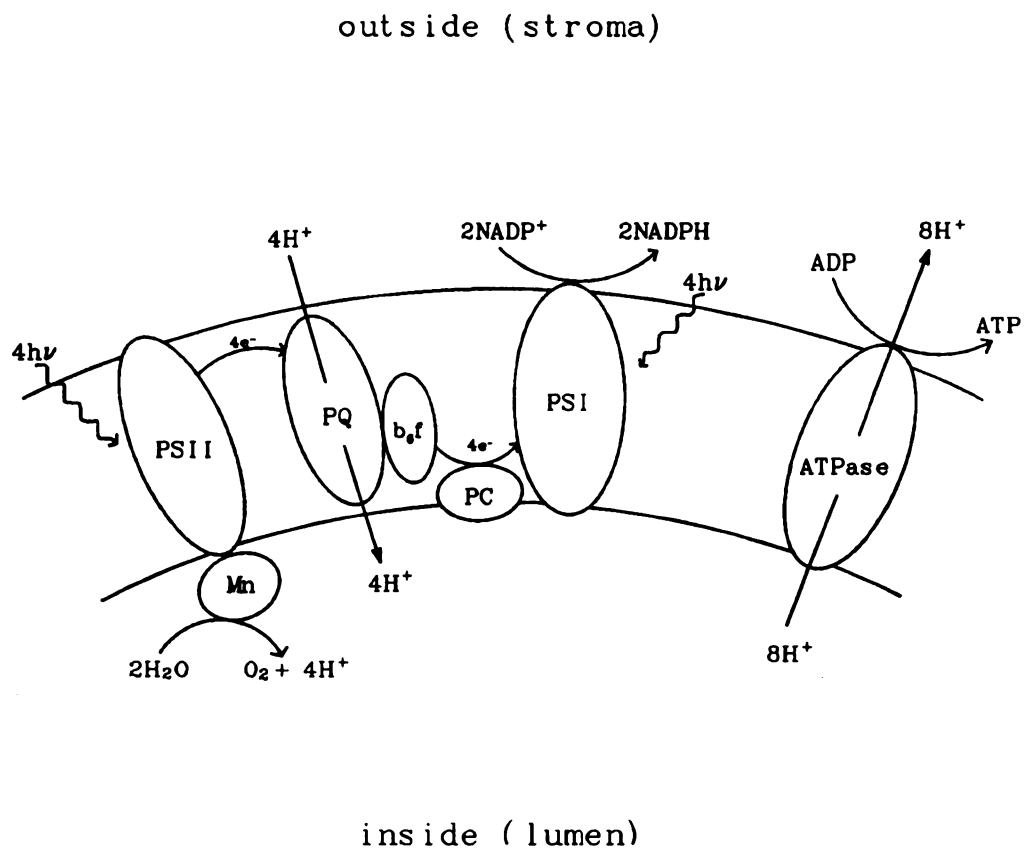


Figure 1-1 The electron transfer and proton transfer patterns of photosynthesis in higher plants

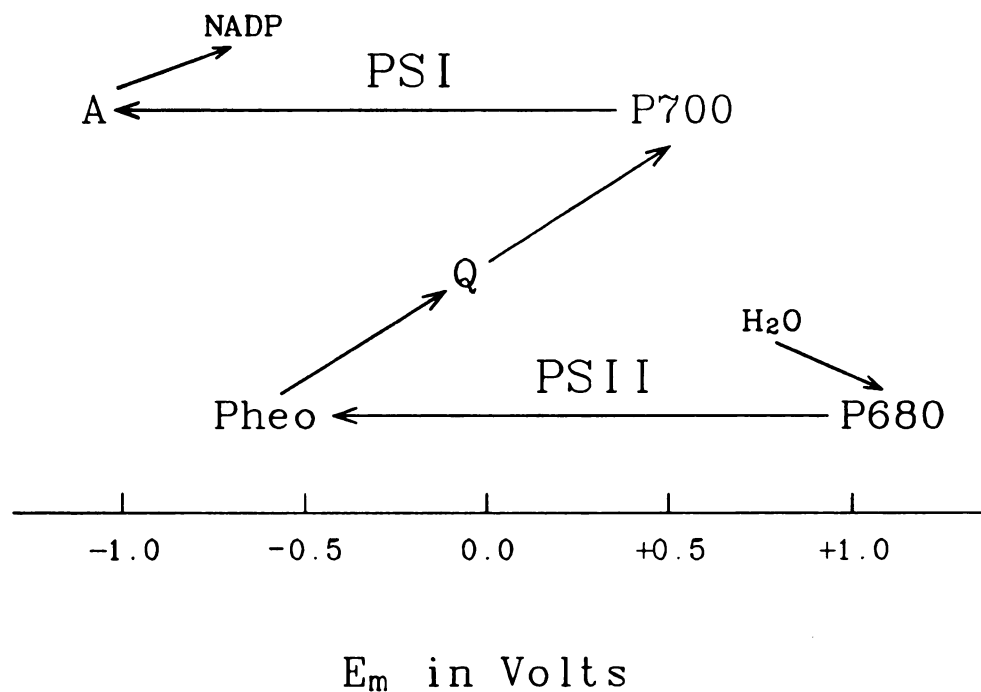


Figure 1-2 Z-scheme of electron transport in higher plants. P700 and P680 are the photochemical reaction centers of the photosystem I and photosystem II respectively. Pheo is a pheophytin molecule that acts as the primary electron acceptor of the P680. A is the primary electron acceptor of P700 and is presumed to be a Fe-S center.

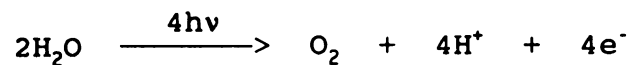
higher plants involves a series electron donors and acceptors of varying redox potential. If the electron transfer diagram is drawn with redox midpoint potential as the X-axis, the diagram looks like a letter Z, thus it is called the Z-scheme for photosynthetic electron transfer (Figure 1-2).

Electron Transfer in Photosystem II

The electron carriers in PSII consist of a manganese cluster (four manganese ions), intermediate electron carrier Y_2 , reaction center P680, which has its absorbance bleaching maximum at 680 nm, primary acceptor Pheo, and plastoquinone acceptors Q_A and Q_B . Upon light excitation, the reaction center P680 (presumably a dimer of chlorophylls) is excited and donates an electron to its nearest acceptor Pheo (pheophytin a) in 3 ps [8]. The charge separation is stabilized in 300 ps [9] by a secondary electron transfer from $Pheo^+$ to a strongly bound plastoquinone molecule called Q_A . The reduced quinone acceptor Q_A^- can be reoxidized in a variety of ways. In intact PSII membrane particles in which the Q_B site is not empty or damaged, or in chloroplasts, Q_A^- is oxidized by a secondary plastoquinone molecule called Q_B in about 200 μ s [10,11]. The Q_A^- to Q_B electron transfer can be inhibited by a number of commercial herbicides, such as DCMU (3(3',4'-dichlorophenyl)-1,1-dimethylurea), which are commonly used in the studies of PSII. In some conditions, Q_A^- can be

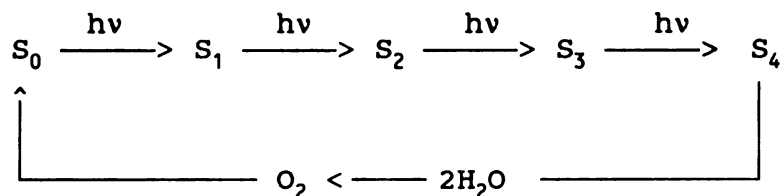
oxidized in approximately 40 μ s by the oxidized non-heme iron located between Q_A and Q_B [12,13]. Q_A^- can be also oxidized by exogenously added acceptors such as 2,5-dichlorobenzoquinone (DCBQ) or ferricyanide, although it is unclear in the ferricyanide case whether Q_A^- is oxidized directly or indirectly [14]. An additional means of Q_A^- oxidation is importance to the research in this thesis, namely, backreaction or charge recombination with P^+680 or Y_2^+ . This reaction takes place when the normal electron transfer on the donor side of PSII is retarded or inhibited. The Q_A^- oxidation by charge recombination is the main topic of this dissertation, and it will be discussed in the following chapters in greater detail.

The water splitting reaction is the least understood part of photosynthesis in higher plants. Although significant progress has been made during the last decade, water oxidation is still an unsolved problem. In order to oxidize water, four oxidizing equivalents are required:



The photochemical reaction that takes place in PSII is a one electron reaction. How this one electron reaction is coupled to the four-electron oxidation of water is a key point in understanding the water splitting process. The single

turnover flash experiments done by Joliot, Kok, and their coworkers [34-36] showed that each oxidizing equivalent is stored in a complex until four have been accumulated. Only when this is accomplished is oxygen released. This is the so-called Kok model



In this scheme, S represents the state of the oxygen evolving complex, and the subscripts represent the oxidizing equivalents stored in the complex.

Although this model has nothing to say about the nature of the S-state complex, it predicts the existence of relatively stable higher S-state intermediates. Manganese has long been known to be essential for water splitting activity [37], as a substantial body of work [37-40] indicates that four manganese are associated with the S-state complex. Transient absorption experiments in UV region [14], the multiline EPR signal [41-44], and K edge manganese X-ray absorption [45] strongly indicate that the manganese cluster is directly involved in the electron transfer reaction between water and Y_2^+ and that it undergoes valence changes during the S-state transitions.

The redox potentials involved on the donor side of PSII

are extremely high and easily lead to non-physiological oxidation products such as chlorophylls [15,16], cytochrome b_{559} [17,18], and carotenoid [19]. The kinetics of electron transfer on the donor side of the PSII are different for the four different redox states of the oxygen evolving complex.

Under normal physiological conditions, the oxidized PSII reaction center $P^{+}680$ is reduced by a component called Y_2 , which has been identified as a tyrosine residue of the D1-polypeptide at the 160 position [20,21]. The electron transfer rate from Y_2 to $P^{+}680$ is highly dependent on the oxidation state of the oxygen evolving complex, pH in the buffer, and polypeptide composition. At physiological pH values, the electron transfer takes place in 20 ns in lower oxidation states of the oxygen evolving complex (S_0 and S_1) and is biphasic in higher oxidation states of the oxygen evolving complex (S_2 and S_3) with halftimes of 50 ns and 250 ns [22,23]. At low pH, the electron transfer is monophasic for all oxidation states of the OEC: the halftime is 40 ns in S_0 and S_1 , and 250 ns in S_2 and S_3 [24]. For tris-washed PSII, in which the manganese cluster and 3 peripheral polypeptides are released, the rate of the electron transfer is much slower, being a few microseconds [25,26].

Photosystem II contains a second tyrosine residue, called Y_D , located on D2-polypeptide at the 161 position [20,27]. It has the same EPR spectrum as Y_2 , but the decay kinetics and

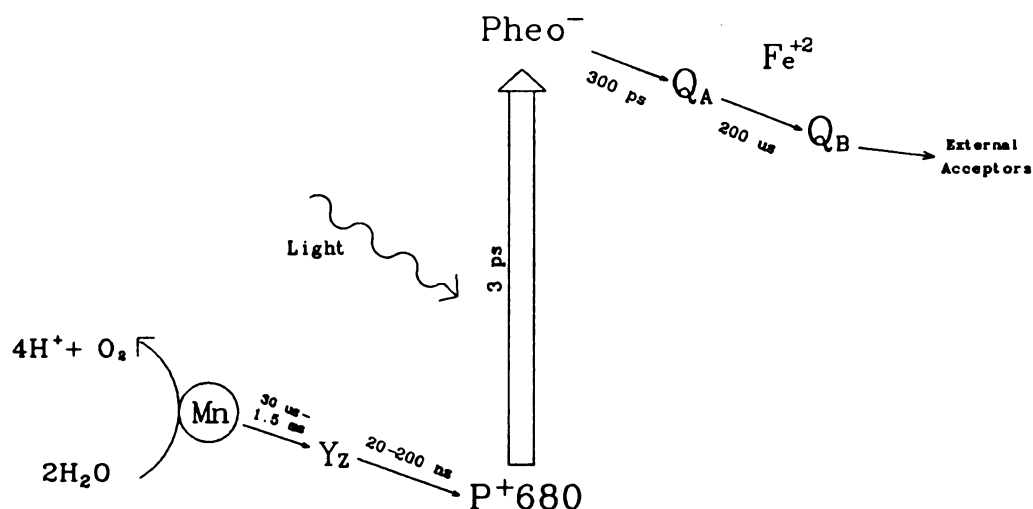


Figure 1-3 The kinetics of electron transfer in photosystem II

interactions with the manganese cluster are different [28-30]. Normally, this tyrosine residue is oxidized and does not participate in electron transport. It is, however, involved in maintaining the system in the S_1 state in the dark [31,32] and preventing over-reduction of the oxygen evolution complex [33]. A potential function in photoactivation of the manganese cluster has also been proposed [27].

It is generally agreed that the manganese cluster functions between substrate water and the intermediate

electron carrier, Y_2 , and that it functions as a four-electron gate. It stores positive charge equivalents prior to the four electron oxidation of two molecules of water. In addition, it is likely that manganese acts as the binding site for the water molecules that are oxidized. For intact PSII membranes, where the manganese cluster is fully functional, Y_2^+ is reduced by the manganese cluster. The rate of this electron transfer is highly depend on the oxidation state of the manganese cluster. In the S_0 state, Y_2^+ is reduced in 30-70 μs , in the S_1 state, it is reduced in 50-110 μs , in the S_2 state, it is reduced in 60-350 μs , and in the S_3 state, the reaction is further slowed down to one millisecond [46-50].

When the manganese cluster is destroyed, such as by tris washing, which releases manganese and peripheral polypeptides from the OEC [51-52], Y_2^+ can be reduced by an external donor or by charge recombination with Q_A^- . These reactions will be discussed in detail in chapter III and chapter IV.

The Structure of Photosystem II

Photosystem II of higher plants is made up of a cluster of at least nine polypeptides (Figure 1-3), six of which are intrinsic, membrane-spanning polypeptides, and three of which are extrinsic, membrane associated polypeptides. The exact locations of the various electron transport components discussed above are not known yet. No single crystal

structure of PSII has been obtained, thus there is no detailed structural information available as there is in the photosynthetic bacteria case [53]. Figure 1-3 shows a possible model of PSII structure, which comes from the assumption that the structure of PSII is similar to the structure of photosynthetic bacteria, though the justification of the assumption is still an open question. Recent results from Yocum's laboratory have strongly challenged this assumption [54].

The six intrinsic polypeptides of PSII include the following: two large chlorophyll-binding polypeptides with apparent molecular masses of 47 and 43 kDA, called CP47 and CP43 respectively, that serve as core antenna subunits; two distinct polypeptides with molecular masses of approximately 32 kDA, named D1 and D2, that bind to each other and are the essential parts of the PSII reaction center; and two other small polypeptides (5 and 10 kDA) that are involved in the binding of the cytochrome b_{559} heme group.

The locations of the reaction center and other electron transfer carriers of PSII within these polypeptides are not clear yet. In early work, the CP47 polypeptide was proposed by several groups to be the site of P680 and pheophytin a binding based upon fluorescence [55], pigment composition and spectral change [56-58]. However, because of the homology in the amino acid sequences of the D1 and D2 polypeptides with

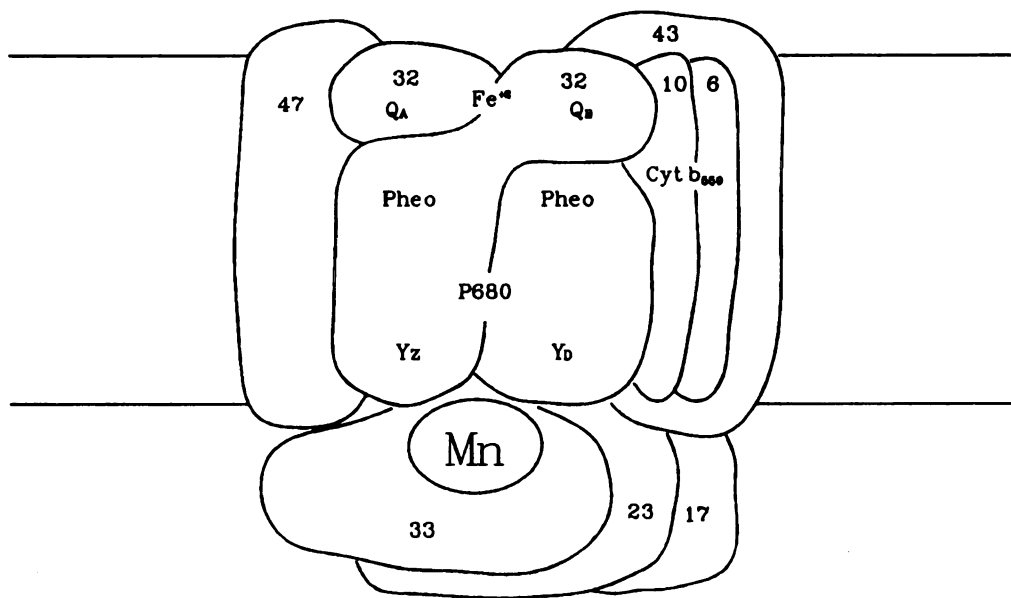


Figure 1-4 A possible structure of photosystem II reaction center

the L and M subunits of the reaction center of purple bacteria [53], it was suggested that D1 and D2, rather than CP47, might provide the binding site for the P680 and pheophytin a [59-61]. Recently, evidence for the binding of pigments to D1 and D2 polypeptides has been provided by Nanba and Satoh [62]. They successfully isolated a complex consisting of the D1 and D2 polypeptides and cytochrome b_{559} from spinach PSII particles with 4-6 Chl a, 2 Pheo a, and 1 β -carotene molecules. This complex shows photochemical activity, as indicated by light induced absorbance changes that could be attributed to the photo-reduced Pheo a, and the formation of a spin-polarized triplet at low temperature that is characteristic of all reaction centers [63]. But the absence of plastoquinone in Nanba and Satoh's preparation indicates that the electron acceptor Q_A and Q_B are lost during the isolation procedure. This raises the question as to whether the pigment composition obtained in the Nanba's particle really reflects the true pigment composition in PSII reaction center. Recent results from Yocum's laboratory indicate that more pigments, 10-12 Chla, 2-3 Pheo a, along with 2 Cyt b_{559} , are bound to the reaction center complex of PSII [54]. There is also some evidence indicating that CP47 and CP43 not only serve as sub-antennae but also play a role in binding quinone molecules and the extrinsic 33 kDA polypeptide [63].

The three extrinsic polypeptides with molecular masses of

17, 23 and 33 kDA are associated with the inner surface of the thylakoid membranes and play important roles in oxygen evolution in higher plants [64,65]. At first it was assumed that these polypeptides were directly involved in the oxidation of water, but more recent evidence has shown that their main function is to shield and stabilize the manganese cluster. Each of the three polypeptides has now been shown to be functionally replaceable with high concentrations of chloride and/or calcium ions. The 17 kDA polypeptide is replaced by 5 mM Cl^- . The 23 kDA polypeptide is replaced by 5 mM Ca^{+} and 30 mM Cl^- . In the absence of the 33 kDA polypeptide oxygen evolution can occur, although at a slower rate, when 200 mM Cl^- is present [66]. Ca^{+} must also be present to overcome the absence of the 23 kDA in these preparations. Thus, it is thought that the extrinsic polypeptides play a role in improving the reaction center capacity for binding Ca^{+} and Cl^- ions. In addition, they play a structural role in protecting the manganese cluster from attack by external reducing agents. It is possible that the 33 kDA may provide some ligands directly to the manganese cluster that are replaced by Cl^- when the polypeptide has been removed [67].

The location of the manganese cluster remains one of the most speculative parts of the PSII structural model. Although the three extrinsic polypeptides are unlikely to be the major

sites of manganese binding [68], none of the six intrinsic polypeptides can be strictly ruled out as the binding polypeptide [69]. Based on mutagenesis experiments on the D1 polypeptide with an unprocessed C-terminal extension [70], photodestruction of the reaction center [71], and cross-linking studies of the complex [72], the prevailing view is that the manganese cluster is more likely to be situated in the D1/D2 reaction center polypeptides.

Transient Absorption Spectroscopy in the Studies of Photosystem II

Transient absorption spectroscopy has been the oldest but the most useful physical technique to study photosynthesis. Although it does not have the high spectral resolution and selection that ESR and ENDOR do, it has better time resolution capability. Rapid development of laser technology has brought transient absorption spectroscopy to preeminence in studying rapid kinetic processes. The picosecond and sub-picosecond laser spectroscopy developed in the last few years has pushed the time resolution of transient absorption spectroscopy close to the theoretical limit. This kind of time resolution is impossible for other kinds of spectroscopies such as ESR, NMR and ENDOR. Transient absorption spectroscopy is a non-destructive technique, and samples used in the measurements are usually closer to their physiological conditions than

those used in other spectroscopies, which reduces the chances of interferences from non-physiological sample conditions.

Almost all redox-active components of photosystem II have absorption changes upon oxidation or reduction following the excitation flash. Thus, they are detectable by transient absorption spectroscopy. Most of the kinetic data on electron transfer in PSII has been obtained by this technique. The spectral overlap of different components, which causes difficulty in interpreting the results, can be greatly improved in transient absorption spectroscopy, because oxidation or reduction of different components may take place on different time scales.

Reaction Center P680

The reaction center of PSII was detected as a flash induced absorption change attributable to chlorophyll a oxidation [73]. Its bleaching maximum is close to 680 nm and it thus was designated P680. The fluorescence of the light harvesting chlorophylls interferes with measurements at this wavelength, however, and many kinetic studies of P⁺680 have been done by measuring the smaller broad absorption increase at around 820 nm [74,75].

In the ultraviolet and visible region, because of the interferences from other components and strong absorption of samples, investigation of the P680 spectrum has not been done

as intensively. The first detailed P⁺680/P680 difference spectrum in the UV/Visible region was published recently by Gerken and coworkers [76]. The UV/Visible region is a very important region because structural or environmental changes may be detected fairly easily in this region.

The appearance kinetics of P⁺680 following light absorption was impossible to monitor few years ago. Recently, however, Wasielewski's laboratory used 500 fs time resolution to resolve this rise time as 3 ps by transient absorption spectroscopy. The data show that P680 donates an electron to a pheophytin a molecule directly without detectable electron transfer participation of the accessory chlorophyll [8]. The P⁺680 decay can be detected optically at 820 nm. Under physiological conditions, P⁺680 is reduced on a time scale of 50 to 250 ns depending on the S-state. When the normal electron transfer is inhibited (e.g. by tris-washing, salt washing, NH₂OH treatment, detergent treatment, or extremes pH), P⁺680 reduction is retarded into the microsecond range and can be easily detected optically.

Acceptor Side

Photoaccumulation of reduced pheophytin in PSII detected by its characteristic absorption changes under reducing conditions was first reported by Klimov et al.[77]. It was proposed that Pheo might play a role as an electron carrier

between the reaction center P680 and the plastoquinone acceptor Q_A , analogous to that of BPheo in purple bacteria. Supporting evidence came from the observation of a split Pheo⁻ EPR signal [78] and from the observation of a characteristic spin-polarized triplet signal from P680 [79]. The difference spectrum of Pheo⁻/Pheo is similar to that of P⁺680/P680 in the red and near infrared region, but the small bleaching at 540 nm and 505 nm are typical of Pheo reduction [80,81]. The most direct proof that Pheo acts as an electron carrier between P680 and Q_A comes from the direct observation by transient absorption spectroscopy of Pheo reduction with sub-picosecond time resolution. It has been shown that Pheo is reduced in 3 ps [8] by P680 and reoxidized in 300 ps as it transfers the electron to acceptor Q_A [9].

A great deal of work on Q_A has been done by using absorption and fluorescence spectroscopy. It has been identified as a firmly bound plastoquinone molecule by absorption spectroscopy and extraction/reconstitution experiments [82]. Q_A is reduced to a semiquinone anion by Pheo⁻ in about 300 ps. The absorption difference spectrum reflecting this transfer is characterized by the appearance of the semiquinone anion absorbance at 325 nm and the disappearance of the oxidized quinone at 265 nm [14]. In the visible region of the spectrum, a second semiquinone absorption band is observed between 400 nm and 450 nm, but

here the spectrum is superimposed on changes due to electrochromic wavelength shifts of the absorbance of chlorophyll and pheophytin molecules. These shifts are caused by the charge on Q_A , and probably involve two pigments in the reaction center, chlorophyll a and pheophytin a. The pheophytin a bandshift around 545 nm is important for diagnostic reasons, since it occurs in a wavelength region in which the absorbance changes can be measured relatively easily. Moreover, Q_A is the only quinone that induces a significant shift of this pigment upon reduction [11,83].

Reduced Q_A donates an electron to another plastoquinone acceptor called Q_B in about 200 μ s [10,11] in intact PSII membrane particles. The reduction of Q_B to Q_B^- gives rise to absorption changes in the UV that are similar to those observed when Q_A is reduced. The spectrum shows characteristic features of plastosemiquinone formation [14]. The Q_B^- minus Q_B optical spectrum is similar in many respects to that of Q_A^- minus Q_A but the bandshifts in the blue and green parts of the spectrum are different [84], indicating that Q_B^- is different from Q_A^- in terms of its proximity to the electrochromically responding pheophytin. The reduced Q_B remains bound to the Q_B -site [85] until a second electron from Q_A^- , produced in a second photoact, reduces it to a doubly reduced quinone. The doubly reduced Q_B (Q_B^{2-}) is protonated to form the hydroquinone Q_BH_2 ; it then leaves the binding site on

the reaction center and becomes part of the membrane plastoquinone pool. This mechanism of plastoquinone reduction exhibits a strong period two oscillation in UV absorption upon flash excitation. Thus, extreme care must be taken when analyzing the flash number dependence of absorption in the UV region.

Donor Side

Although the electron transfer rate from Y_2 to reaction center P^+680 is strongly dependent on the S-state, ranging from 20 ns to 250 ns, its absorption difference spectrum appears to be very similar in all these S-states [11,14,23]. It consists of absorbance increases around 260 nm and 300 nm and of a chlorophyll a bandshift around 435 nm. Because of the strong overlap of the absorption difference spectrum between Q_A^-/Q_A and Y_2^+/Y_2 in the UV region, where the major peaks of Y_2^+/Y_2 are located, care must be taken when the data are analyzed. However the EPR signal of Z^+ is relatively easy to detect, so most studies of Y_2^+ to date have been done by EPR rather than optically.

Transient absorption spectroscopy provides an excellent tool to study S-state transitions, since other techniques, such as EPR and EXAFS that require cryogenic temperature, can not be done at physiological temperature. The kinetics of S-state transitions can be studied with single turnover

flashes with dark adapted PSII particles, and the period four oscillation of absorbance changes, which corresponds to four different S-state transition, can be observed in the UV region [46,86]. In dark adapted PSII, about 75% of the reaction centers are in the S_1 state. The first flash induces the S_1 to S_2 transition, which produces an absorbance increase at 362 nm with a half time about 40 μ s [46]. The second flash induces the S_2 to S_3 transition with an absorbance increase similar to the first flash with a half time of about 100 μ s. The third flash, which induces the S_3 -(S_4)- S_0 transition and is coupled with oxygen evolution, reverses the absorbance increases of the first and the second flashes and resets the system to the S_0 state with a half time about 1.5 ms. The fourth flash, which induces the S_0 to S_1 transition, shows a very small absorbance increase with a halftime about 50 μ s [46]. Experiments done at different wavelength show very similar results [87].

The absorption difference spectrum of S-state transitions has a peak around 300 nm with extinction difference coefficients on the order of 4500-6000 $M^{-1}cm^{-1}$. Above 400 nm, absorption changes directly related to the manganese cluster are very small. The absorption difference spectrum of S_1 to S_2 transition and S_2 to S_3 transition are very similar. Both are tentatively assigned to a Mn(III) to Mn(IV) transition based on the experiments of multiline EPR signal [41,88-90],

XANES K-edge [91], and NMR proton relaxation rate [92]. The small absorption changes of the S_0 to S_1 transition are assumed to be due to a Mn(II) to Mn(III) transition based on other techniques [93].

Description of Work to be Presented

In intact PSII membranes, the forward electron transfer is carried out very efficiently and the quantum yield is very close to 1. This high efficiency of electron transfer is achieved by rapid reduction of the P^+680 by its physiological donor Y_2 in less than 250 ns [22]. Certain chemical treatments, which inhibit oxygen evolution, greatly increase the lifetime of P^+680 so that the charge recombination reaction of the state Q_A^-/P^+680 is extended into the microsecond time scale. The time evolution of the state Q_A^-/P^+680 is highly depended on the micro-environments of the electron carriers and the presence of inhibitors.

Gerken and coworkers [76] studied the charge recombination reactions of Q_A^-/P^+680 in tris-washed PSII in cyanobacterium. They found three decay phases with halftimes of 170 μ s, 800 μ s and 6 ms, and attributed the multiphasic kinetics to a distribution of different structural states of the reaction center proteins. Ford and Evans [94] observed that, after NH_2OH inhibition, the sub-microsecond decay phase of P^+680 in PSII was transferred into the microsecond time range. The

decay was biphasic with halftimes of 90-150 μ s and 600-900 μ s. Both phases were attributed to charge recombination between Q_A^- and P^+680 . They explained the different kinetic phases in terms of different charge states of other redox-active components in the reaction center complex. Other inhibitory treatments include trypsination [95], which retards P^+680 reduction to 200 μ s and may be relieved by the addition of Ca^{2+} cations, and addition of acetate [96], which slows the forward reduction of P^+680 by almost four orders of magnitude and the back reaction with Q_A^- five-fold, were explained as modifications of the micro-environment of PSII.

The wide differences of decay pathways and decay rates of the charge separated state, Q_A^-/P^+680 , under different treatments raises interesting questions as to how the time evolution of Q_A^-/P^+680 is modified by these treatments and as to what information we can obtain by monitoring the time courses of the state Q_A^-/P^+680 following these different treatments. In the experiments described in chapter III, we used the transient absorption spectroscopy technique, described in chapter II, to monitor the decay time course of Q_A^-/P^+680 with tris, NaCl, and NH_2OH treated PSII. Our results show that the charge recombination reactions can be observed in these inhibited PSII preparations. The halftimes of the charge recombination reaction are similar in tris-washed PSII and NH_2OH treated PSII, but it is faster in NaCl-washed PSII.

These differences are attributed to the different micro-environments at the donor side of PSII. The Q_A^- to Q_B electron transfer, which has not been analyzed fully in prior studies, may not occur in these samples because of the positive charge on P^+680 or the modification of Q_B site.

An obvious way to identify the components of the electron transfer reactions and the effects of different treatments by transient absorption spectroscopy is to obtain the absorption difference spectrum of the individual components. The first full absorption difference spectrum of Q_A^-/Q_A was obtained by Van Gorkom [82] and identified as arising from a plastoquinone molecule because of its similarities to the in vitro spectrum of plastoquinone. Dekker and coworkers [14] obtained detailed absorption difference spectra of Q_A^-/Q_A and Y_2^+/Y_2 in tris-washed PSII by analysis of flash-induced absorption changes in the millisecond time range. The absorption difference spectrum of $P^+680/P680$ in the UV range has not been studied as extensively as that of Q_A^-/Q_A and Y_2^+/Y_2 because of its very short lifetime. The first detailed $P^+680/P680$ absorption difference spectrum in the UV-Visible region was obtained very recently by Gerken et. al. [76] in tris-washed PSII from cyanobacterium *Synechococcus* sp. by measuring the charge recombination reactions between Q_A^- and P^+680 . They found that the $P^+680/P680$ absorption difference spectrum is dominated by a very sharp bleaching around 434 nm, which resembles the in

vitro difference spectrum of $\text{Chla}^+/\text{Chla}$.

The absorption difference spectrum can be used to identify the various components as well as their micro-environments. Weiss and Renger [95] claimed that the difference spectrum of $\text{P}^*\text{680}/\text{P680}$ was affected by the trypsination at pH 7.5 or by incubation with NH_2OH . In the work described in Chapter IV, we measured the absorption difference spectrum of $\text{P}^*\text{680}/\text{P680}$ and Y_2^+/Y_2 by monitoring the decay kinetics of $\text{Q}_\text{A}^-/\text{P}^*\text{680}$ under different treatments in tris-washed PSII. The results we obtain support a model in which the microsecond decay phase comes from the charge recombination reaction between Q_A^- and $\text{P}^*\text{680}$ and the millisecond phase comes from electron transfer between Q_A^- and Y_2^+ . The difference spectra we obtained with NH_2OH treated tris-PSII show that the spectrum of $\text{P}^*\text{680}/\text{P680}$ is not affected by the NH_2OH treatment, contrary to the claim by Weiss and Renger [95], but that the spectrum of Y_2^+/Y_2 is dramatically modified by NH_2OH treatment. We conclude that the NH_2OH inhibition site is closer to Y_2 than to the reaction center P680 site.

References

1. T. Forster (1948), Ann Physik., 2, 55
2. R. Van Grondelle (1985) Biochim. Biophys. Acta, 811, 147
3. W.W. Parson and B. Ke (1982) in Photosynthesis, Vol.I, Energy Conversion by Plants and Bacteria, (Govindjee, ed.) 331, Academic Press, New York
4. R. K. Klayton and W. Sistrom (1978), The Photosynthetic Bacteria, Plenum Press, New York
5. A.L. Lehninger (1970), Biochemistry, Worth Publishers, New York
6. B.K. Pierson and J.M. Olson (1987) in Photosynthesis, edited by J. Ames, 21, Elsevier Science Publishing Company, New York
7. R.K. Clayton, Photosynthesis: Physical Mechanisms and Chemical Patterns 79, Cambridge University Press 1980
8. M.R. Wasielewski, D.G. Johnson, M. Seibert, and Govindjee, Proc. Natl. Acad. Sci. USA, Vol. 86, 524-528, January 1989
9. Eckert, H.-J, Wiese, N., Bernarding, J., Eichler, H.-J. and Renger, G. FEBS Lett. 1988, 240, 153
10. J.M. Bowes and A.R. Crofts, Biochim. Biophys. Acta 1980, 590, 373
11. G.H. Schatz and H.J. van Gorkom, Biochim. Biophys. Acta 1985, 810, 283

12. V. Petrouleas and B.A. Diner, Biochim. Biophys. Acta 1987, 893, 126
13. B.A. Diner and V. Petrouleas, Biochim. Biophys. Acta 1987, 895, 107
14. Dekker, J.P., van Gorkom, H.J., Brok, M. and Ouwehand, L. Biochim. Biophys. Acta 1984, 764, 301
15. Visser, J.W.M., Rijersberg, C.P. and Gast, P. Biochim. Biophys. Acta 460, 1977, 36
16. De Paula, J.C., Innes, J.B. and Brudvig, G.W. Biochemistry Vol. 24, 1985, 8114
17. Vermeglio, A. and Mathis, P. Biochim. Biophys. Acta 314, 1973, 57
18. Malkin, R. and Vänngård, T. FEBS Lett. 111, 1980, 228
19. Mathis, P. and Rutherford, A.W. Biochim. Biophys. Acta 767, 1984, 217
20. Debus, R.J., Barry, B.A., Babcock, G.T., and McIntosh, L. Proc. Natl. Acad. Sci. USA 85, 1988, 427
21. Barry, B.A. and Babcock, G.T. Proc. Natl. Acad. Sci. USA 84, 1987, 7099
22. Brettel, K., Schlodder, E., and Witt, H.T. Biochim. Biophys. Acta 766, 1984, 403
23. Gerken, S., Brettel, K., Schlodder, E., and Witt, H.T. FEBS Lett. 1988, 237, 69
24. Meyer, B., Schlodder, E., Dekker, J.P., and Witt, H.T. Biochim. Biophys. Acta submitted
25. Reinman, S., Mathis, P., Conjeaud, H., and Stewart, A. Biochim. Biophys. Acta 1981, 635, 429
26. Boska, M., Sauer, K., Buttner, W., and Babcock, G.T.

- Biochim. Biophys. Acta 1983, 722, 327
27. Vermaas, W.F.J., Rutherford, A.W., Hansson, D., Proc. Natl. Acad. Sci. USA 1988, 85, 8477
 28. Hoganson, C.W. and Babcock, G.T., Biochemistry 1988, 27, 5848
 29. Babcock, G.T. and Sauer, K. Biochim. Biophys. Acta 1973, 325, 504
 30. Warden, J.H., Blankenship, R.E. and Sauer, K. Biochim. Biophys. Acta 1976, 423, 462
 31. Boussac, A. and Etienne, A.L. Biochim. Biophys. Res. Commun. 1982, 109, 1200
 32. Vermass, W.F.J., Renger, G., and Dohnt, G. Biochim. Biophys. Acta 1984, 764, 192
 33. Styring, S. and Rutherford, A.W. Biochemistry 1987, 26, 2401
 34. Joliot, P., Barbieri, G. and Chabaud, R. Photochem. Photobiol. 1969, 10, 309
 35. Kok, B., Forbush, B. and McGloin, M. Photochem. Photobiol. 1970, 11, 457
 36. Weiss, C., Jr. and Sauer, K. Photochem. Photobiol. 1970, 11, 495
 37. Cheniae, G. Methods Enzymol. 1980, 69, 349
 38. Ames, J. Biochim. Biophys. Acta 1983, 726, 1
 39. Radmer, R. and Cheniae, G.M. in Primary Processes of Photosynthesis (Barber, J., ed.) 1977, 308, Elsevier, Amsterdam
 40. Cheniae, G.M. and Martin, I.F. Biochim. Biophys. Acta 1970, 197, 219

41. Dismukes, G.C. and Siderer, Y. Proc. Natl. Acad. Sci. USA 1981, 78, 724
42. Zimmerman, J.L. and Rutherford, A.W. Biochim. Biophys. Acta 1984, 767, 160
43. Hansson, O. and Andreasson, L.-E. Biochim. Biophys. Acta 1982, 679, 261
44. de Paula, J.C. and Brudvig, G.W. J. Am. Chem. Soc. 1985, 107, 2643
45. Goodin, D.B., Yachandra, V.K., Britt, R.D., Sauer, K. and Klein, M.K. Biochim. Biophys. Acta 1984, 765, 524
46. Saygin, O. and Witt, H.T. Biochim. Biophys. Acta 1987, 893, 452
47. Dekker, J.P., Plijter, J.J., Ouwehand, L., and van Gorkom, H.J. Biochim. Biophys. Acta 1984, 767, 176
48. Renger, G. and Weiss, W. Biochem. Soc. Trans. 1985, 14, 17
49. Koike, H., Hanssum, B., Inoue, Y., and Renger, G. Biochim. Biophys. Acta 1987, 893, 524
50. Hoganson, C.W. and Babcock, G.T. Biochemistry 1988, 27, 5848
51. Radmer, R. and Cheniae, G.M. in Primary Processes of Photosynthesis (Barber, J., ed.) 1977, 303, Elsevier, Amsterdam
52. Åkerlund, H.-E., Jansson, C. and Andersson, B. Biochim. Biophys. Acta 1982, 681, 1
53. Deisenhofer, J., Epp, O., Mikki, K., Huber, R. and Michel, H. J. Mol. Biol. 1984, 180, 385
54. Dekker, J.P., Bowlby, N.R. and Yocum, C.Y. FEBS Lett. 1989, 254, 150

55

5

5

5

5

6

6

55. Nakatani, H.Y., Ke, B., Dolan, E. and Arntzen, C.J. Biochim Biophys. Acta 1984, 765, 347
56. Yamagishi, A. and Katoh, S. Biochim Biophys. Acta 1984, 765, 118
57. De Vitry, C., Wollman, F.A. and Delepelaire, P. Biochim Biophys. Acta 1984, 767, 415
58. Camm, E.L. and Green, B.R. J. Cell Biochem. 1984, 23, 171
59. Trebst, A. and Draber, W. Photosynth. Res. 1986, 10, 381
60. Trebst, A. Z. Naturforsch. 1986, 41C, 240
61. Michel, H. and Deisenhofer, J. in Encyclopedia of Plant Physiology: Photosynthesis III (Staehelin, L.A. and Arntzen, C.J. eds.), 1986, 371, Springer, Berlin
62. Nanba, O. and Sotoh, K. Proc. Natl. Acad. Sci. USA 1987, 84, 109
63. Evans, M.C.W. Nature 1987, 327, 284
64. Ghanotakis, D.F. and Yocum, C.F. Photosynth. Res. 1985, 7, 97
65. Dismukes, G.C. Photochem. Photobiol. 1986, 43, 99
66. Miyao, M., Murata, N., Lavorel, J., Maisson-Peteri, B., Boussac, A. and Etienne, A.L. Biochim. Biophys. Acta 1987, 890, 151
67. Dismukes, G.C. Chemica Scripta 1988, 28A, 99
68. Murata, N. and Miyao, M. Trends Biochem. Sci. 1985, 10, 122
69. Ghanotakis, D.F., Waggoner, C.M., Bowlby, N.R., Demetriou, D.M., Babcock, G.T. and Yocum, C.F. Photosynth. Res. 1987, 14, 191

70. Taylor, M.A., Packer, J.C.L. and Bowyer, J.R. FEBS Lett. 1988, 237, 229
71. Virgin, I., Styring, S. and Andersson, B. FEBS Lett. 1988, 233, 408
72. Enami, I., Miyaoka, T., Mochizuki, Y., Shen, J. Satoh, K. and Katoh, S. Biochim. Biophys. Acta 1989, 973, 35
73. Döring, G., Stiehl, H.H. and Witt, H.T. Z. Naturforsch. 1967, 22b, 639
74. Van Best, J.A. and Mathis, P. Biochim. Biophys. Acta 1978, 503, 178
75. Brettel, K., Schlodder, E. and Witt, H.T. Biochim. Biophys. Acta 1984, 766, 403
76. Gerken, S, Dekker, J.P., Schlodder, E. and Witt, H.T. Biochim. Biophys. Acta 1989, 977, 52
77. Klimov, V.V., Klevanik, A.V., Shuvalov, V.A. and Krasnovsky, A.A. FEBS Lett. 1977, 82, 183
78. Klimov, V.V., Dolan, E., Shaw, E.R. and Ke, B Proc. Natl. Acad. Sci. USA 1980, 77, 7227
79. Rutherford, A.W., Paterson, D.R. and Mullet, J.E. Biochim. Biophys. Acta 1981, 635, 205
80. van Gorkom, H.J., Pulles, M.P.J. and Wessels, J.S.C. Biochim. Biophys. Acta 1975, 408, 331
81. Shuvalov, V.A., Klimov, V.V., Dolan, E., Parson, W.W. and Ke, B. FEBS Lett. 1980, 118, 279
82. Van Gorkom, H.J. Biochim. Biophys. Acta 1974, 347, 439
83. Lavergne, J. FEBS Lett. 1984, 173, 9
84. Mathis, P. and Haveman, J. Biochim. Biophys. Acta 1977, 461, 167

9

9

9

93

94

95

96

85. Velthuys, B.R. in Function of Quinones in Energy Conserving Systems (Trumpower, B.L., ed.) Academic Press, New York, 1982, 401
86. Pulles, M.P.J., van Gorkom, H.J. and Willemsen, J.G. Biochim. Biophys. Acta 1976, 449, 536
87. Dekker, J.P., van Gorkom, H.J., Wensink, J. and Ouwehand, L. Biochim. Biophys. Acta 1984, 767, 1
88. Casey, J.L. and Sauer, K. Biochim. Biophys. Acta 1984, 767, 21
89. Zimmermann, J.L. and Rutherford, A.W. Biochim. Biophys. Acta 1984, 767, 160
90. Pecoraro, V.L. Photochem. Photobiol. 1988, 48, 249
91. Yachandra, V.K., Guiles, R.D., McDermott, A.E., Cole, J.L., Britt, R.D., Dexheimer, S.L., Sauer, K. and Klein, M.P. Biochemistry 1987, 26, 5974
92. Srinivasan, A.N. and Sharp, R.R. Biochim. Biophys. Acta 1986, 850, 211
93. Srinivasan, A.N. and Sharp, R.R. Biochim. Biophys. Acta 1986, 851, 369
94. Ford, R.C. and Evans, M.C.W. Biochim. Biophys. Acta 1985, 807, 1
95. Weiss, W. and Renger, G. Biochim. Biophys. Acta 1986, 850, 173
96. Bock, C.H., Gerken, S., Stehlik, D. and Witt, H.T. FEBS Lett. 1988, 227, 141

CHAPTER II

TRANSIENT ABSORPTION SPECTROSCOPY

It has been 42 years since the first spectrometers working in the ultraviolet and visible regions of the spectrum came into general use [1], and over this period they have become an extremely important analytical instrument in many chemical and biological laboratories. Absorption spectrometry is a non-destructive technique and most measurements can be carried out at physiological temperature, this makes it a suitable technique to study biological system. Transient absorption spectroscopy measures the time evolution of the absorbance changes of a system after excitation. It has been widely used to study kinetics of chemical reactions. Rapid development of laser technology has brought the transient absorption spectroscopy to preeminence in studying ultrafast reactions with picosecond or even sub-picosecond time resolution, which no other spectroscopy can match.

Transient absorption spectroscopy has been heavily used in the studies of the electron transfer reactions of photosynthesis. In the experiment, the probe beam is usually kept

very weak so that it will not cause extensive photochemical reaction. The sample is excited by an intense flash of short duration and the absorbance changes after the flash are monitored by the probe beam. The time course of the absorbance changes and its dependence on wavelength provide important information on the electron transfer reactions taking place and the components involved in the reactions.

System Design

Because the transient absorption system is designed specifically for the study of electron transfer reactions in photosynthesis, special considerations must be taken. First, the probe beam power must be kept low enough so that it does not cause significant photochemical reaction; Second, the optical path must be designed in a such way that fluorescence from the sample is blocked from reaching the detector; Third, because the absorbance changes to be detected are small compared with the background, the DC component of the signal must be subtracted out before it can be input into the analog to digital converter.

The original system was built by D. Lillie [2], who interfaced a NICOLET 1074 (Fabri Tek, equipped with an SD-72/2A 9-bit A/D converter and a SW 71A sweep controller; Madison, WI) to a DEC (Digital Equipment Corporation) PDP-11 minicomputer. Because of frequent failure of the hardware and

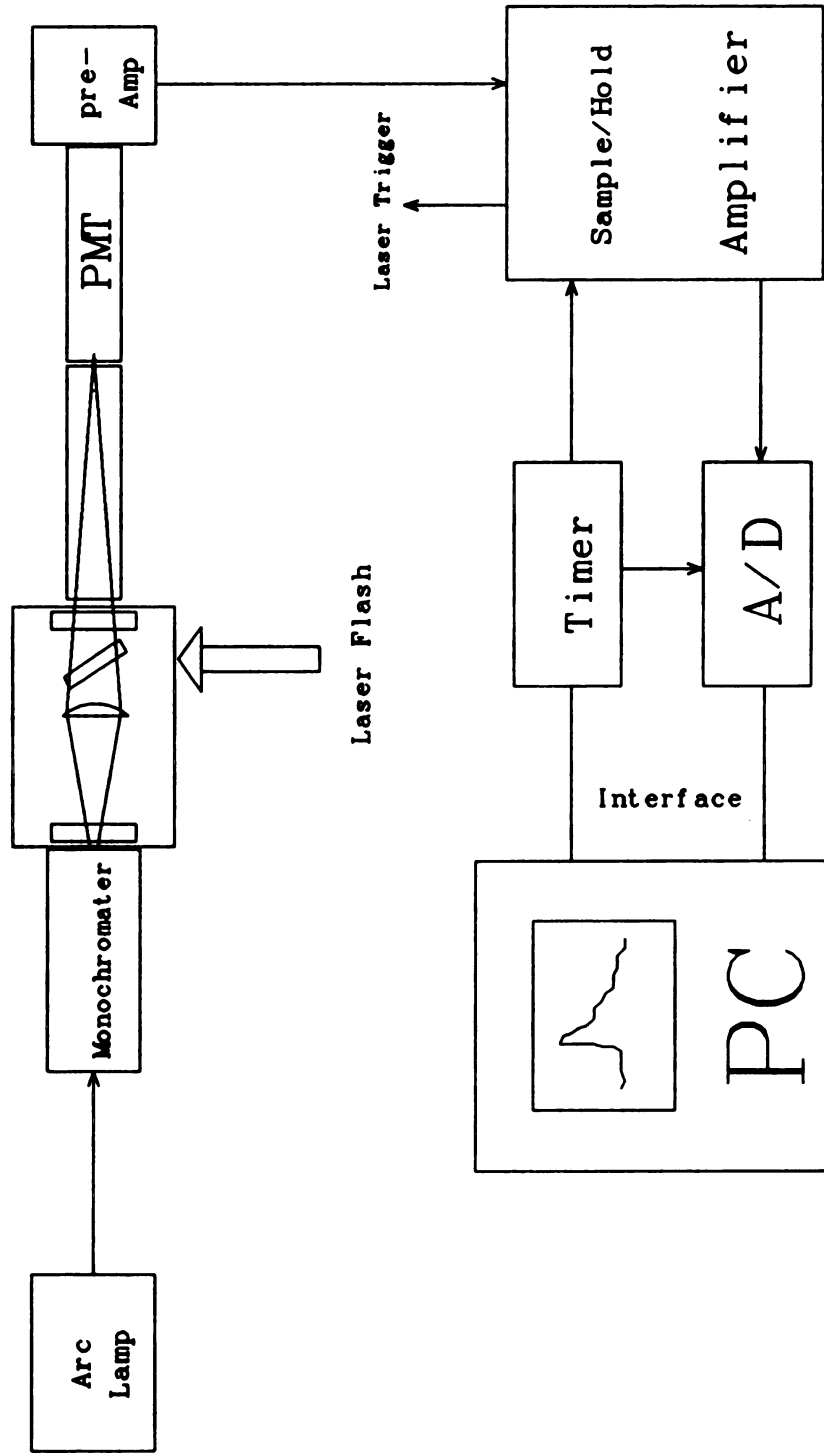


Figure 2-1 Instrument setup.

inconvenience of using the PDP-11 minicomputer to control the instrument, it was rebuilt by me with a new data acquisition board (WAAG-1000 from Marckrich Corp.) and timer board (CTM-05 from Metrabyte Corp.), and interfaced to an IBM/AT compatible Zenith 248 personal computer. This made it possible to integrate the new system with the laser facility located in the chemistry department at Michigan State University.

The system (Figure 2-1) consists of three major subsystems: (1) the optical subsystem, which includes the probe light source, monochromator, silica lens, and cutoff filters; (2) the detecting and signal processing subsystem, which includes the photomultiplier tube, signal pre-amplifier, sample/hold amplifier, and fourth order low pass filter; and (3) the computer interface, which includes analog to digital conversion board, five channel timer board, driver circuit and software interface. The excitation flash is provided by a Nd:YAG pulsed laser (DCR-1 or DCR-2 from Quanta-Ray) at 532 nm (frequency doubled) or at 355 nm (frequency tripled) with a pulse width of about 10 ns. The laser is triggered externally by the computer.

Optical Subsystem

The optical subsystem was built by D. Lillie originally, but modification has been made in the following aspects in order to enhance the instrument performance and reduce the

fluorescence and other interferences: (1) The photomultiplier tube, is moved farther away from the sample cell excitation flash is provided with an extension tube. The distance between the sample and the detector is increased from 4 cm to 40 cm. The probe beam is focused at the detector instead of at the sample and a slit is placed near the detector to limit the solid angle of fluorescence from the sample. This modification reduces the fluorescence interferences and excitation laser flash artifactual effects tremendously, and makes the instrument capable of detecting P^*680 decay in the near infrared region where the sample has very strong fluorescence [3]. (2) The probe beam is defocused at the sample, which reduces the intensity of the probe beam on the sample so that photo-excitation of the sample is not a serious problem. The electronic shutter that was designed to protect the sample from the probe beam is no longer needed. (3) The sample is oriented at about 45 degree to the actinic flash in order to obtain more effective and more uniform excitation.

The modified optical subsystem layout is shown in Figure 2-2. All components are mounted on an optical rail bolted to a heavy length of colorlithe, secured to a laboratory table top. This helps to suppress the noise from environment.

The probe beam light source is provided by a 75 W Xenon Arc Lamp from Photon Technology with a LSP-200 universal power

s
ha
ra
ne
pho
pro
It h
and
grat
with
givin
respec

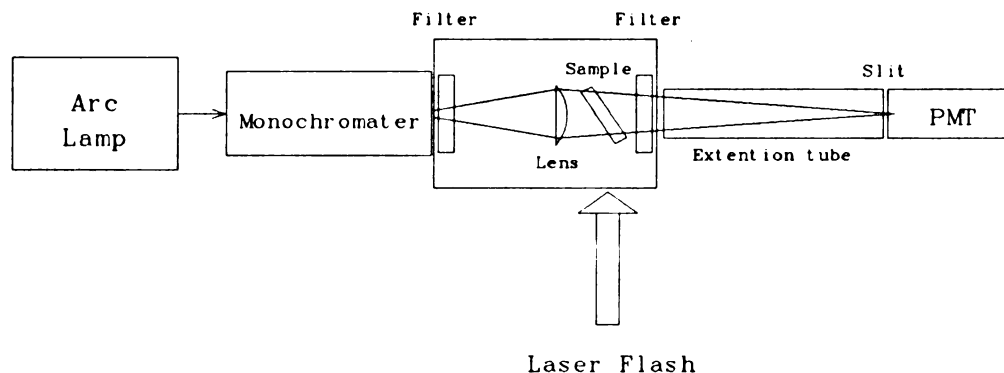


Figure 2-2 Optical layout of the transient absorption spectrometer used in the studies of the electron transfer in PSII (only relative positions are shown).

supply. Though the arc lamp is not as good as a tungsten-halogen lamp in term of signal/noise level, its spectral radiation covers the visible as well as the ultraviolet and near infrared regions, which makes it convenient for studying photosystem II. The wavelength selection of the probe beam is provided by an H-20 UV-VIS monochromator from Instruments SA. It has two ion-etched concave holographic gratings for the UV and the near-IR, as well as a normal concave holographic grating for the UV-VIS region. The monochromator is equipped with fixed interchangeable slits of 0.5, 1.0, and 2.0 mm, giving an optical bandwidth of 2.0, 4.0, and 8.0 nm respectively, which are suitable for transient absorption studies.

The sample compartment consists of a filter holder, sample holder, and a 50 mm diameter silica concave lens with a focal length of 10 cm. The optical filter before the sample is used to prevent second order diffraction from the monochromator from reaching the sample. The filters after the sample are used to cut off the excitation laser flash and fluorescence from the sample which allowing the probe beam to pass through. The sample holder is modified in a such way that the sample can be oriented at any angle between 0 and 90 degree, which makes it possible to optimize the cross section for both probe beam and excitation flash. The long focus UV lens is used to reduce the intensity of the probe beam on the sample and to focus the probe beam farther away from the sample so that the detector can be mounted at a distance of 50 cm from the sample. This arrangement reduces the solid angle of fluorescence from the sample tremendously and makes the interference of fluorescence from the sample insignificant when measurements are made at 820 nm.

A Nd:YAG pulsed laser from Quantum-Ray is used as the excitation source. The 10 ns excitation pulse at 532 nm is generated by frequency doubling the 1064 nm laser radiation in a KDP crystal. The 355 nm pulse can be generated by frequency tripling. The 355 nm exciting pulse is necessary when measurements are made around 550 nm region to monitor the C550 band shift in PSII.

a
s
p

th
ra
on
det
dist

phot
sens
stron
backgr

Detecting and Signal Processing

The detector used in the instrument is a 50 mm diameter photomultiplier tube, 9659QB from EMI. It has 11 venetian blind dynodes and an extended S-20 window. The signal from the PMT is first sent to the pre-amplifier that is located behind the PMT housing. The amplified signal is then sent to the fourth order low pass active filter to filter out high frequency noise and the filtered signal is input to the sample/hold amplifier for further amplification and DC level subtraction. Finally the processed signal is sent to the analog to digital converter for digital processing and data storage. The block diagram for the detecting and signal processing subsystem is shown in Figure 2-3.

The signal to be detected is the change of absorbance of the sample following the actinic flash. It is usually in the range of 0.01% to 0.1%. Because the signal to be detected is on top of a strong background, special considerations of the detecting system must be made so that the signal is not distorted.

The detector used in the instrument is an 11 dynode photomultiplier tube, which has very high gain and sensitivity. Since the signal to be detected comes with a strong background, the PMT can be easily saturated by background radiation. In order to avoid this, the gain of the

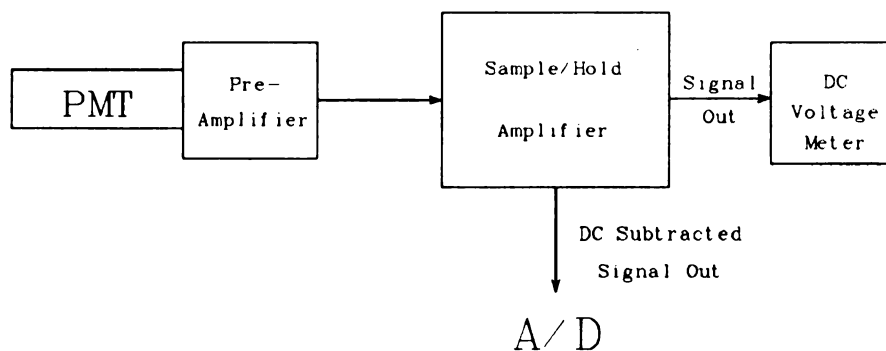


Figure 2-3 The block diagram of the detecting and signal processing subsystem

PMT must be limited to its linear region. At same time, the sensitivity of the PMT must be kept high to detect the small absorbance changes. This is achieved by modifying the wiring of the PMT. A PMT consists of three parts: the cathode, the anode, and the dynode chain. The most important parts in determining the sensitivity of a PMT are the cathode and anode; the dynodes mainly control the gain. One way to limit the gain of a PMT and at same time to keep its high sensitivity is to reduce the number of effective dynodes. Based on the above analysis and different connection trials, the PMT used in the instrument is modified as follows for measurements in the UV and near-IR regions (in the region around 500 nm, the gain of PMT needs to be further reduced in

order to obtain the best signal to noise ratio): the fourth dynode and the fifth dynode are connected together, and the sixth dynode and the seventh dynode are connected together. This modification of the PMT greatly increases the signal to noise ratio and improves the performance of the instrument.

The pre-amplifier is used to boost the signal from the PMT before it is sent to the main amplifier to process. This increases the time response of the PMT and reduces radio frequency pickup. The pre-amplifier is attached to the rear of the PMT housing. The pre-amplifier circuitry is shown in Figure 2-4. It has two stages. The first stage is in the current-follower mode. The second stage is an inverting amplifier that both amplifies the signal and provides offset control.

The signal from the pre-amplifier is sent to a low pass filter, which is a fourth order Chebyshev type active filter [4]. This filter has an adjustable time constant so that no digital sampling is performed on an analog signal containing frequencies higher than the nyquist frequency [5].

The sample/hold amplifier provides user adjustable gain and time constant. It provides an amplifier signal out for DC level readout and as well as a DC subtracted signal for the signal digitizer. The reason for using a sample/hold amplifier instead of normal amplifier is straightforward. The instrument operates in a single beam mode and consequently

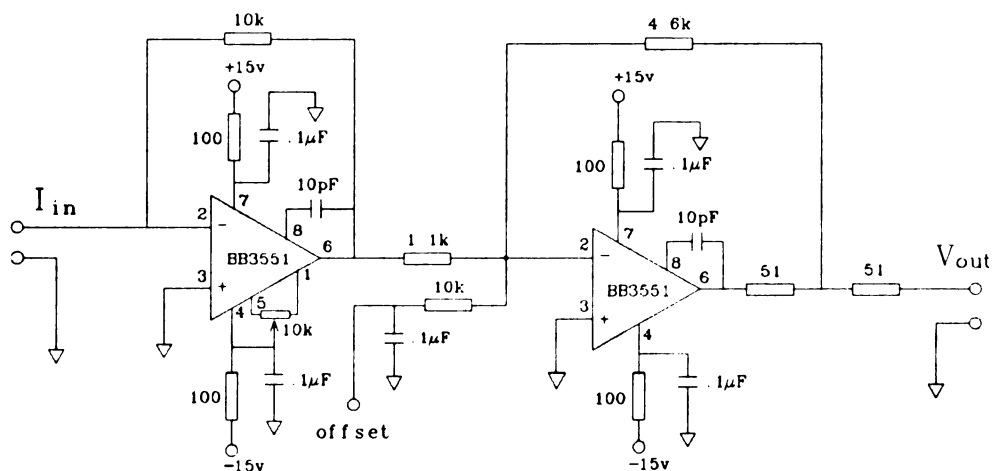


Figure 2-4 Pre-amplifier circuit. I_{in} comes from the PMT anode, V_{out} goes to the fourth order low pass active filter. The offset is controlled from the instrument panel. The operational amplifiers used are Burr Brown 3551 with 50 MHz GBP.

there is significant variation of the output DC voltage level due to fluctuations over time (seconds) in the power supplies of the PMT and the probe source, in changes of the output from the probe beam, component heating, sample distortion, etc. Conventional double beam spectrometers resolve this problem by using a reference sample. In a conventional single beam spectrometer the user has to set the 0%T (transmittance) and 100%T by hand before making a measurement. A single beam transient absorption spectrometer, however, does not allow for readjustment of the 0%T and 100%T before every flash, and the

2
a
c
a
wh
ti
si
of
cin
sub
inv
has
the

analog to digital (A/D) converter has a finite voltage range over which it converts (in our case, the range is -0.64 V to $+0.64\text{ V}$). For optimal use of the digitizing range it is best to have the DC voltage level occur at 0.0 V . The detector amplifier has DC offset control which is set at the beginning of a flash series. However, if slow fluctuations in the DC level are not compensated for, the signal can drift out of the digitization range. This becomes more serious when the signal to be detected is small and comparable with the DC fluctuation level, as in our case. Thus a sample/hold amplifier that compensates the fluctuation automatically is needed.

The sample/hold amplifier circuitry is shown in Figure 2-5. It consists of two major circuits, the conventional amplifier and the DC level subtraction circuit. The conventional amplifier has two stages, the first of which is an inverting amplifier with fixed gain 4.0 and the second of which is an inverting amplifier with user adjustable gain and time constant. The output of the second stage is sent to a signal output driver for DC voltage level readout. The output of the second stage is also sent to the DC level subtraction circuit to subtract out the DC level. The DC level subtraction circuit consists of a sample/hold stage, a signal inverter, and a summing amplifier. The sample/hold amplifier has two external trigger inputs, "sample" and "hold". When the circuit is triggered into the "sample" mode via the

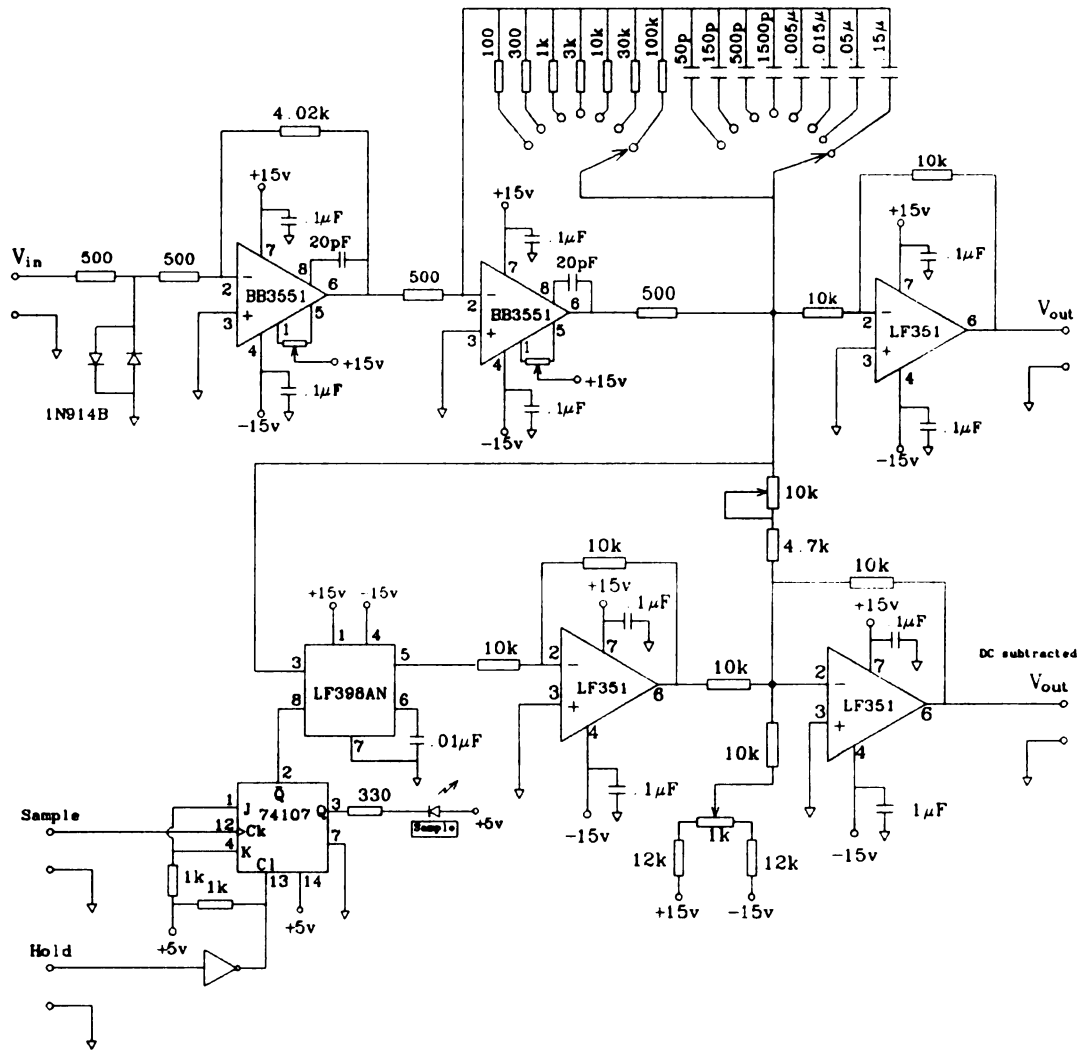


Figure 2-5 The sample/hold amplifier. The two outputs, one is normal output (the upper output) for DC level measurement, another is DC subtracted output (the lower output) for the signal digitizer. Two variable resistors are used to balance the inverted signal.

"sample" trigger input, the sample/hold stage passes the input signal completely, and the signal is then inverted by the inverter and summed with the un-inverted signal for an output of 0.0 V. When the circuit is triggered into the "hold" mode, the DC level at the time of triggering is stored on the capacitor and held on the output line of the sample/hold stage, it is then inverted, and subtracted from the present signal resulting in an output signal centered at 0.0 V DC. The sample/hold amplifier is idling in the "sample" mode, monitoring and compensating the baseline continuously. When the "hold" mode is triggered, it suspends the baseline monitoring and opens a time window for the signal to pass through. Because the time required in making the measurements is usually much shorter than the time scale of the DC level fluctuations, the DC subtracted signal from the sample/hold amplifier is an accurate representation of the input signal minus only the DC level.

Computer Interface

Spectrometers generate and computers use data in fundamentally different ways. In order for them to communicate with each other, it is necessary to create an interface between them to serve as a bridge between the analog world and the digital world. With the data processing power of the computer, the performance of the instrument can be

greatly improved. With the increasing availability of cheap computing power, computers have become essential instrumental component and the computer interface has been a very important aspect of modern instrument development.

The computer interface has two basic tasks: (1) It must ensure that the data generated by an instrument are converted correctly into a form that can be accepted by a computer. (2) It must transmit information between the instrument and the computer that to carry out necessary control functions. In our instrument, these two tasks are performed by two interface boards, a data acquisition board WAAG-1000 from Markenrich Corporation and a timer board CTM-05 from Metrabyte Corporation. The computer used with our instrument interface is an IBM/AT compatible Zenith 248 personal computer that runs at 8.0 MHz. It controls all data acquisition and timing operations, and at same time, functions as a data storage and processing unit. A mathcoprocessor 80287 is installed in the computer to increase the data processing speed.

Data Acquisition

Data acquisition is a process that converts the real world signal into a computer acceptable format and makes it computer accessible. Acquisition requires three tasks, signal conversion, data transfer, and interrupter and control handling. In our instrument these functions are performed by

a WAAG-1000 (Waveform Acquisition and Arbitrary Generator) data acquisition board from Markenrich Corporation. It has a digitization window of -0.64 V to $+0.64\text{ V}$ with 8 bit resolution. The sampling rate can be programmed at 2 KHz, 20 KHz, 200 KHz, 2 MHz, and 20 MHz. The maximum number of data points that can be accumulated is 16,384 with the on board 16 KB ultrafast (45 ns) static RAM (random access memory). The

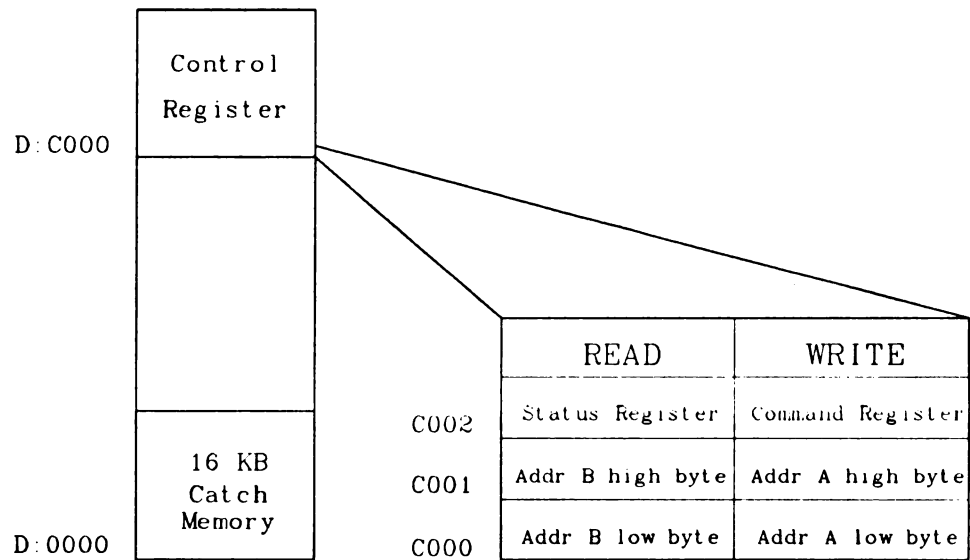


Figure 2-6 The address map of the WAAG-1000 data acquisition board.

board is plugged into an expansion slot in the computer that makes all necessary electronic connections. The board address is set at D0000 of the computer's memory block D and all controls are via the four registers (two 8 bits control registers and two 16 bits address registers) on the board (Figure 2-6).

Data acquisition is achieved by setting the proper parameters (sampling rate, number of data to be collected, trigger signal, and the channel of the input signal) via the command register and then monitoring the data acquisition process via the status register. When data collection is completed, stop the counter and place the on board catch memory that holds the data on the system bus by writing control code into the command register, and then transfer the data from the on board catch memory to the computer base memory.

The command register and the status register are shown in the Table 1 and Table 2 respectively. The data acquisition process can be described in the following eight steps:

1) Place the data acquisition board on system bus

The command register is an 8 bit write only register addressed at D:C002 that selects operating mode, input channel, and sampling rate. The bit 0 controls whether the RAM on the data acquisition

Table 1 Command Register

Bit	High (1)	Low (0)
0	system mode	acquisition mode
1	disable counter	enable counter
2	channel selection	
3		
4	sampling rate selection*	
5		
6		
7	negative trigger	positive trigger

* sampling rate selection

Bit 4	Bit 5	Bit 6	sampling rate
0	0	0	20 MHz
1	0	0	2 MHz
0	1	0	200 KHz
1	1	0	20 KHz
0	0	1	2 KHz

Table 2 **Status Register**

Bit	High (1)	Low (0)
0	data acquisition finished	data acquisition in processing
1	data overflow	non-overflow
2	not triggered	been triggered

board resides in the system bus or locally to the board. This bit is set to 1 to set the board on the system bus.

2) Set data acquisition parameters

Bit 1 of the command register controls the internal address counter and is set to 1 to disable the counter. Bits 2 and 3 control input channel and are set to 00 (binary) to select channel A as input. Bits 4, 5 and 6 control the sampling rate and are set according to the experiment requirement. Bit 7 selects the trigger polarity. It is set to 0 for positive trigger. Thus, writing

0XXX0011 (binary, XXX is the sampling rate set by experiment) into the command register sets input at channel A, positive trigger, desired sampling rate, and disables the internal counter.

3) Select number of data to be collected

The address register A is a write only register addressed at D:C000 (low byte) and D:C001 (high byte), it holds a 14 bit value that determines the number of sampled points desired during data acquisition. The selection of the number of data to be collected is made by writing the appropriate value (to get the correct number of data to be collected, add 257 to the number and complement) into this register.

4) Put the board into data acquisition mode

Setting both bits 0 and 1 to 0 will enable the address counter and put the board into the data acquisition mode.

5) Start the data acquisition process

The data acquisition process is started by triggering the board externally. The trigger signal comes from the timer board.

6) Monitor the data acquisition process

The data acquisition process is monitored by continuously reading the status register located at

D:C002. When the bit 0 goes high, the data acquisition is completed.

7) Place the data acquisition board on system bus

Writing XXXXXX11 into the command register stops the counter and places the data acquisition board on the system bus so that the data on the board is accessible to the computer.

8) Transfer the data into the computer base memory

Once the data acquisition board is placed on the system bus, the data stored on the board's catch memory can be transferred to the computer base memory. When this data transfer process is completed, the next cycle of the data acquisition process can begin.

The data acquisition process is completed after the data are transferred into computer base memory. Once the data are stored in the computer base memory, they can be manipulated in various standard ways. The data manipulation will be discussed in the software design section.

Timing Control

The discrete components of the spectrometer are controlled by the computer via timing signals sent to these components. The timing signals are provided by a timer board, CTM-05 from

Metabyte Corporation. It is a five channel counter-timer, it has five 16 bit up/down counters, a 1 MHz timebase with divider so that the delay of each counter can be set from 1 microsecond to 655.36 seconds. It is plugged into an expansion slot of the computer that provides all necessary electronic connections.

The timing sequences required for the instrument are: (1) Trigger the data acquisition board; (2) Trigger the sample/hold amplifier into hold mode; (3) Trigger the excitation laser flash; (4) Trigger the sample/hold amplifier to the "sample" mode. These four timing sequences are triggered via four of the five channels of the timer, the one channel left is used to trigger an oscilloscope.

The operation of the timer is controlled by its command register, master mode register, and individual counter mode register. It is set to software-triggered one-shot delayed pulse mode without gating. The reason for choosing this operation mode is its simplicity and flexibility. In this mode the delay of all five channels can be programmed independently. This is particular useful when different lasers are used as the excitation source. Since different lasers have different internal delay times, we can accommodate these internal delay differences simply by changing the delay of the laser trigger without changing other timing sequences. The advantages to using the software trigger are twofold.

First, it starts the next cycle as soon as the prior data acquisition process is completed so that the possible conflict between the setting of the repetition rate of the measurements and the computer processing speed is avoided, second, it also saves one channel for other applications.

The measurement is started by sending a trigger pulse to the data acquisition board. After a very short time delay that is determined by the delay of the laser flash trigger, a trigger pulse is sent to the sample/hold amplifier by the computer to set it to the "hold" mode. Then a pulse to trigger the laser initiates the photochemical reactions in PSII. The time course of the absorbance changes is digitized and stored in the catch memory of the data acquisition board. When the data acquisition process is finished, a trigger signal is sent to the sample/hold amplifier to set it to the "sample" mode. After the computer transfers all collected data to its base memory, a software trigger is generated by the computer to start another cycle of measurement.

Software Design

The software is the ultimate user interface that integrates the various hardware interfaces and allows user control of the instrument via the keyboard. The software design for our experiment has to be straightforward, user friendly, easy to understand and easy to modify by users other

than the author in order to accommodate future experimental requirements. Based on these considerations, the software is written in Microsoft QuickBASIC (version 4.0). Basic is the easiest high level language, but it also has excellent device interface and graphics functions that are extremely important for instrument interface software. The problem of the slow execution speed of the BASIC language is resolved by using a compiled version that has execution speed close to the program written in FORTRAN.

The software is designed as two separated programs. One program, TASCII (Transient Absorption Spectrometer Computer Interface), is designed for data acquisition and instrument control. The second program, DTDSP (Data Treatments and Display), is designed for retrieving the data, doing simple data manipulation and format transfer so that the data can be input into other available data manipulation software to do further data manipulation and analysis.

Program TASCII

The program TASCII (Transient Absorption Spectrometer Computer Interface) is a computer interface program that controls data acquisition, timing sequences and the instrument. It consists of three major parts, data acquisition, timing control and graphic display. It is designed in a menu drive manner for easy use.

The program TASCII is started by typing TASCII in the default directory. The experimental parameters, such as wavelength, sampling rate, number of data to be collected, number of averages, laser trigger time delay, PMT voltage, and screen display refresh rate, are input via keyboard. The program first initiates the timer, selects appropriate clock speed for each channel of the timer according to the input time delay, and loads the time delays into the individual counters of each channel. Then the program initiates the data acquisition board and selects the correct sampling rate and number of samples to be collected for the internal counter on the board. Although the hardware sampling rates are limited at 20 MHz, 2 Mhz, 200 KHz, 20 KHz, and 2 KHz, the software sampling rates can be selected at 20 MHz, 10 Mhz, 5 MHz, 2 MHz, 1 MHz, 500 KHz, 200 KHz, 100 KHz, 50 KHz, 20 KHz, 10 KHz, 5 KHz, 2 KHz, 1 KHz, 500 Hz, 200 Hz, 100 Hz, 50 Hz, and 20 Hz. This variety of software selectable sampling rate is achieved by taking every second, every fourth, or every tenth data point out of the data set that has been collected. After these initial setting, the timer is triggered by writing an "arm" command into its command register by the program; the process of data acquisition is performed by a sequence of timing signals sent to the different components of the instrument. The program is designed in a such way that before each measurement, a background scan (with identical setting

except that the laser flash is not triggered) is performed. Background subtracted data is stored in the computer. In order to increase the processing speed, the data are summed with the data collected on previous scans instead of real time averaging during the data acquisition process. The data are averaged only when they are saved to the disk.

The program allows interrupts to the data acquisition process; the process may be resumed after necessary instrument adjustments. The graphic display routine allows real time display of the digitized signal. A portion of the display can be enlarged for a closer look by using the View or Window commands. The refresh of the screen display can be programmed for any number of scans, which is useful if the high repetition rate is needed. The data are saved in terms of signal amplitude (DC level subtracted signal) in voltage, together with other parameters such as DC level of the signal, sampling rate, number of data, etc..

Program DTDSP

The program DTDSP is designed for retrieving the data that are saved by program TASCII and translating the data into absorbance units according to the following equation:

$$\begin{aligned} A &= -\log(T) = -\log(\Phi/\Phi_0) \\ &= -\log(V/V_0) \end{aligned}$$

$$\begin{aligned}
\Delta A &= A' - A = -\log(V'/V_0) - (-\log(V/V_0)) \\
&= -\log(V'/V_0) + \log(V/V_0) \\
&= -\log(V'/V) = -\log((V+\Delta V)/V) \\
&= -\log(1 + \Delta V/DC)
\end{aligned}$$

The program reads the desired data file from the disk and transfers the raw data (the data are saved as the signal amplitude in voltage and the DC level) into absorbance according to the above equation automatically. The program consists of data display, data manipulation, format transfer and print routines. The print routine is performed by DOS function call, it does not have its own printer driver. In most cases it is more convenient to use commercially available graphic package to obtain hard copies. The display routine is similar to that in the program TASCII, a portion of the spectrum can be zoomed in or out by using View or Window commands. The data manipulation routine has the capability to perform subtraction and digital filtering (a data smooth method that has similar results as a low pass filter). The format transfer routines consist of three subroutines for three different programs. It has a subroutine for OLIS KFIT program (a kinetic fit program from On-Line-Instrument System, Inc.) to perform kinetic fit and analysis, it has the second subroutine for program PLOTIT (an integrate graphic package with many data manipulation functions and output supports) to

use its plot driver to get high resolution hard copies, it has the third subroutine for using program PFF on PDP-11 minicomputer that has spectrum manipulation capability.

Although the program can do simple data analysis and manipulation, it is not designed to perform complex data analysis and manipulation rather than as an intermediate to the commerce available software. The program is written in such a way that it can be easily modified to accommodate any new software package.

References

1. Knowles, A. and Burgess, C. in Practical Absorption Spectrometry 1984, Chapman and Hall
2. Lillie, D. Ph.D. Dissertation 1989, Michigan State University
3. Van Best, J.A. and Mathis, P Biochim. Biophys. Acta 1978, 503, 178
4. Johnson, D.E. and Hilburn, J.L. in Rapid Practical Designs of Active Filters 1975, page 6, John Wiley & Sons, Inc.
5. Malmstadt, H.V., Enke, C.G. and Crouch, S.R. in Electronics and Instrumentation for Scientists 1981, Benjamin/Cummings Publishing Company, Inc.

CHAPTER III

THE CHARGE RECOMBINATION REACTIONS OF THE CHARGE SEPARATED STATE Q_A^-/P^+680

Introduction

The photochemical reaction of photosystem II in higher plants, which begins with the excitation of the reaction center chlorophyll P680 [1,2] by light, induces a series of electron transfer reactions that leads to the reduction of a plastoquinone molecule and water oxidation. Transient absorption spectroscopy shows that a charge separated state between the reaction center P680 and the first stable acceptor, a strongly bounded plastoquinone molecule, Q_A is created within 300 ps following visible excitation [3-6]. The relatively slow recombination reactions between the charge separated species allow forward, charge-conserving electron transfer reactions to compete effectively and accounts for the near unit quantum efficiency with which PSII operates. Under oxygen-evolving conditions the most rapid redox reaction that occurs after the creation of the state Q_A^-/P^+680 is the reduction of P^+680 by the tyrosine donor Y_2 , which occurs in the nanosecond time range [8]. The rate of this reaction, as

we

in

re

ma

va

pl

tr

un

in

sp

di

an

sp

fo

in

re

co

pe

wi

an

de

tu

fla

sin

well as that of the somewhat slower reoxidation of Q_A^- , is influenced by a variety of factors, such as the biochemical resolution of the preparation [7], oxidation state of the manganese cluster [8-12], pH value of the buffer [13-15], valence state of the non heme iron Fe^{+2} [16,17], state of the plastoquinone acceptor site [18,19], and various inhibitory treatments [20,21].

The time evolution of the charge separated state Q_A^-/P^+680 under different conditions and treatments has been studied intensively during the last decade by transient absorption spectroscopy and time resolved EPR techniques. The first direct measurements of the P^+680 decay was made by Van Best and Mathis in 1978 by using the transient absorption spectroscopy technique with nanosecond time resolution. They found that P^+680 was reduced with a half time of 25 to 45 ns in untreated, dark-adapted chloroplasts and attributed this reduction to an electron donor between the oxygen evolution complex and the reaction center P^+680 [22]. Further studies performed by Schlodder, Brettel and coworkers [8,23] in 1984, with photosystem II preparations instead of chloroplasts and an improved instrument, showed that the P^+680 reduction depended strongly on flash number in a series of single turnover flashes given to the dark adapted samples, and the flash number dependence behavior of the P^+680 reduction was similar to that of the S state transitions with the

characteristic period four oscillation. The half times of the P^+680 reduction obtained in their experiment were 23 ns (monophasic) for the S_0 and S_1 states, 50 ns and 260 ns (biphasic) for the S_2 and S_3 states. The retardation of the P^+680 reduction in the higher S states was explained in terms of Coulomb attraction by a positive charged oxygen evolving complex on the primary donor Y_2 . The recent results from Gerken and coworkers [9,18] supported the argument that the P^+680 was reduced by the donor Y_2 directly.

The charge separated state Q_A^-/P^+680 is sensitive to various treatments that inhibit oxygen evolution. Völker and coworkers [13,21] studied P^+680 reduction with trypsin treated PSII and found, after trypsin treatment at pH 6.0, a slow phase with a halftime of 200 μ s that appeared as the nanosecond phase decreased. The retardation of the P^+680 reduction with trypsin treatment could be restored by $CaCl_2$ addition. They claimed that the trypsin treatment induced structural modification of the PSII donor side [24,25] that affects the electron transfer rate between the manganese cluster and Y_2^+ , as well as between Y_2 and P^+680 , and that this modification could be functionally compensated to a significant extent by the specific action of Ca^{2+} cations.

The state Q_A^-/P^+680 is also stabilized when the three extrinsic polypeptides and manganese are released by tris(hydroxymethyl)aminomethane washing [26,27]. The

nanosecond phases in $P^{+}680$ reduction in untreated preparations are replaced by microsecond components in tris-washed PSII [28]. The $P^{+}680$ lifetime ranges from 2 μ s at pH 8.0 to 40 μ s at pH 4.0 and is determined by its direct reduction by Y_2 [12-14,28]. If the charge separated state $Q_A^{-}/P^{+}680$ is created when the primary donor Y_2 is still in its oxidized state Y_2^{+} , $Q_A^{-}/P^{+}680$ decays by direct charge recombination between Q_A^{-} and $P^{+}680$. The halftime of the charge recombination has been measured by several laboratories, the results range from 80 μ s to 800 μ s depending on the preparations [11,29-31].

Hydroxylamine, NH_2OH , has been known to be an inhibitor to donor side electron transfer in PSII for some time, though the inhibition site is not clear yet [32]. NH_2OH treatment inhibits water oxidation and electron transfer from Y_2 to $P^{+}680$ [33]. $Q_A^{-}/P^{+}680$ decays mainly via the charge recombination under millimolar NH_2OH treatment and repetitive flash excitation. The kinetics of the $Q_A^{-}/P^{+}680$ recombination with NH_2OH treated PSII has been studied by both optical and EPR techniques [11,19,28,33-36]; the halftimes range between 150 μ s and 800 μ s. The wide range of the charge recombination rate was explained by Ford and Evans in terms of different charge states of the donor and acceptor side of PSII [19]. Further studies of NH_2OH inhibition on PSII electron transfer showed that the inhibition is complex and that at least two inhibiting sites were involved [11,19,37-39].

1

r

I

a

t

w

tr

an

ra

mo

acc

Recent work reported by Hoganson and Babcock [35] explored the Q_A^-/P^+680 recombination reaction in tris-washed, in NH_2OH treated, and in salt-washed photosystem II membrane particles by time resolved EPR. They showed that the rate of the recombination reaction varied in these preparations and was more rapid in the salt-washed system, in which both the 33 KDa polypeptide and the manganese ions associated with the water splitting complex are retained. These components are removed in the other two classes of preparations. They also monitored the EPR linewidth of P^+680 and observed a narrower signal when Y_2 was maintained in its reduced, diamagnetic state by NH_2OH treatment than when Y_2^+ was present concurrently with P^+680 . From this observation, a distance of $\sim 12 \text{ \AA}$ between Y_2 and $P680$ was estimated.

Despite these efforts in characterizing the recombination reaction, a number of important questions remain unresolved. In the experiments described here we have used transient absorption spectroscopic techniques (described in chapter II) to monitor the decay of the charge separated state Q_A^-/P^+680 with tris-washed PSII, NaCl washed PSII, and NH_2OH treated tris-PSII. P^+680 decay and Q_A^- decay were detected at 820 nm and 325 nm, respectively, with different flash repetition rates. The pheophytin band shift induced by Q_A^- was also monitored in order to obtain a better understanding of acceptor side effects.

s

2

a

We

pr

ho

The

RC-

fir

(g=7

proc

throu

disca

(g=77

mediu

MES, P

Materials and Methods

Photosystem II Membrane Preparation

Photosystem II membranes were prepared from spinach according to the method described by Berthold et al.[40] with some modifications [41]. Spinach obtained from the supermarket was depetiolated and washed in cold distilled water. All operations were performed at 4°C unless stated otherwise. The spinach was broken in a Waring blender for 30 seconds in a buffer solution of 0.4 M NaCl, 20 mM HEPES, 2.0 mM MgCl₂, 1.0 mM ethylenediamine tetraacetic acid (EDTA), and 2 mg/ml bovine serum albumin, pH 7.5. About 250 ml buffer was used for every 300 gram of spinach. The whole preparation process was performed under low light conditions. The homogenate was filtered through eight layers of cheese cloth. The filtrate was then poured into centrifuge tubes (RC-5 or RC-5B with SS-34 Sorvall rotor) for centrifugation. In the first step the centrifuge was allowed to reach to 2000 rpm (g=750) and then braked to a stop. This first centrifuge process removed any large unbroken spinach that had passed through the cheese cloth filtration. The pellets were discarded, and the supernatant was centrifuged at 8000 rpm (g=7700) for 10 minutes. The pellets were resuspended in a medium consisting of 0.15 M NaCl, 0.4 mM MgCl₂, and 20.0 mM MES, pH 6.0. This suspension was centrifuged again at 8000

rpm ($g=7700$) for 10 minutes. The pellets were collected and resuspended in a small volume of the buffer solution containing 50.0 mM MES, 15.0 mM NaCl, 5.0 mM $MgCl_2$, and 1.0 mM ascorbic acid, pH 6.0. The chlorophyll concentration of the suspension was determined according to the Sun and Sauer method [42]. Triton detergent solution, made by mixing 25 ml Triton-X100 with 75 ml buffer solution consisting of 50.0 mM MES, 15.0 mM NaCl, 5.0 mM $MgCl_2$, and 1.0 mM ascorbic acid at pH 6.0, was added dropwise in the dark to this suspension so that a final chlorophyll concentration of 2 mg/ml and a Triton-X100 to chlorophyll ratio of 35 mg to 1 mg resulted. After the addition of the Triton-X100 solution, the sample solution was incubated and stirred slowly in an ice bucket in the dark for 30 minutes.

After the incubation with Triton-X100, the sample solution was centrifuged at 3000 rpm ($g=1086$) for about 1 minute to remove starch granules. Then the supernatant was centrifuged at 20000 rpm ($g=48246$) for 30 minutes. The pellets were resuspended in an SMN buffer that consisted of 0.4 M Sucrose, 50.0 mM MES, 15.0 mM NaCl, pH 6.0. The suspension was centrifuged again at 20000 rpm ($g=48246$) for 30 minutes. The pellets were collected and dissolved in a small amount of SMN buffer solution for storage. The final chlorophyll concentration of the PSII membrane preparation was usually between 2.0 and 3.5 mg/ml.

i
c
et
in
co
li
was
pel
aga
diss
stor

The oxygen evolution activity was measured with a Clark-type oxygen electrode at room temperature in a buffer containing 20.0 mM MES, 50.0 mM NaCl, and 5.0 mM MgCl_2 (pH 6.0). 2.5 mM $\text{K}_3\text{Fe}(\text{CN})_6$ and/or 250 μM DCBQ were added as electron acceptors. The rates of oxygen evolution varied between 500 and 1000 μmol of O_2 (per mg of Chl)/hr, typical rates were about 800 μmol of O_2 (per mg of Chl)/hr. The contamination from photosystem I was less than 5% in these preparations as determined by EPR [36,40], which allows us to neglect contributions from the photosystem I in the optical measurements.

Tris Treatment

Tris inactivation of PSII membranes was performed by incubating the preparation described above in a solution containing 0.8 M tris(hydroxymethyl)aminomethane and 0.5 mM ethylenediamine tetraacetic acid (EDTA) at pH 8.0. The incubation process was carried out at a chlorophyll concentration of 0.5 mg/ml at 0°C for 20 minutes under room light. After the 20 minutes incubation, the sample solution was centrifuged at 20000 rpm ($g=48246$) for 30 minutes. The pellets were resuspended in the SMN buffer and centrifuged again at 20000 rpm ($g=48246$) for 30 minutes. The pellets were dissolved in a small amount of SMN buffer solution for storage.

A

N

de

pr

50

pro

mg/

samp

minu

cent

pell

N

and e

few t

the m

restor

Tris treatment releases the 33 KDa, 23 KDa, and 17 KDa polypeptides and manganese from the PSII membrane preparations. Thus after tris treatment, the oxygen evolving activity is totally destroyed and leaves Y_2 as the terminal electron carrier on the donor side of PSII. In addition to the oxygen evolving capacity, tris treatment also removes most of the residual PSI activity [44], and possibly some plastoquinones.

NaCl Treatment

The NaCl washing was carried out according to the method described by Ghanotakis et al. [41]. The PSII membrane preparations described above were incubated in 2.0 M NaCl, 50 mM Mes, 5 mM $MgCl_2$ solution at pH 6.0. The incubation process was carried out at a chlorophyll concentration of 1.0 mg/ml at 0°C for 1 hour in dark. After the incubation, the sample solution was centrifuged at 20000 rpm ($g=48246$) for 30 minutes. The pellets were resuspended in the SMN buffer and centrifuged again at 20000 rpm ($g=48246$) for 30 minutes. The pellets were stored in a small amount of SMN buffer solution.

NaCl washing removes the 23 KDa and 17 KDa polypeptides and electron transfer on the donor side is inhibited after a few turnovers [41]. However, NaCl washing does not destroy the manganese cluster; oxygen evolution activity can be restored by addition of Ca^{+2} [52,53].

r
e
r
t
i
fe
Fe
op
30
our

Mea

conc

Hydroxylamine Treatment

Hydroxylamine treatment was performed about 5 to 10 minutes before the measurements were began. After 2.5 mM $K_3Fe(CN)_6$ and $K_4Fe(CN)_6$ were added to the tris-washed PSII membrane preparations at a chlorophyll concentration of 200 $\mu g/ml$, 2.0 mM NH_2OH was added to the sample solution. Each NH_2OH treated sample was put into a 0.1 cm optical path length cuvette and given 60-80 laser flashes ($\lambda=532$ nm, FWHM \approx 10 ns, $W\approx$ 2 mJ/per pulse) before the measurement was taken. The light requirement of NH_2OH inactivation has been reported by several laboratories [13,19,33]. In our experiments, we found that it gave us better NH_2OH inhibition results to use a pre-flash sequence as the light source for the NH_2OH inactivation rather than continuous projector lamp illumination. The chemical reaction between NH_2OH and the ferri/ferrocyanide system is slow, producing about 10% Fe^{+2}/Fe^{+3} concentration change in 30 minutes. Because our optical measurements were completed in most cases in less than 30 minutes, this reaction does not have significant effects on our results.

Measurement Conditions

The optical measurements were performed with a chlorophyll concentration of approximately 200 $\mu g/ml$ in a buffer solution

consisting of 0.4 M Sucrose, 50.0 mM MES, 15.0 mM NaCl, pH 6.0. The chlorophyll concentration was higher for the C-550 bandshift measurements because of the low sample absorption in that region. The experiments were carried out on the transient absorption spectrometer described in chapter II. The sample cell used was a 0.1 cm optical path quartz cuvette which gave an effective optical path length of 0.14 cm when it was oriented at 45 degree relative to the probe beam. The slit used with the monochromator was 1.0 mm for the measurements at 325 nm, which gave a spectral resolution of 4.0 nm. For the measurements at 820 nm, a larger slit width, 2.0 mm, was used, which gave a spectrum resolution of 8.0 nm, since at this wavelength the excitation of the sample by the probe beam is not significant. Moreover, because P⁺680 has a broad absorbance increase around 820 nm, using of larger slit width improves the signal to noise ratio. A smaller slit width, 0.5 mm, which gave a spectral resolution of 2.0 nm, was used for the measurements of the C-550 bandshift in order to increase the spectrum resolution and to avoid excitation of the samples by the probe beam. Three glass filters (U340 for the measurements at 325 nm and IR80 for the measurements at 820 nm, the filters were from Hoya Corp.) were used, one behind the monochromator to block the secondary diffraction from the monochromator and two in front of the PMT to protect it from the excitation laser flash. For the C-550 bandshift

measurements, two broad band interference filters centered at 550 nm (from Oriel Corp.) were placed in front the PMT and a glass filter (BG-18) was placed behind the monochromator. The instrument time constants used was 5 μ s for microsecond scans and 1 ms for the millisecond scans. The excitation flash was provided by a Quanta Ray Nd:YAG laser, DCR-1A or DCR-2A, which has a pulse width (FWHM) of about 10 ns. The wavelengths of the excitation flash was 532 nm for the measurements made at 325 nm and 820 nm. For the C-550 bandshift measurements, the excitation flash was at 355 nm.

For the evaluation of the kinetic parameters, the data were fit by means of the least squares method by using the kinetics fit program KFIT from OLSI. All measurements were performed at room temperature.

Results

Excitation Saturation Profile

The saturation behavior of the flash induced absorption changes at 325 nm was measured with tris-washed PSII. The wavelength of the excitation flash was 532 nm and the Chl concentration of the sample was 186 μ g/ml. The flash energy was modified with neutral density filters. The amplitudes of the absorption changes at 325 nm induced is shown in Figure 3-1 as a function of the excitation flash energy. The data

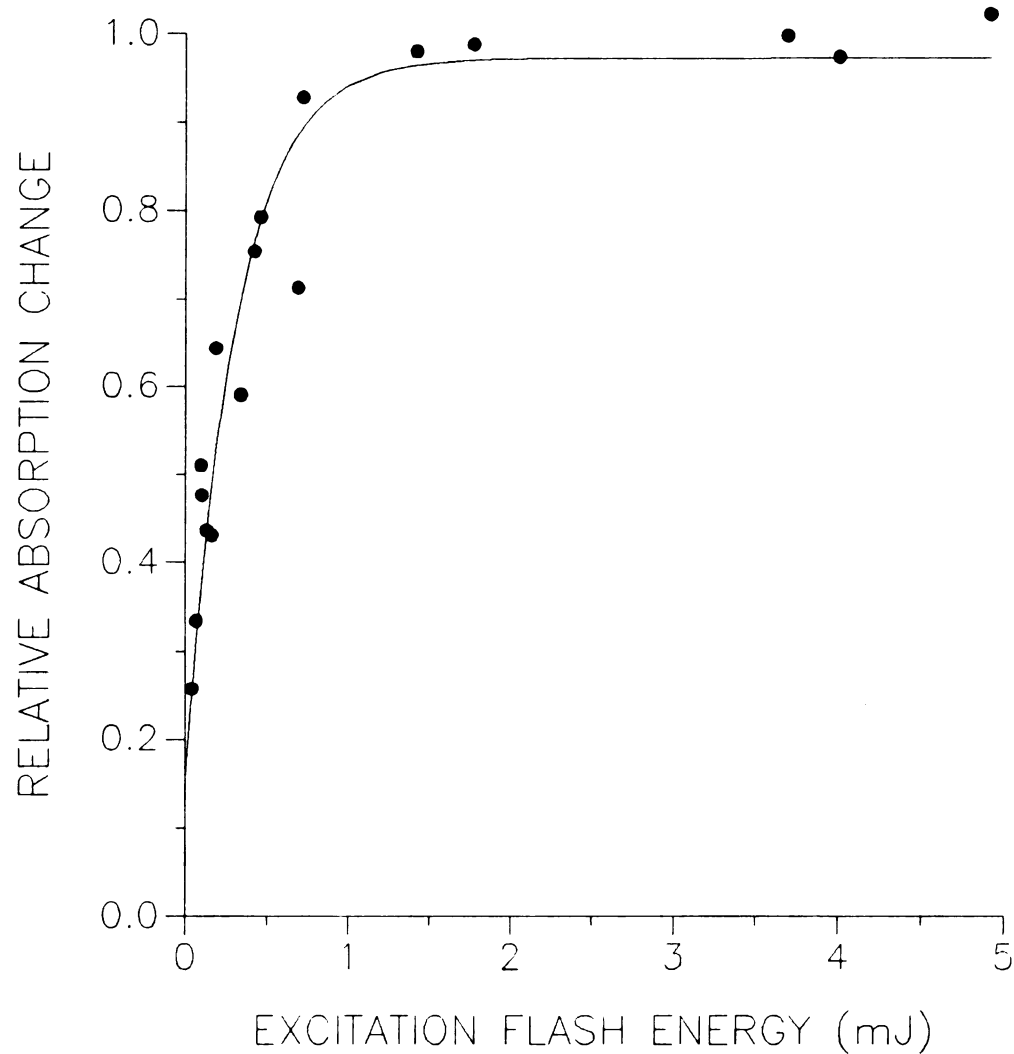


Figure 3-1 Amplitude of the absorption changes at 325 nm as a function of the excitation flash energy in tris-washed PSII. [Chl]=196 $\mu\text{g/ml}$, optical path=0.14 cm, 2.5 mM $\text{K}_3\text{Fe}(\text{CN})_6$ and $\text{K}_4\text{Fe}(\text{CN})_6$ were added as the electron acceptor system.

were fit according to the following equation [23]:

$$\text{relative absorption change} = 1 - e^{-\delta I}$$

with I = energy (per cm^2) of the laser flash and δ = effective optical cross section for the P680 photo-oxidation at 532 nm. The curve shows a 50% saturation at the excitation flash energy of 0.33 mJ per flash, this corresponds to about 4 photons per reaction center of PSII. The effective optical cross section calculated from the 50% saturation energy is about $1.2 \times 10^{-15} \text{ cm}^2/\text{J}$.

Q_A^-/P^+680 Recombination in Tris-PSII

The charge recombination of Q_A^-/P^+680 was observed in the microsecond range with tris-washed PSII under high repetition rate of the excitation laser flash. Under these conditions, the physiological electron source on the donor side of the PSII is destroyed and Y_2 becomes the terminal electron carrier on the donor side of the PSII. When high flash repetition rate is applied, most of the Y_2 remains oxidized prior to the excitation of the reaction center P680. In this case, the oxidized reaction center P^+680 can not be reduced by its physiological donor Y_2 fast enough to compete with the charge recombination process. Consequently, the lifetime of P^+680 is extended into the hundreds of microseconds range and

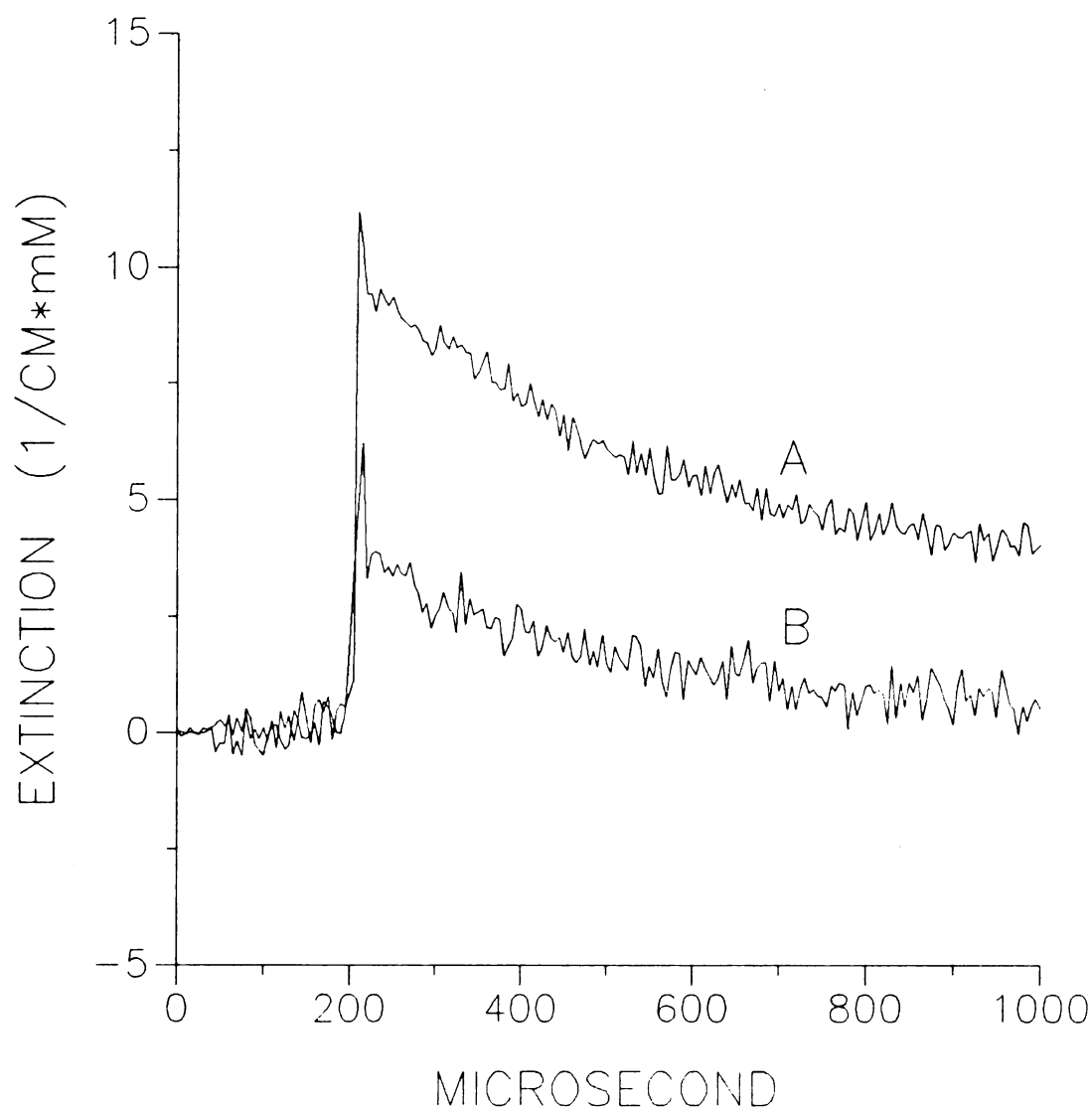


Figure 3-2 Microsecond time courses of the absorption changes at 325 nm (trace A) and 820 nm (trace B) with tris-washed PSII. [Chl]=215.7 $\mu\text{g/ml}$, optical path=0.14 cm, excitation flash repetition rate 5.8 Hz. 2.5 mM $\text{Fe}(\text{CN})_6^{-3}/\text{Fe}(\text{CN})_6^{-2}$ were added as the electron acceptor system. The transient in the first few μs was unreliable because of flash artifacts.

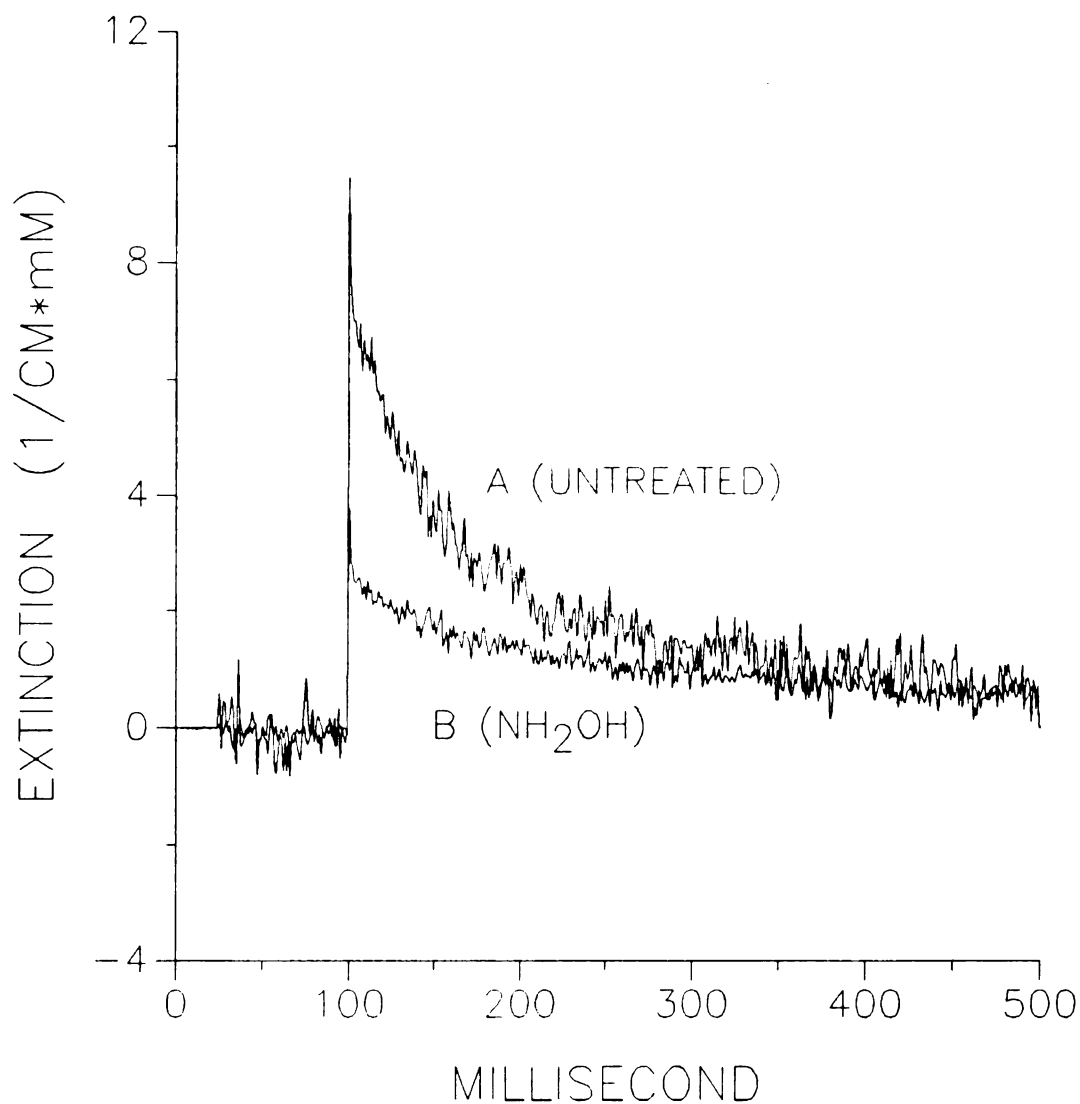


Figure 3-3 Millisecond time courses of the absorption changes at 325 nm with tris-washed PSII (trace A) and NH_2OH treated tris-PSII (trace B). $[\text{Chl}] = 215.3 \mu\text{g/ml}$, optical path = 0.14 cm, the time between the excitation flashes was 1.98 second. $2.5 \text{ mM } \text{Fe}(\text{CN})_6^{-3}/\text{Fe}(\text{CN})_6^{-2}$ were added as the electron acceptor system. The transient in the first few μs was unreliable because of flash artifacts.

e
a
i
o
t
2
w
o
r
A
tl
Q
o
re
re
ti
in
Fo
of
be
es
in
ab
re

determined by the rate of the charge recombination.

Figure 3-2 and Figure 3-3 shows the kinetic traces of the absorption changes at 820 nm and 325 nm in the microsecond and in the millisecond time scales, which represent Q_A^- and P^+680 decays, respectively. The P^+680 (trace B in Figure 3-2) in the microsecond scan shows monophasic decay with a halftime of $226 \pm 27 \mu s$, whereas the Q_A^- (trace A) shows a biphasic decay with halftimes of $223 \pm 11 \mu s$ and $45 \pm 1 ms$. The amplitudes of both P^+680 and Q_A^- depend strongly on the flash repetition rate, this is shown in Figure 3-4 (trace A) and Figure 3-5. At low flash repetition rate, the P^+680 amplitude is small on the tens of microseconds time scale (Figure 3-4, trace A), and Q_A^- decays mainly in the millisecond time range. More than 80% of the Q_A^- decays in the millisecond time scale at a flash repetition rate of 1.2 Hz. Upon increasing the flash repetition rate, P^+680 becomes observable in the microsecond time range, and at the same time, the microsecond Q_A^- phase is increased at the expense of its millisecond phase decay. Following Haveman and Mathis [54], we attribute the appearance of Q_A^-/P^+680 recombination to those centers in which Y_2^+ has not been reduced in the time between flashes. From Figure 3-4, we estimate that the halftime for Y_2^+ reduction by ferrocyanide in tris-washed PSII is approximately 300 ms. This reaction is about 40 times faster than is observed for the $Y_2^+/\text{ferrocyanide}$ reaction in tris-washed chloroplasts [55], which may reflect

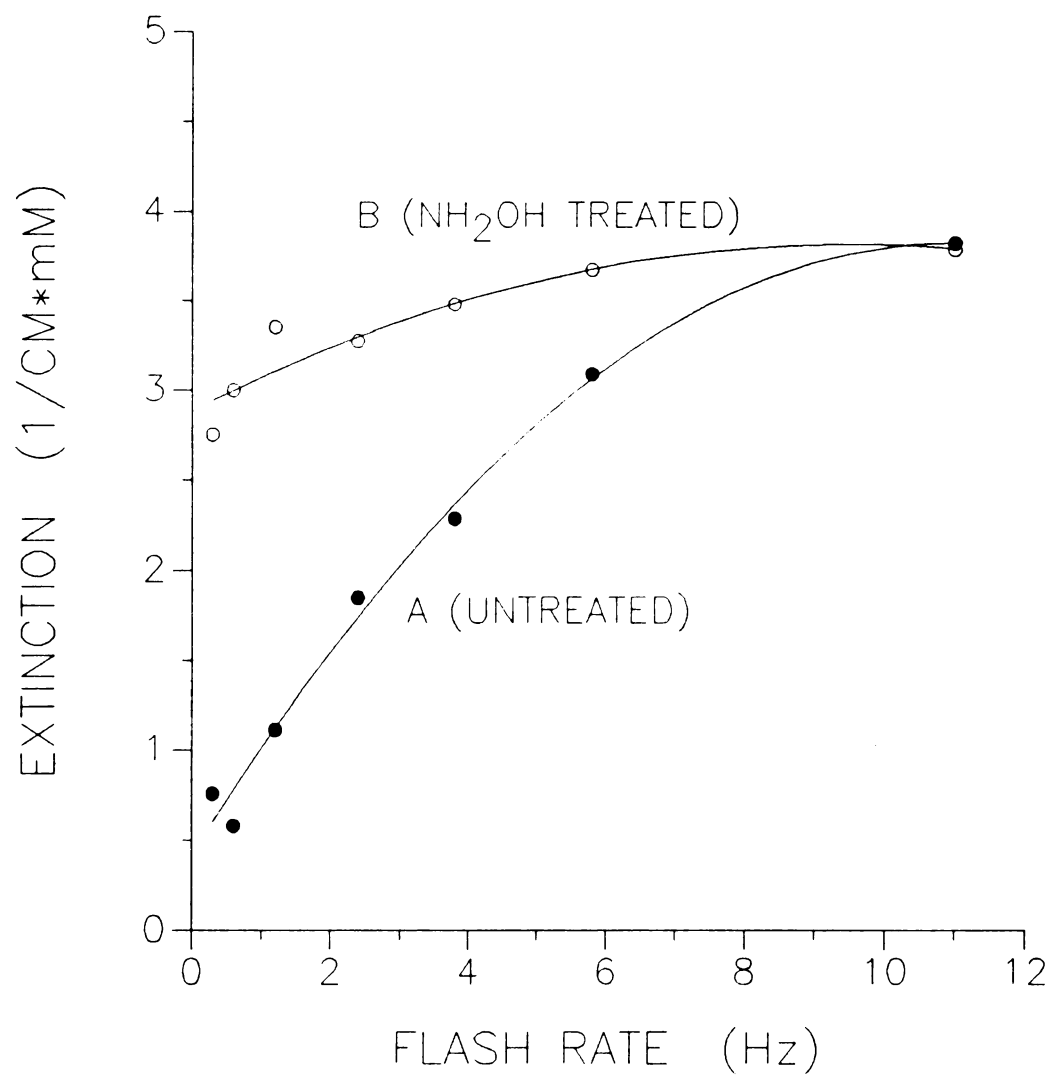


Figure 3-4 The dependence of the absorption changes at 820 nm on the flash repetition rate. Trace A is tris-washed PSII, trace B is NH₂OH treated tris-PSII.

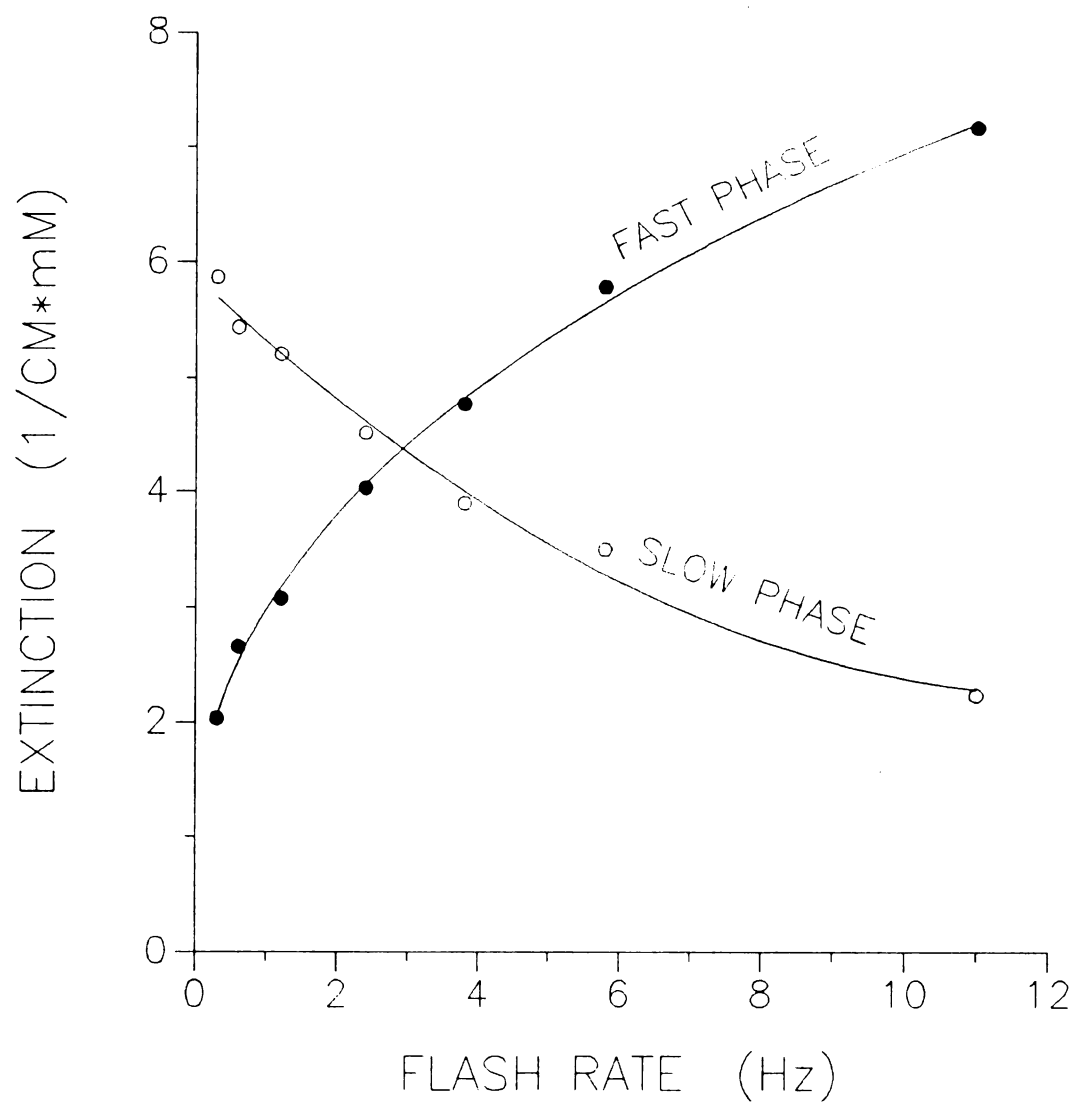


Figure 3-5 The dependence of the absorption changes at 325 nm on the flash repetition rate in tris-washed PSII.

the greatly reduced diffusion barrier to the external reductants in the resolved PSII preparation.

The extinction coefficient for P680 at 820 nm has not been defined precisely, the reported value has a range of 4.2 to 7.0 $\text{mM}^{-1}\text{cm}^{-1}$ [11,23]. The measurements we performed at 325 nm and 820 nm allowed us to calibrate the extinction coefficient of P680 at 820 nm against the better defined value of Q_A . Knowing the percentage of the Q_A^- that undergoes recombination with P^+680 , 63% at excitation repetition rate of 5.8 Hz, and the extinction coefficient of Q_A , 13.0 $\text{mM}^{-1}\text{cm}^{-1}$ at 325 nm, we obtained an extinction coefficient for P680 at 820 nm of $6.6 \pm 0.3 \text{ mM}^{-1}\text{cm}^{-1}$.

Q_A^-/P^+680 Recombination in NaCl Washed PSII

Without addition of Ca^{2+} , NaCl washed PSII membrane fragments are unable to carry out the normal electron transfer reactions that result in oxygen evolution [52,53]. Under repetitive excitations, electron transfer on the donor side of PSII in NaCl washed PSII is retarded and charge recombination between Q_A^- and P^+680 occurs. Figure 3-6 shows the microsecond decay traces of Q_A^- and P^+680 in NaCl washed PSII. The decay is similar to that in tris-washed PSII except that it is somewhat faster. By fitting the data, we obtained decay halftimes of $125 \pm 6 \mu\text{s}$ for Q_A^- (fast phase), and $138 \pm 9 \mu\text{s}$ for P^+680 .

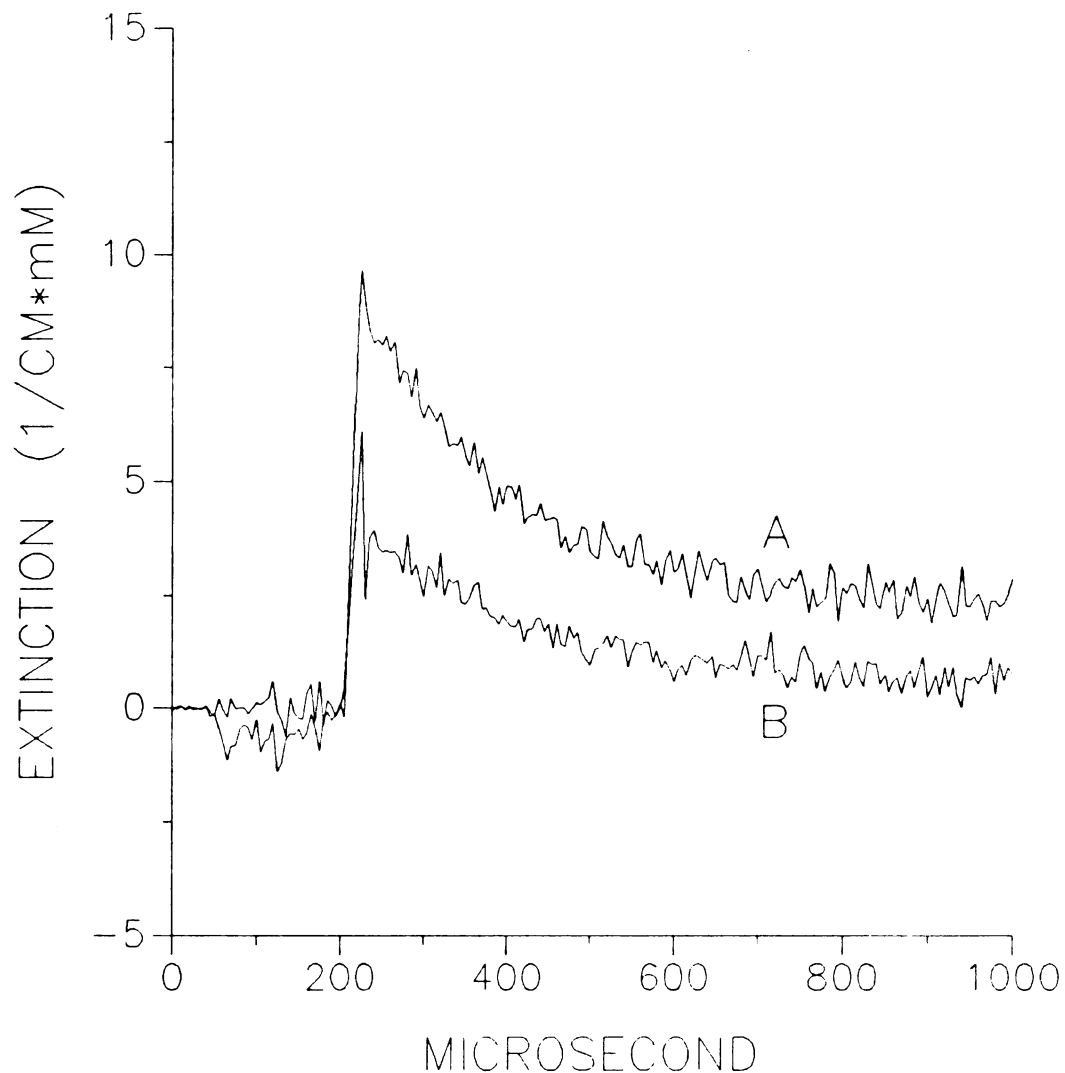


Figure 3-6 Microsecond time courses of the absorption changes at 325 nm (trace A) and 820 nm (trace B) in NaCl washed PSII. [Chl]=214.1 $\mu\text{g/ml}$, optical path=0.14 cm, excitation flash repetition rate 5.8 Hz. 2.5 mM $\text{Fe(CN)}_6^{-3}/\text{Fe(CN)}_6^{-2}$ were added as the electron acceptor system. The transient in the first few μs was unreliable because of flash artifacts.

Q_A^-/P^+680 Recombination in NH_2OH Treated Tris-PSII

NH_2OH treatments of PSII have been reported to inhibit water oxidation and electron transfer from Y_2 to P^+680 [19,33,34]. When electron transfer in PSII is inhibited, the decay of the charge separated state Q_A^-/P^+680 occurs primarily by charge recombination. The absorption changes following the excitation with NH_2OH treated tris-PSII are shown in Figure 3-7 and Figure 3-3 (trace B). The P^+680 decay was fit to a halftime of $236 \pm 24 \mu s$. Q_A^- decays in a biphasic manner with halftimes of $240 \pm 12 \mu s$ and $80 \pm 2 ms$. Compared to recombination in tris-washed PSII, NH_2OH treated PSII show a similar fast rate, but the ratio of the microsecond phase Q_A^- decay is higher. The extinction coefficient for P680 at 820 nm in NH_2OH treated tris-PSII, $7.2 \pm 0.3 mM^{-1}cm^{-1}$, is slight higher than the value in tris-washed PSII.

With NH_2OH treated PSII, high flash repetition rate are no longer required in order to observe the charge recombination reaction. This is shown in Figure 3-8 and Figure 3-4 (trace B). The decays of P^+680 and Q_A^- are almost independent of the flash repetition rate. The high repetition rate is not needed since the electron donation from Y_2 to P^+680 is blocked by NH_2OH treatment. The EPR experiments performed by Hoganson et al. [35] and Ghanotakis et al. [33] showed that the Y_2 is unable to be oxidized by P^+680 under the treatment of NH_2OH .

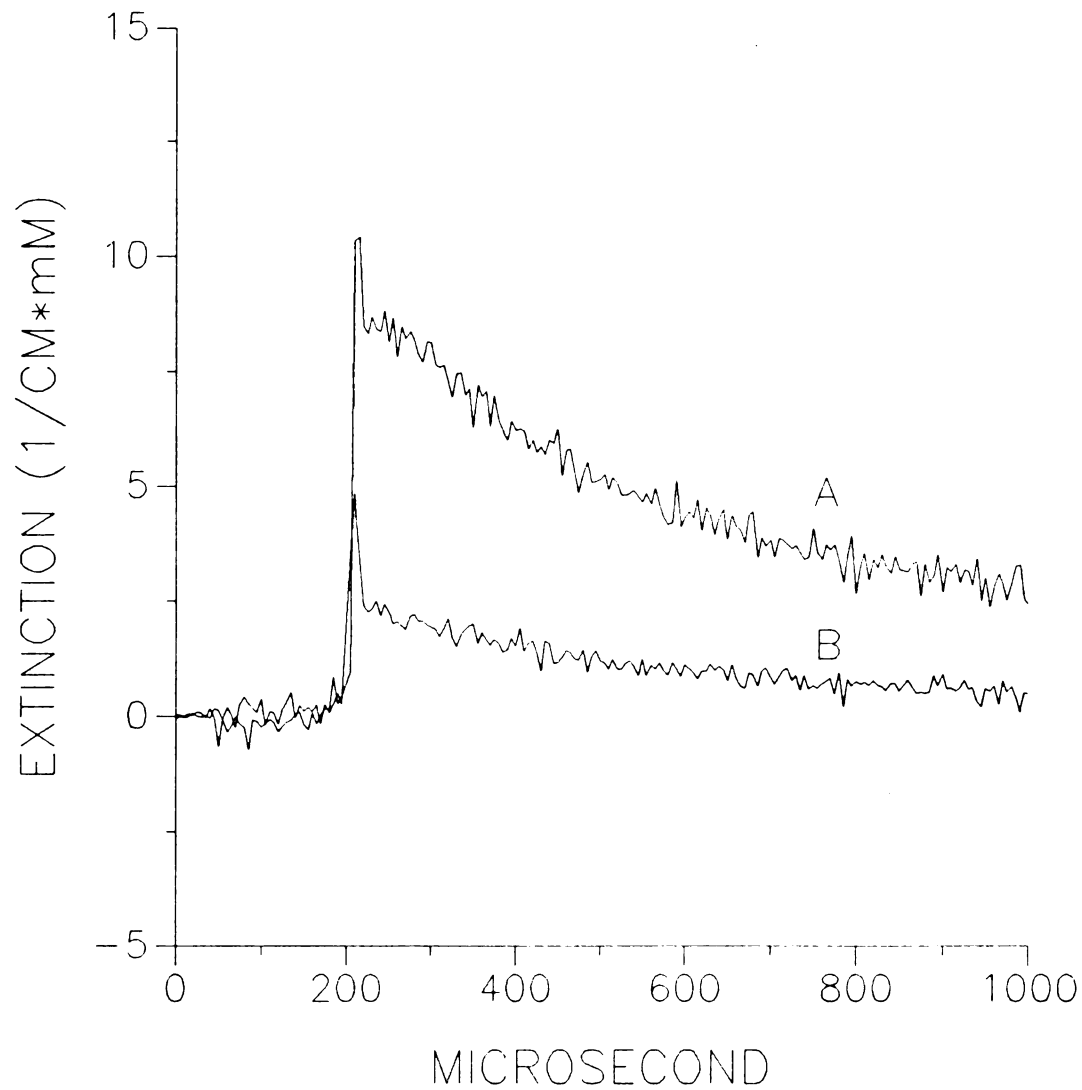


Figure 3-7 Microsecond time courses of the absorption changes at 325 nm (trace A) and 820 nm (trace B) with NH_2OH treated tris-PSII. Experiment conditions were same as those in Figure 3-2. The transient in the first few μs was unreliable because of flash artifacts.

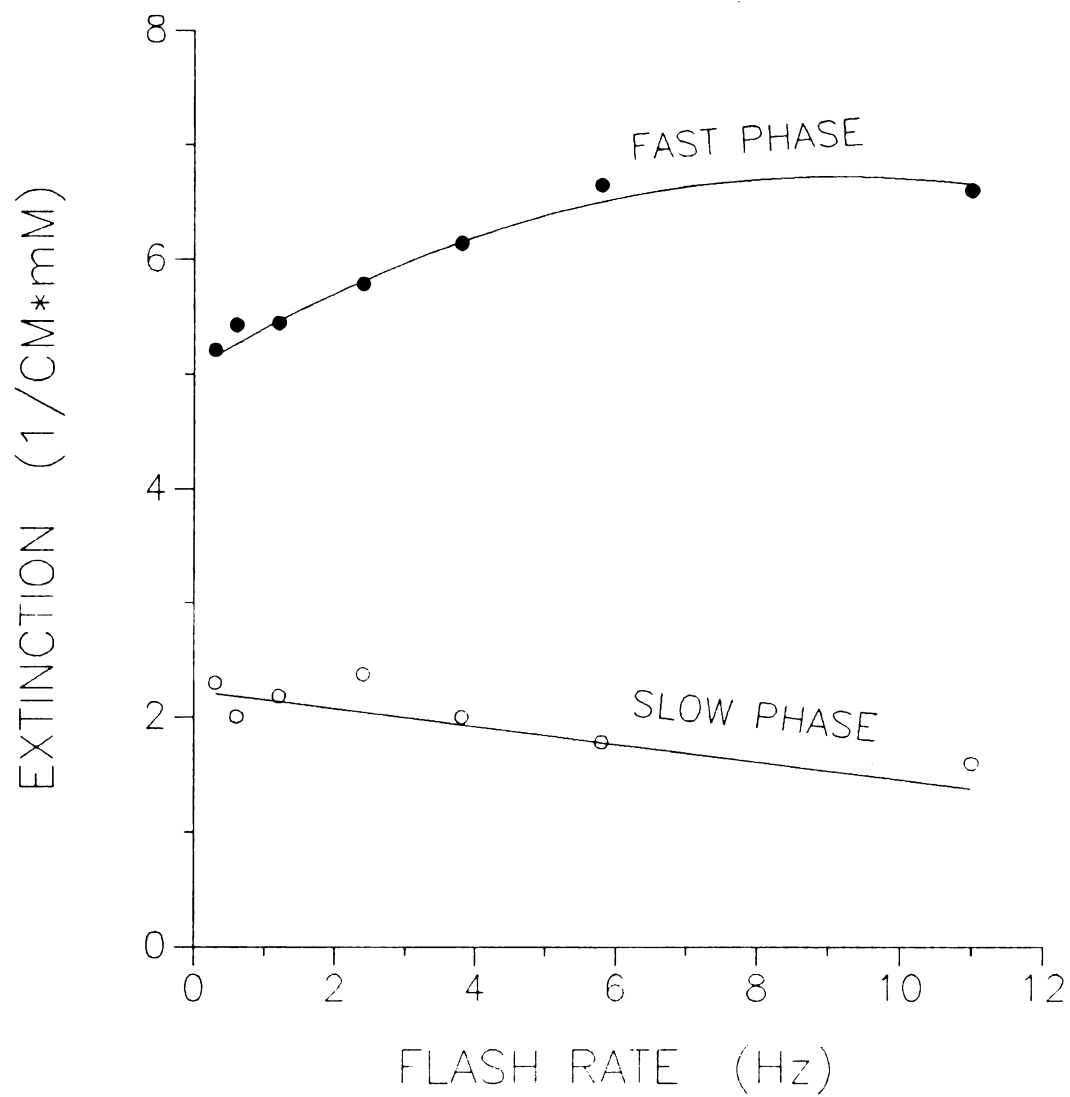


Figure 3-8 The dependence of the absorption changes at 325 nm on the repetition rate of the excitation flash in NH_2OH treated tris-PSII.

Light is required for NH_2OH to react with the donor side of PSII to disable the electron transfer capability of Y_2 . Consistent with this earlier observation, it was also observed in our experiments (data not show) that without illumination after the addition of NH_2OH , the decay trace of the first 20 scans is different from that of the second 20 scans. After about 50 flashes these differences become unnoticed. The experiments we performed here used 60 to 80 flashes to meet the light requirement of the NH_2OH inhibition before the measurements were taken. Using pre-flashes instead of pre-illumination for NH_2OH inhibition treatment provided a better way to control the inhibition process and avoid non-uniform illumination and heat damage to the samples.

C-550 Bandshift

In photosystem II, Q_A^-/Q_A and Q_B^-/Q_B have very similar UV absorption difference spectra. Thus, it is impossible to distinguish the Q_B^- contributions from that of Q_A^- when measurements are made only at 325 nm. However, the reduction of Q_A induces an absorption band shift of the pheophytin a molecule centered at 545 nm [44-46]. The charge on Q_B , on the other hand, has very little effect on this shift. Thus, the absorption difference at 540 nm minus that at 550 nm has been often used as a measure of the amplitude of C550, a local electrochromic indicator of the concentration of Q_A^- [16,44].

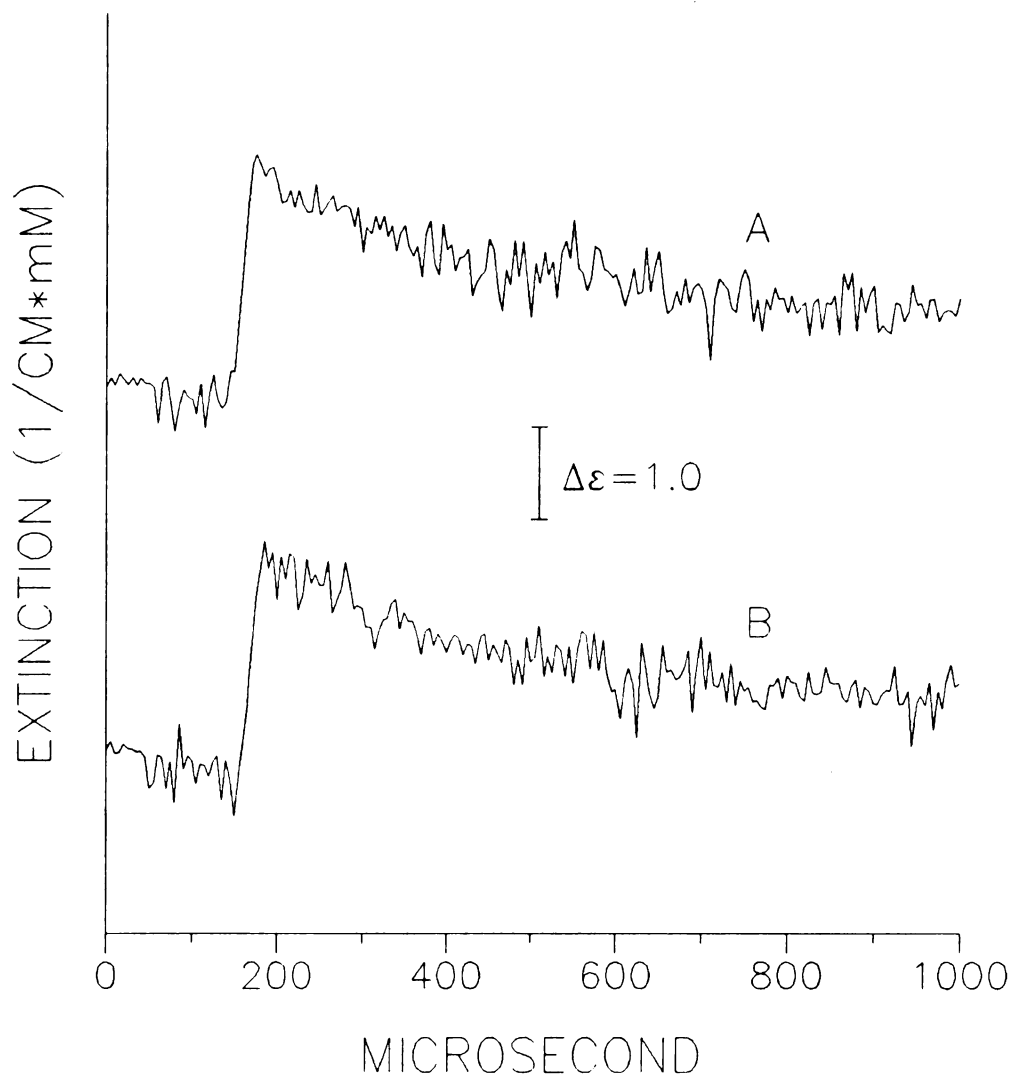


Figure 3-9 Microsecond time courses of the C550 band shift in tris-washed PSII (trace A) and NH_2OH treated tris-PSII (trace B). $[\text{Chl}] = 315.7 \mu\text{g/ml}$, $2.5 \text{ mM } \text{Fe}(\text{CN})_6^{-3}/\text{Fe}(\text{CN})_6^{-2}$ were added as the electron acceptor system.

Table Halftimes of the Microsecond Decays

Treatment	P^+680 (μs)	Q_A^- (μs)	C550 (μs)
Tris	223 ± 11	226 ± 27	225 ± 29
NaCl	125 ± 6	138 ± 9	
NH ₂ OH	240 ± 12	236 ± 24	233 ± 29

Measurements of the C550 band shift were performed with tris-washed PSII and NH₂OH treated tris-PSII membrane preparations. Figure 3-9 shows the time courses of the C550 band shift measured as the absorption difference at 540 nm minus that at 550 nm. The decays are biphasic, with the fast phase in the microsecond and the slow phase in the millisecond range. The halftimes of the faster phase are $225 \pm 29 \mu s$ for tris-washed PSII and $233 \pm 29 \mu s$ for NH₂OH treated tris-PSII. The ratio of the microsecond phase of C550 decay is about 70%. These results are in good agreement with the measurements made at 325 nm, and imply that the contribution from Q_B^- is small. The differential extinction coefficient for the 540 nm minus

550 nm obtained in our experiment was $2.1 \text{ mM}^{-1}\text{cm}^{-1}$, this is close to the reported value of $2.2 \text{ mM}^{-1}\text{cm}^{-1}$ [46].

Discussion

The results we obtained here show that the reaction we observed is the charge recombination reaction from the charge separated state Q_A^-/P^+680 . This contention is strongly supported by the decay kinetics of Q_A^- and P^+680 , which show near identical decay halftimes. The charge recombination process depends on the different inhibition treatments and experimental conditions. Both decay pathways and rates can be modified by using different inhibitors or changing conditions.

In tris-washed PSII, the electron donation by Y_2 to the reaction center P^+680 is still active. This is demonstrated in our experiments by the fact that at low excitation rates, almost no P^+680 can be detected in the one hundred microsecond time scale. The rate limiting step of the electron transfer on the donor side of tris-washed PSII is the reduction of the oxidized secondary donor Y_2^+ . From the results of the dependence of the absorption changes of P^+680 on the excitation repetition rate we estimated that the halftime of Y_2^+ reduction in tris-washed PSII in the presence of 2.5 mM ferri/ferrocyanide at pH 6.0 is about 300 ms.

Our data do not show any direct involvement of Q_B during the charge recombination process. In intact PSII membrane

f

be

al

tr

re

ex

th

of

cha

the

tra

ban

to

comp

P*68

reco

Syne

poss

samp

site.

retar

charg

by th

change

fragments or chloroplasts, the Q_A^- to Q_B electron transfer has been shown to take place in about 200 μ s [16,47]. If this is also the case in tris-washed PSII, the Q_A^- to Q_B electron transfer should compete effectively with the charge recombination process; however, this is not observed in our experiments. Our results show a very similar kinetic trace of the absorption changes detected at 325 nm and the time course of the C550 band shift that is caused mainly by the negative charge on Q_A . This rules out any significant contribution of the electron transfer from Q_A^- to Q_B , since this electron transfer reaction will change the decay kinetics of the C550 band shift dramatically.

It is not clear why the electron transfer reaction of Q_A^- to Q_B , though it has a comparable rate constant, can not compete with the charge recombination reaction between Q_A^- and P^+680 . Very recently Gerken et al. [18] measured the charge recombination reactions between Q_A^- and P^+680 in cyanobacterium *Synechococcus* sp. and obtained similar results. It is possible that plastoquinone is severely depleted during the sample preparation, which will effectively deplete the Q_B site. However, another possible reason for the dramatic retardation of the Q_A^- to Q_B electron transfer is the positive charge on the reaction center P^+680 . The Coulomb attraction by the positively charged reaction center P^+680 can induce changes of the free energies of nearby reactions, which

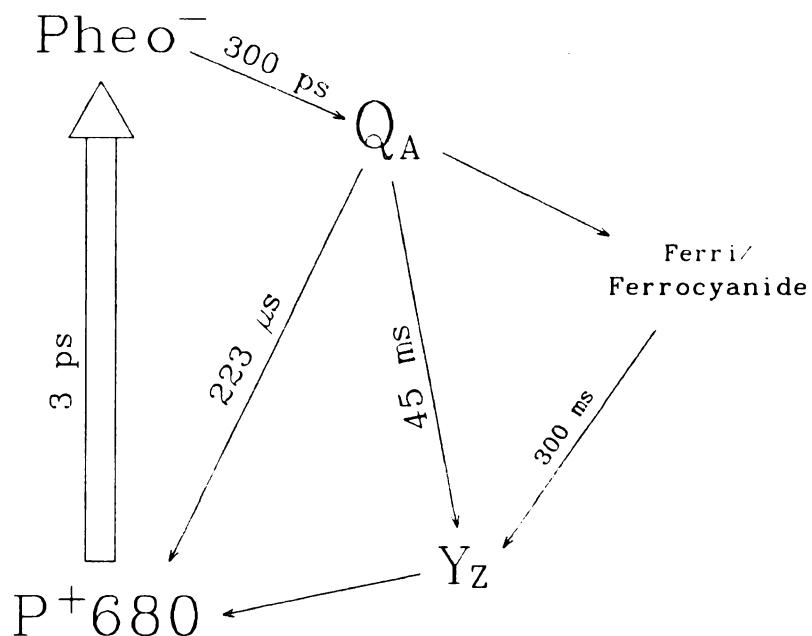


Figure 3-10 The scheme of the electron transfer pathways in tris-washed PSII.

according to Marcus electron transfer theory [48], will alter the rates of electron transfer.

The different behavior of the dependence of the charge recombination reaction on the repetition rate of the excitation flash with NH_2OH treated PSII implies that a different inhibition mechanism is in place. In tris-washed PSII, the inhibition is achieved by removing electron donors to Y_z^+ , while the electron transfer from Y_z to P^+680 is not

affected greatly. However, in NH_2OH treated tris-PSII, the electron transfer from Y_2 to P^+680 is greatly retarded or blocked and the electron donation of Y_2 to P^+680 no longer competes with the Q_A^-/P^+680 charge recombination reaction.

At least two inhibitory actions of NH_2OH treatment have been reported [19,33]. In one case it acts as an electron donor to PSII, possibly competing with water, and in the other case, it inactivates the donor side of PSII, retarding the electron transfer from Y_2 to P^+680 . Our results clearly favor the second of these two models. Hoganson and Babcock [35] has suggested that the NH_2OH inhibition may involve a reversible oxime formation at one of the carbonyl groups of P680, which might lower the redox potential of P^+680 and prevent it from oxidizing Y_2 . Our results suggest that the NH_2OH inhibition site is more likely localized near Y_2 rather than at the reaction center P680. This will be discussed in more detail in chapter IV.

The decay of the state Q_A^-/P^+680 via the charge recombination reaction has been studied by using both optical and EPR techniques; the halftimes obtained range from 100 to 800 μs [11,18,19,22,28-31,35]. Recently, Gerken and coworkers [18] observed that three exponential decay phases with half times of 170 μs , 800 μs and 6 ms are involved in the charge recombination reactions in cyanobacterium PSII membrane preparations, and claimed that these multiphasic kinetics were

due to a distribution of different structural states of the reaction center polypeptides. Our results with tris-washed PSII from spinach do not resolve significant multiphasic kinetics of the charge recombination reaction. Instead a single exponential decay with a halftime of 223 μ s is observed in the microsecond range. The charge recombination reactions in our preparations are most likely taking place from the same structural states of the reaction center polypeptides, since heterogeneity in these states can result in a non-exponential behavior of the reactions [49]. Such behavior is not observed in our experiments. NH_2OH treatment of tris-PSII does not change the rate of the charge recombination process, which suggests that the valence of Y_2 is not critical in influencing the kinetics of the reaction.

In NaCl washed PSII, the charge recombination reaction of $\text{Q}_\text{A}^-/\text{P}^+680$ is faster, with a halftime of about 130 μ s. Unlike tris washed-PSII, NaCl washing removes only the 17 KDa and 23 KDa polypeptides, the 33 KDa polypeptide and the manganese ions associated with the water splitting complex are retained [31,41]. The NaCl washed PSII membrane preparations is able to undergo several turnovers before the normal electron transfer is inhibited [41]. Moreover, oxygen evolution activity can be restored up to 75% upon the addition of Ca^{2+} [52,53]. However, in tris-washed PSII membrane preparations, all three extrinsic polypeptides, as well as the manganese

ions, are released, and the redox properties of Y_2 are modified. These differences in the micro-environment at the donor side of PSII influence the rate of the charge recombination reaction. The positively charged species at the donor side of PSII may exert Coulomb effects and result in a faster charge recombination reaction. The changes of the redox potential of Y_2 under tris-washing treatment may also play a role in the recombination rate. The mutagenesis experiment carried out by Metz and coworkers [50] shows that when Y_2 is replaced by phenylalanine, a residue with higher redox potential, the charge recombination reaction between Q_A^- and P^+680 is slowed down to 1 ms.

Conclusion

The time evolution of the charge separated state Q_A^-/P^+680 under different treatments can be used to obtain valuable information of the micro-environment of PSII. The charge recombination of the state Q_A^-/P^+680 can be detected optically by measuring the time courses of the absorption changes at 325 nm (Q_A^-) and 820 nm (P^+680). Our results show that charge recombination occurs in tris-washed PSII at high repetition rates of the excitation flash. NH_2OH treatment removes the requirement of high flash repetition rate. This difference comes from the different inhibitory states. Tris washing inhibits the re-reduction of Y_2^+ by its physiological donor

whereas the electron transfer from Y_2 to P^+680 is not blocked. NH_2OH treatment greatly retards the electron transfer from Y_2 to P^+680 and keeps Y_2 in its reduced state. The rate of the charge recombination reaction in NaCl washed PSII is faster than that in tris and NH_2OH treated PSII. This difference presumably comes from effects on the micro-environment around the reaction center. Our results do not show any direct involvement of secondary acceptor Q_B during the charge recombination reactions. We attribute this to the effects of the positive charge on the reaction center P^+680 or to depletion of the Q_B site during sample preparation.

REFERENCES

1. Döring, G., Stiehl, H.H. and Witt, H.T. Z. Naturforsch 1967, 22b, 639
2. Döring, G., Renger, G., Vater, J. and Witt, H.T. Z. Naturforsch 1969, 24b, 1139
3. Stiehl, H.H and Witt, H.T. Z. Naturforsch 1968, 23b, 220
4. Stiehl, H.H and Witt, H.T. Z. Naturforsch 1968, 24b, 1588
5. Wasielewski, M.R., Johnson, D.G., Seibert, M. and Govindjee, Proc. Natl. Acad. Sci. USA, Vol. 86, 524-528, January 1989
6. Eckert, H.-J, Wiese, N., Bernarding, J., Eichler, H.-J. and Renger, G. FEBS Lett. 1988, 240, 153
7. Dekker, J.P., Ghanotakis, D.F., Plijter, J.J., van Gorkom, H.J. and Babcock, G.T. Biochim. Biophys. Acta 1984, 767, 515
8. Brettel, K., Schlodder, E., and Witt, H.T. Biochim. Biophys. Acta 766, 1984, 403
9. Gerken, S., Brettel, K., Schlodder, E., and Witt, H.T. FEBS Lett. 1988, 237, 69
10. Meyer, B., Schlodder, E., Dekker, J.P., and Witt, H.T. Biochim. Biophys. Acta submitted
11. Reinman, S., Mathis, P., Conjeaud, H., and Stewart, A. Biochim. Biophys. Acta 1981, 635, 429

12. Boska, M., Sauer, K., Buttner, W., and Babcock, G.T. Biochim. Biophys. Acta 1983, 722, 327
13. Weiss, W. and Renger, G. Biochim. Biophys. Acta 1986, 850, 173
14. Schlodder, E. and Meyer, B. Biochim. Biophys. Acta 1987, 890, 23
15. Golbeck, J.H. and Warden, J.T. Biochim. Biophys. Acta 1985, 806, 116
16. Petrouleas, V. and Diner, B.A. Biochim. Biophys. Acta 1987, 893, 126
17. Diner, B.A. and Petrouleas, V. Biochim. Biophys. Acta 1987, 893, 138
18. Gerken, S. Dekker, J.P., Schlodder, E. and Witt, H.T. Biochim. Biophys. Acta 1989, 977, 52
19. Ford, R.C. and Evans, M.C.W. Biochim. Biophys. Acta 1985, 807, 1
20. Bock, C.H., Gerken, S., Stehlik, D. and Witt, H.T. FEBS Lett. 1988, 227, 141
21. Volker, M., Eckert, H.J. and Renger, G. Biochim. Biophys. Acta 1987, 890, 66
22. Van Best, J.A. and Mathis, P. Biochim. Biophys. Acta 1978, 503, 178
23. Schlodder, E., Brettel, K., Schatz, G.H. and Witt, H.T. Biochim. Biophys. Acta 1984, 765, 178
24. Völker, M., Ono, T., Inoue, Y. and Renger, G. Biochim. Biophys. Acta 1985, 806, 25
25. Renger, G., Völker, M. and Weiss, W. Biochim. Biophys. Acta 1984, 766, 582

26. Åkerlund, H.E., Jansson, C. and Andersson, B. Biochim. Biophys. Acta 1982, 681, 1
27. Radmer, R. and Cheniae, G.M. in Primary processes of Photosynthesis (Barber, J., ed.) 1977, 303, Elsevier, Amsterdam
28. Conjeaud, H., Mathis, P. and Paillotin, G. Biochim. Biophys. Acta 1979, 546, 280
29. Conjeaud, H. and Mathis, P. Biochim. Biophys. Acta 1980, 590, 353
30. Satoh, K. and Mathis, P. Photobiochem. Photobiophys. 1981, 2, 189
31. Reinman, S. and Mathis, P. Biochim. Biophys. Acta 1981, 635, 249
32. Cheniae, G.M. and Martin, I.F. Plant Physiol. 1971, 47, 568
33. Ghanotakis, D.F. and Babcock, G.T. FEBS Lett. 1983, 153, 231
34. Ford, R.C. and Evans, M.C.W. FEBS Lett. 1983, 160, 159
35. Hoganson, C.W. and Babcock, G.T. Biochemistry 1989, 28, 1448
36. Hoganson, C.W. and Babcock, G.T. Biochemistry 1988, 27, 5848
37. Radmer, R. and Ollinger, O. FEBS Lett. 1982, 144, 103
38. Hanssum, B. and Renger, G. Biochim. Biophys. Acta 1985, 810, 225
39. Frank, F. and Schmid, G.H. Biochim. Biophys. Acta 1989, 977, 215

40. Berthold, D.A., Babcock, G.T. and Yocum, C.F. FEBS Lett. 1981, 134, 231
41. Ghanotakis, D.F., Babcock, G.T. and Yocum, C.F. Biochim. Biophys. Acta 1984, 765, 388
42. Sun, A.S.K. and Sauer, K. Biochim. Biophys. Acta 1973, 325, 301
43. R.K. Clayton, Photosynthesis: Physical Mechanisms and Chemical Patterns 79, Cambridge University Press, 1980
44. Dekker, J.P., Van Gorkom, H.J., Brok, M. and Ouwehand, L. Biochim. Biophys. Acta 1984, 764, 301
45. Klimov, V.V., Klevanik, A.V. and Shuvalov, V.A. FEBS Lett. 1977, 82, 183
46. Van Gorkom, H.J., Tamminga, J.J. and Haveman, J. Biochim. Biophys. Acta 1974, 347, 417
47. Bowes, J., Crofts, A.R. and Arntzen, C.J. Arch. Biochem. Biophys. 1980, 200, 303
48. Marcus, R.A. J. Chem. Phys. 1956, 24, 966
49. Kleinfeld, D., Okamura, M.Y. and Feher, G. Biochemistry 1984, 23, 5780
50. Metz, J.G., Nixon, P.J., Rögner, M, Brudvig, G.W. and Diner, B.A. Biochemistry 1989, 28, 6960
51. Barry, B.A. and Babcock, G.T. Proc. Natl. Acad. Sci. USA 1987, 84, 7099
52. Ghanotakis, D.F., Babcock, G.T. and Yocum, C.F. FEBS Lett. 1984, 167, 127-130
53. Miyao, M. and Murata, N. FEBS Lett. 1984, 168, 118-120
54. Haveman, J. and Mathis, P. Biochim. Biophys. Acta 1976, 440, 346-355

55. Yerkes, C.T. and Babcock, G.T. Biochim. Biophys. Acta
1980, 590, 360-372

e

s

c

to

mi

cha

ful

[5]

sim

Dekh

CHAPTER IV
CHARACTERIZATION OF P⁺680/P680
AND Y₂⁺/Y₂ ABSORPTION DIFFERENCE SPECTRUM

Introduction

Photosynthesis in higher plants involves a series of electron transfer reactions that lead to water oxidation and CO₂ reduction. These electron transfer reactions are carried out by individual electron carriers that undergo reduction or oxidation during the electron transfer process. The absorption changes associated with the redox activity of these electron carriers can be detected by transient absorption spectroscopy. The wavelength dependence of the absorption changes, i.e. the absorption difference spectra, can be used to identify and characterize these electron carriers and their micro-environments.

Absorption difference spectra have been widely used to characterize the electron carriers in PSII [1-4]. The first full absorption spectrum of Q_A⁻/Q_A was obtained by Van Gorkom [5] and was identified as a plastoquinone molecule due to its similarities to the in vitro spectrum of plastoquinone. Dekker and coworkers in 1984 [3] reported the detailed

s

pr

ab

its

a p

abs

Howe

Y_2 i

poly

tyros

simil

obtain

al. [1

Y_2 was

absorption difference spectrum of Q_A^-/Q_A and Y_2^+/Y_2 in tris-washed PSII in the presence of ferricyanide and 3-(3',4'-dichlorophenyl)-1,1-dimethylurea (DCMU) by analysis of the flash induced kinetics of millisecond absorption changes, prompt and delayed fluorescence, and EPR signal II_f . It was shown that the absorption difference spectrum of Q_A^-/Q_A consists of two negative peaks at 268 nm and 433 nm, and four positive peaks at 325, 398, 416, and 449 nm. The spectrum of Y_2^+/Y_2 consists mainly of positive bands at 260 nm, 300 nm, and 390-450 nm on which a chlorophyll band shift around 438 nm is superimposed. Similar results were obtained with native preparations [6].

The chemical identification of the donor Y_2 by its absorption difference spectrum was not successful because of its low spectral resolution. It was originally assigned to be a plastoquinone molecule [3,7] due to the similarity of its absorption difference spectrum in the ultraviolet range. However, recent mutagenesis experiments [8-11] have shown that Y_2 is a tyrosine residue located at position 161 of the D1 polypeptide. The in vitro absorption difference spectrum of tyrosine radical [12,13], $TyrO^\cdot/TyrOH$, has features that are similar to those of the Y_2^+/Y_2 absorption difference spectrum obtained by Dekker et al. [3] and more recently by Gerken et al. [14] in the UV range. The original misassignment of the Y_2 was due to the low resolution of the absorption difference

t
s
tr
re
wh
di
abs
et
Syn
diff
arou
and a
aroun
Chla⁺/
wavele

spectrum as well as to the unresolved EPR spectrum of Y_2^+ [15-17].

The absorption difference spectrum of $P^+680/P680$ in the UV range has not been studied as extensively as that of Q_A^-/Q_A and Y_2^+/Y_2 . The reasons for this are that the decay of P^+680 is fast (in the nanosecond time scale) and that there are difficulties in separating contributions from other components. Weiss and Renger [18] measured the $P^+680/P680$ absorption difference spectrum from 250 nm to 400 nm in trypsinized and NH_2OH treated PSII membranes. They found that there were differences in the $P^+680/P680$ absorption difference spectrum near 300 nm and 360 nm in trypsinized and NH_2OH treated PSII membranes. However, the spectra were not well resolved and the measurements were not performed above 400 nm where the most characteristic features of the $P^+680/P680$ difference spectrum are located. A more detailed $P^+680/P680$ absorption difference spectrum was obtained recently by Gerken et al. [1] in tris-washed PSII from cyanobacterium *Synechococcus* sp.. They found that the $P^+680/P680$ absorption difference spectrum is dominated by a very sharp bleaching around 434 nm, by absorption increases around 305, 345, 400 nm and above 450 nm, and absorption decreases below 290 nm and around 375 nm. A comparison with the in vitro spectrum of $Chla^+/Chla$ in CH_2Cl_2 [19] reveals similarities in the wavelength range over which absorption changes occur, although

significant differences are apparent. These differences might be caused by differences in aggregation state as well as in the local environment.

The absorption difference spectrum of $P^{+}680/P680$ and Y_2^{+}/Y_2 can be obtained by various methods. However, the most important aspect to be considered is how to separate the contributions from other components that are active during the electron transfer reactions. An inaccurate subtraction of those interferences can result in distorted spectrum. In the experiments described here we obtained the absorption difference spectrum of $P^{+}680/P680$ and Y_2^{+}/Y_2 by monitoring the charge recombination reactions of the state $Q_A^{-}/P^{+}680$ in tris and NH_2OH treated PSII. The advantages of this method are the following: (1) It involves fewer electron transfer reactions so that the different pathways can be defined more accurately; (2) The different electron transfer reactions can be relatively easily separated since they occur on different time scales (e.g., $Q_A^{-}/P^{+}680$ recombination occurs in the microsecond time scale, while Q_A^{-}/Y_2^{+} recombination occurs in the millisecond time scale).

The NH_2OH treatment that inhibits the electron transfer from Y_2 to $P^{+}680$ is not well understood. Whether the inhibition takes place at the reaction center P680, at the Y_2 site, or remotely in the protein is still an open question. In the experiments described here we have performed

1
a
p
in
th
tr
tet
car
for
init
take
memb.
200 μ
light
of th
chapte

measurements in NH_2OH treated tris-PSII in order to determine how NH_2OH treatment affects the difference spectrum. The modifications of the absorption difference spectra of $\text{P}^+680/\text{P}680$ and of Y_2^+/Y_2 with NH_2OH treated samples provides us insight into the mode of NH_2OH inhibition.

Materials and Methods

The experiments were performed with tris-washed photosystem II membranes. The PSII membranes were isolated from spinach according to the method described by Berthold et al. [20] with some modifications [21]. The preparation procedures were described in detail in chapter III. Tris inactivation of PSII membranes was performed by incubation of the PSII membranes in a solution containing 0.8 M tris(hydroxymethyl)aminomethane and 0.5 mM ethylenediamine tetraacetic acid (EDTA) at pH 8.0. The incubation process was carried out at a chlorophyll concentration of 0.5 mg/ml at 0°C for 20 minutes under room light. The NH_2OH treatment was initiated about 5 to 10 minutes before the measurements were taken. 2.0 mM NH_2OH was added to the tris-washed PSII membrane preparations at a chlorophyll concentration of about 200 $\mu\text{g}/\text{ml}$. 60-80 pre-laser flashes were given to meet the light requirement of NH_2OH inactivation [18,22,23]. Details of the tris and NH_2OH treatments were described in the chapter III.

c
c
m
4
of
th
we
di
to
flu
use
scar
Nd: Y
nm.
?
progr
were

The optical measurements were performed with a chlorophyll concentration around 200 $\mu\text{g/ml}$ in a buffer consisting of 0.4 M Sucrose, 50.0 mM MES, 15.0 mM NaCl, and pH 6.0. Lower Chl concentration, around 100 $\mu\text{g/ml}$, was used in the 250-280 nm range because of the strong sample absorption in that region. The experiments were carried out with the transient absorption spectrometer described in the chapter II. The sample cell used was a 0.1 cm optical path quartz cuvette that gave an effective optical path length 0.14 cm when oriented at 45 degree relative to the probe beam. The slit used with the monochromator were 1.0 mm that gave a spectral resolution of 4.0 nm. Three glass filters (U330 for the wavelength range of 250-280 nm, U340 for the range of 280-370 nm, and B390 for the range of 370-480 nm; the filters were from Hoya Corp.) were used, one behind the monochromator to block the secondary diffraction from the monochromator and two in front of the PMT to protect the PMT from the excitation laser flash and fluorescence from the samples. The instrument time constants used were 5 μs for microsecond scans and 1 ms for millisecond scans. The excitation flash was provided by a Quanta Ray Nd:YAD laser. The wavelength of the excitation flash was 532 nm. All measurements were performed at room temperature.

The data were analyzed by using the kinetic fitting program KFIT from OLSI. The absorption difference spectrum were constructed by plotting the amplitudes of the absorption

e
r
5
ex
se
wi
Thu
und
equ

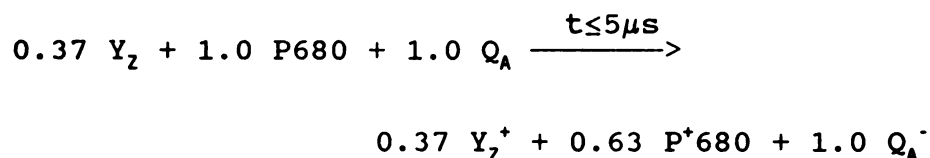
About
excit

changes of corresponding phases against the wavelength. The extinction coefficients were calculated under the assumption of 250 Chl molecules per reaction center.

Results

P⁺680/P680 Difference Spectrum

The charge separated state $Q_A^-/P^{+}680$, which is created in about 300 ps following the visible excitation [24-27], decays in the microsecond time scale when high repetition rate flash excitation was applied to tris-washed PSII. At 5.8 Hz flash repetition rate, about 63% of the $Q_A^-/P^{+}680$ is still present at 5 μ s (the time constant used in the experiments) following the excitation flash (Figure 3-4 in the chapter III). The charge separated state decays by recombination between Q_A^- and $P^{+}680$ with a halftime of 230 μ s (Figure 3-2 in the chapter III). Thus, the electron transfer reactions in tris-washed PSII under the above conditions can be represented by the following equation:



About 37% of Y_2 is still in reduced state prior to the excitation flash and results in a 63% detectable $P^{+}680$ in the

c
c

tr
no

the
 $Q_A /$

res
spec

over
compa

I
to p'
state

microsecond time scale. The initial amplitudes of the absorption changes after 5 μ s (the instrument response time) following the excitation flash are plotted against wavelength in Figure 4-1.

The 230 μ s phase of the Q_A^-/P^+680 decay arises from the charge recombination reaction between Q_A^- and P^+680 , a contention that is strongly supported by the observations that Q_A^- and P^+680 have near identical decay halftimes. Thus, the absorption difference spectrum of the 230 μ s phase as shown in Figure 4-2 should represent the total absorption difference spectrum of $Q_A^-P^+680/Q_AP680$. The $P^+680/P680$ absorption difference spectrum can be obtained by subtracting the Q_A^-/Q_A contributions from the $Q_A^-P^+680/Q_AP680$ difference spectrum.

Figure 4-3 shows the $P^+680/P680$ difference spectrum in tris-washed PSII. The subtraction was carried out by normalizing the spectrum at 325 nm under the assumption that the absorption change at 325 nm is due to Q_A^- only [3]. The Q_A^-/Q_A absorption difference spectrum was taken from the results of Dekker et. al. [3]. The absorption difference spectrum of Chlorophyll a^+ /Chlorophyll a in CH_2Cl_2 [19] is overlayed with the $P^+680/P680$ spectrum in Figure 4-3 for comparison.

In NH_2OH treated tris-PSII, the electron transfer from Y_2 to P^+680 is inhibited [22,28,29] and the charge separated state Q_A^-/P^+680 decays mainly via the charge recombination

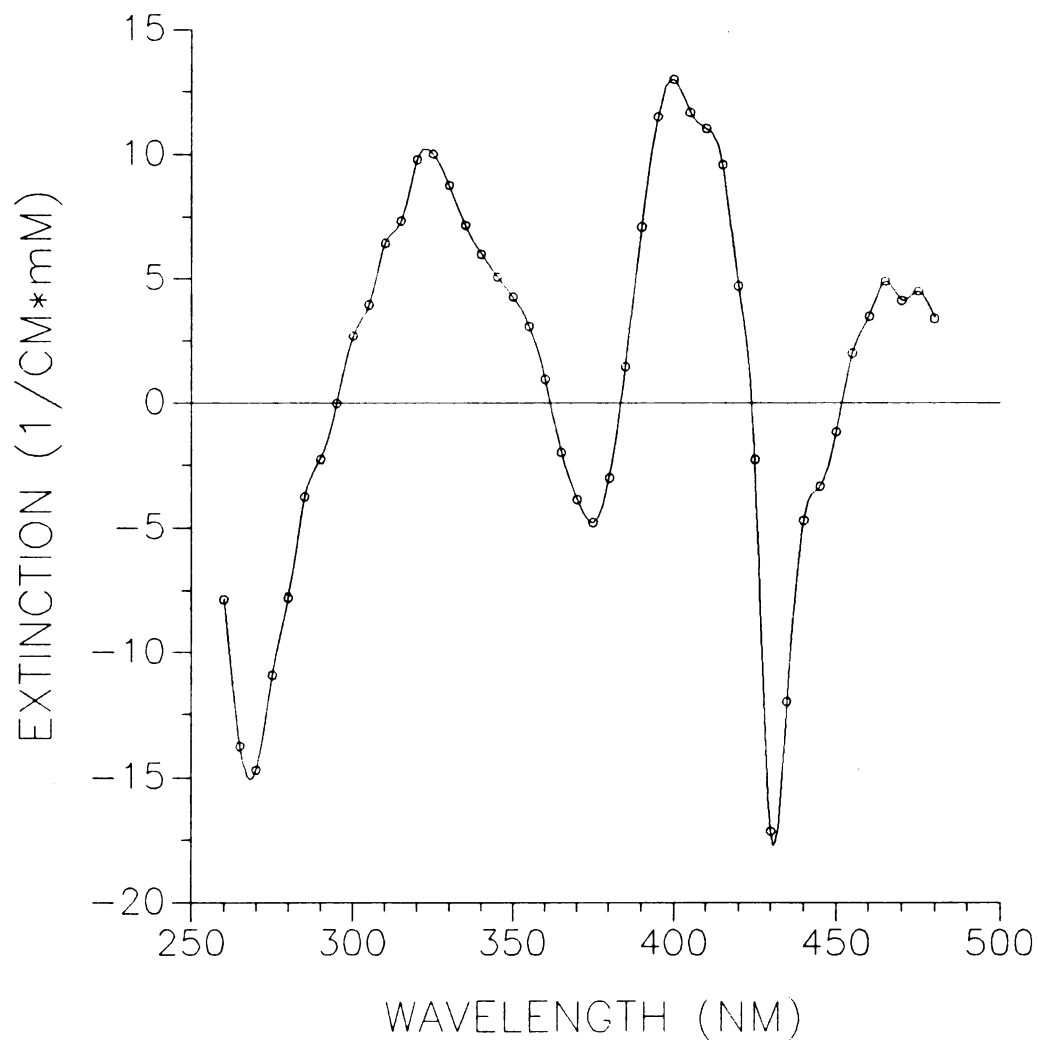


Figure 4-1 Absorption difference spectrum of the initial amplitudes of the total absorption changes after 5 μ s following the flash excitation in tris-washed PSII. [Chl]=215 μ g/ml, optical path=0.14 cm, excitation flash repetition rate 5.8 Hz. 2.5 mM $\text{Fe}(\text{CN})_6^{3-}/\text{Fe}(\text{CN})_6^{4-}$ were added as the electron acceptor system.

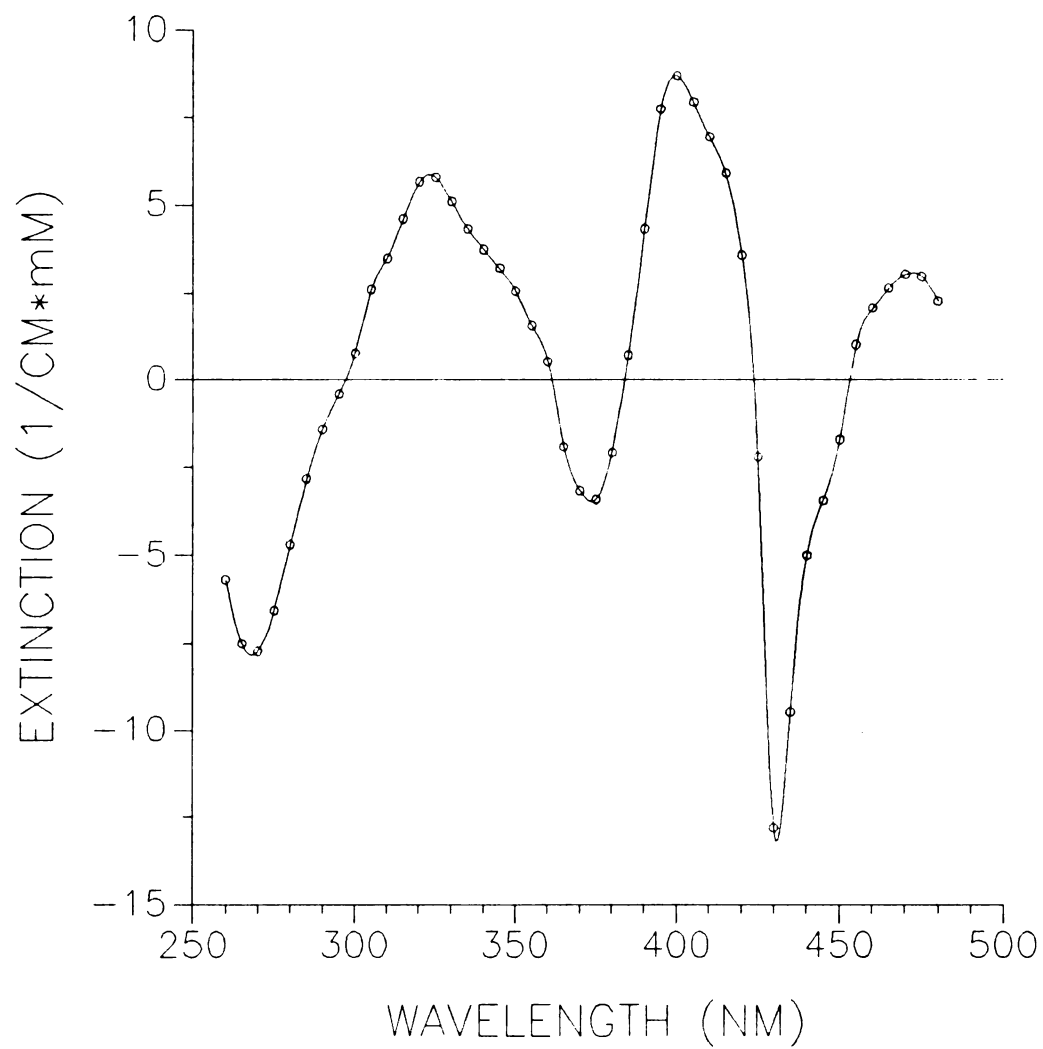


Figure 4-2 Absorption difference spectrum of the 230 μ s decay phase in tris-washed PSII.

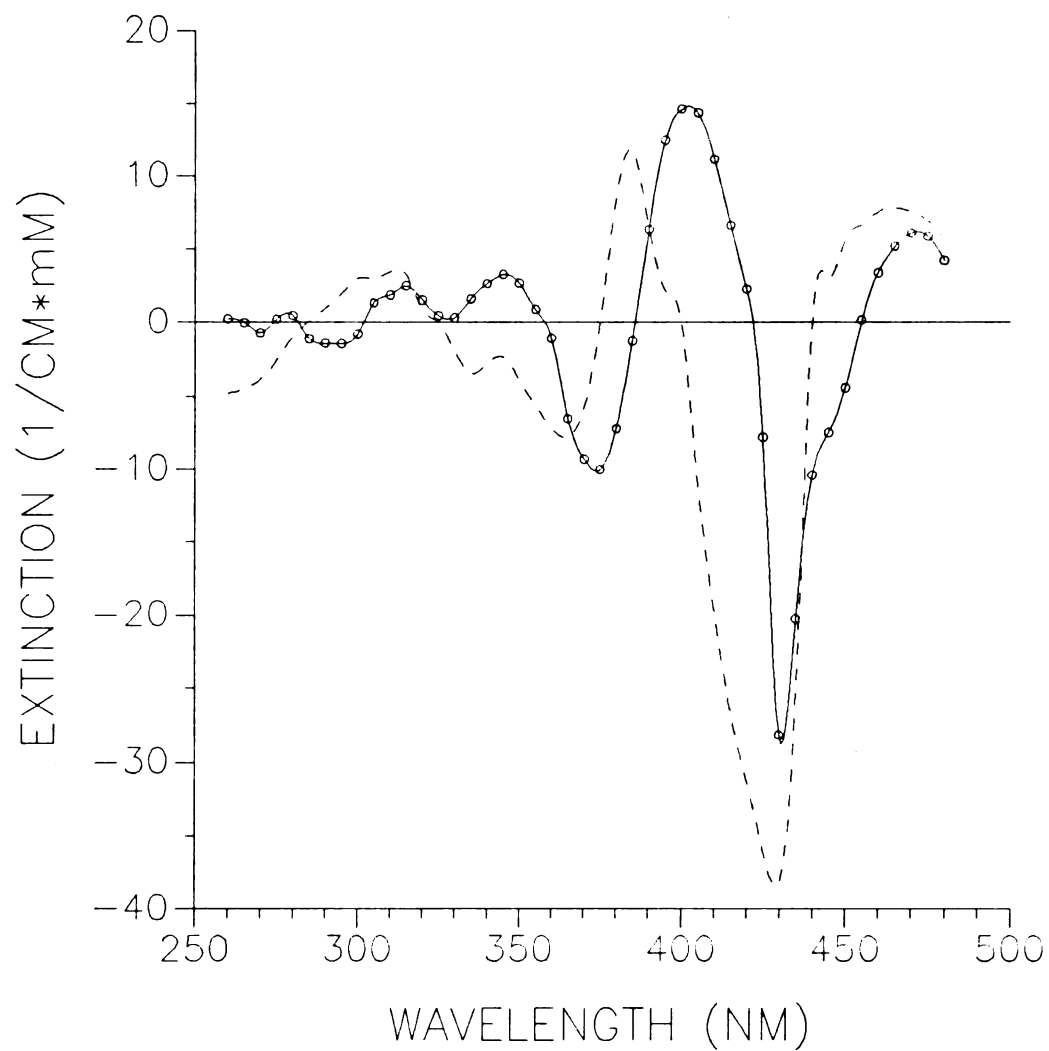
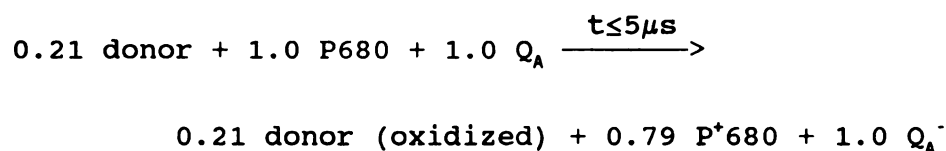


Figure 4-3 Absorption difference spectrum of the reaction center P⁺680/P680 in tris-washed PSII (open circle, continuous line) and the spectrum of Chl a⁺/Chl a in CH₂Cl₂ (dash line).

reaction between Q_A^- and P^+680 . Under the conditions of 2.0 mM NH_2OH , 60 pre-flashes, and 5.8 Hz flash repetition rate, NH_2OH treated tris-PSII shows that about 79% of the state Q_A^-/P^+680 is still present after 5 μs following the excitation flash (Figure 3-8 in the chapter III). The fraction of reaction centers, 21%, that are reduced in the sub-microsecond time scale might be the result of incomplete inhibition by NH_2OH treatment, or reflect reduction by electron donors other than Y_2 [30].

The electron transfer reactions of the state Q_A^-/P^+680 after 5 μs following the excitation flash in the NH_2OH treated tris-PSII can be represented by the following equation:



Reaction centers, not reduced in the sub-microsecond time scale, undergo charge recombination between Q_A^- and P^+680 with a halftime of 230 μs . Thus, the absorption difference spectrum of the 230 μs phase of the Q_A^-/P^+680 decay represents the total spectrum of $Q_A^-P^+680/Q_A P680$ in NH_2OH treated tris-PSII. Subtracting the Q_A^-/Q_A contributions from this total spectrum, we obtained the absorption difference spectrum of $P^+680/P680$ in NH_2OH treated tris-PSII (Figure 4-4 open triangle). The $P^+680/P680$ spectrum in tris-washed PSII is

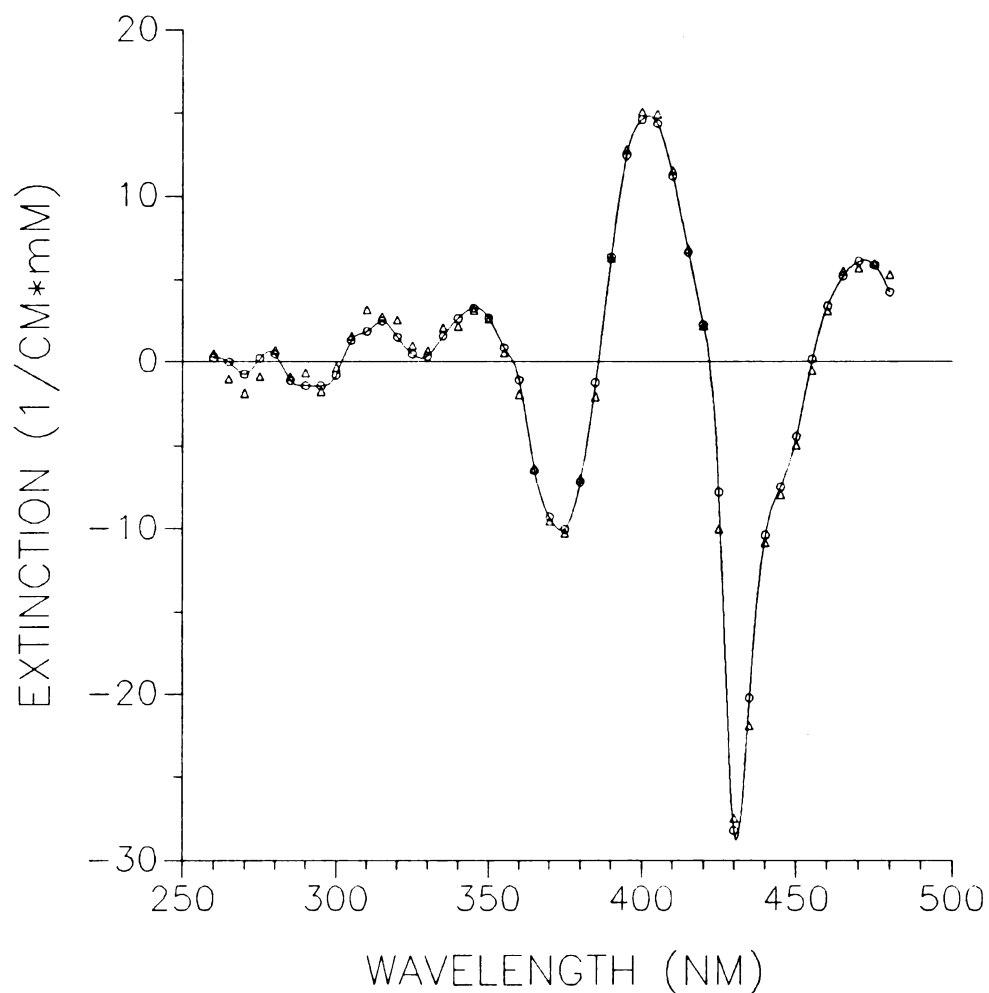


Figure 4-4 Absorption difference spectrum of the reaction center P*680/P680 in tris-washed PSII (open circle) and in NH₂OH treated tris-PSII (open triangle). The NH₂OH treatment was performed with the addition of 2.0 mM NH₂OH and 60 pre-flashes before the measurements were taken in tris-washed PSII. The experiment conditions were the same as in Figure 4-1.

1

a

de

wa

spe

y_2^*

con

subt

spec

carr

at 32

diffe

and Ha

also presented in the Figure 4-4 as a comparison.

Y_2^+/Y_2 Difference Spectrum

In tris-washed PSII, the millisecond decay phase is dominated by the recombination reaction between Q_A^- and Y_2^+ . In order to increase the amplitude of the millisecond decay phase signal, the time between flashes was extended to 1.98 seconds. Under this condition, about 71% Q_A^- decays in the millisecond time scale with a halftime of 45 ms (Figure 3-5 in the chapter III). This 45 ms decay phase presumably arises from the charge recombination reaction between Q_A^- and Y_2^+ [3]. EPR data on the decay of Y_2^+ are also consistent with this assumption [3,31].

The absorption difference spectrum of the millisecond decay phase of the charge separated state Q_A^-/P^+680 in tris-washed PSII is shown in Figure 4-5 (open circle). This spectrum represents the $Q_A^-Y_2^+/Q_A Y_2$ difference spectrum. The Y_2^+/Y_2 spectrum can be obtained by subtracting the Q_A^-/Q_A contributions from this spectrum. Figure 4-6 shows the subtracted spectrum that represents the absorption difference spectrum of Y_2^+/Y_2 in tris-washed PSII. The subtraction was carried out under the assumption that the absorption changes at 325 nm are due to Q_A^- only [3]. The in vitro absorption different spectrum of tyrosine taken from the results of Bent and Hayon [12] is overlayed in the Figure (dashed line). The

o
s
tr
fo
in
(F.

spe
samp
of t
afte
spect
compl
contr
chloro
spectr
contril

in vitro tyrosine spectrum in Figure 4-6 is attributed to the formation of the phenoxy radical TryO^\cdot resulting from the loss of the phenolic hydrogen from tyrosine in water.

In NH_2OH treated tris-PSII, the amplitude of the millisecond decay phase is very small even at very low flash repetition rate (Figure 4-5, open triangle). NH_2OH treatment inhibits electron transfer from Y_2 to P^+680 and results in the decay of the charge separated state $\text{Q}_\text{A}^-/\text{P}^+680$ mainly via the charge recombination reaction between Q_A^- and P^+680 . Under the same conditions as the untreated tris-washed PSII, NH_2OH treated tris-PSII shows that only 29% Q_A^- is present at 1 ms following the excitation flash. This fraction of Q_A^- decays in the millisecond time scale with a halftime of about 80 ms (Figure 3-3 in the chapter III).

The same procedure used to obtain the Y_2^+/Y_2 difference spectrum in tris-washed PSII was employed for NH_2OH treated samples. Figure 4-7 shows the absorption difference spectrum of the 80 millisecond decay phase in NH_2OH treated tris-PSII after subtracting the $\text{Q}_\text{A}^-/\text{Q}_\text{A}$ contributions from the total spectrum in 4-5 (open triangle). The spectrum shows very complicated features. In the visible region, the contributions may arise from the oxidized reaction center chlorophyll P^+680 . The complicated absorption difference spectrum in NH_2OH treated tris-PSII might be the result of the contributions of several electron transfer components.

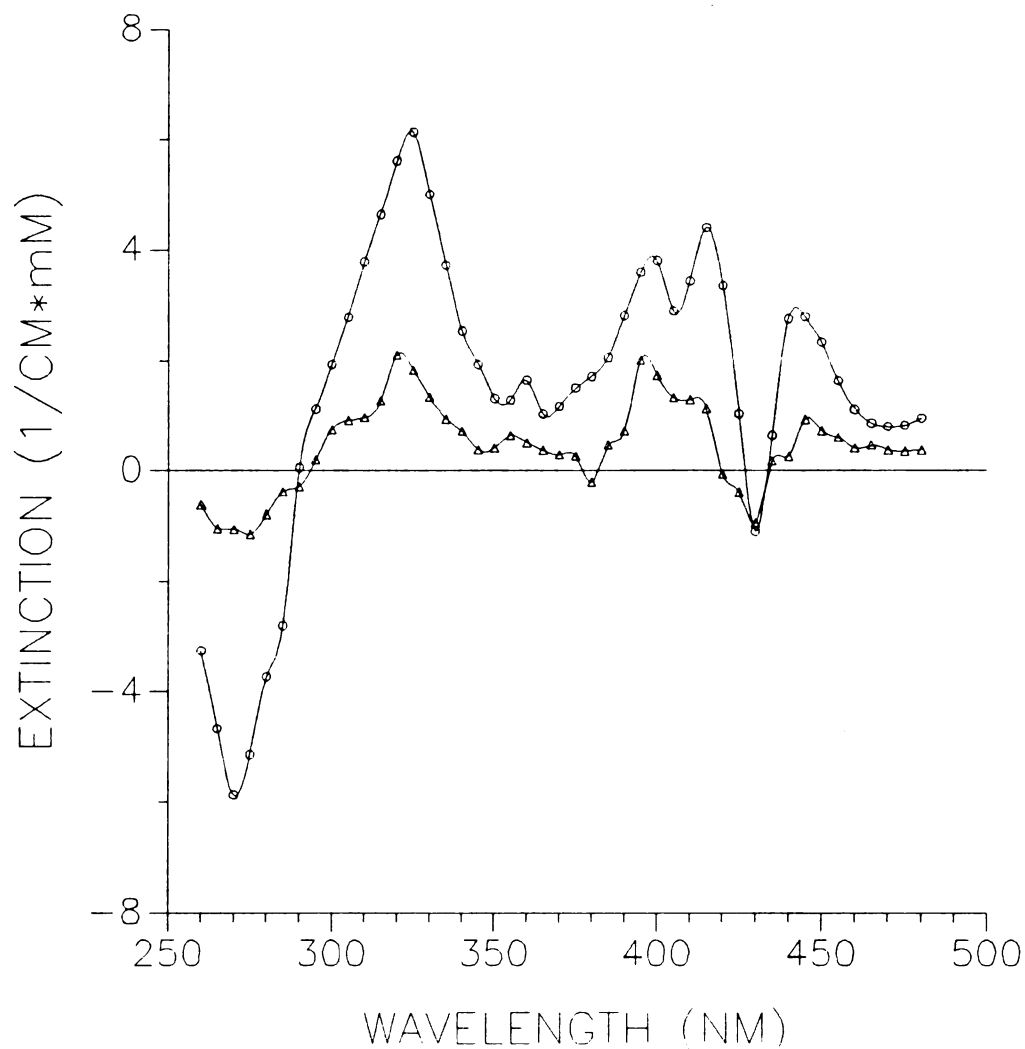


Figure 4-5 Absorption difference spectrum of the millisecond decay phase in tris-washed PSII (open circle) and in NH₂OH treated tris-PSII (open triangle). [Chl]=215 μ g/ml, the time between excitation flashes was 1.98 second. 2.5 mM Fe(CN)₆⁻³/Fe(CN)₆⁻⁴ were added as the electron acceptor system.

Fig
tri
 $Q_A /$
circ
absc
wate

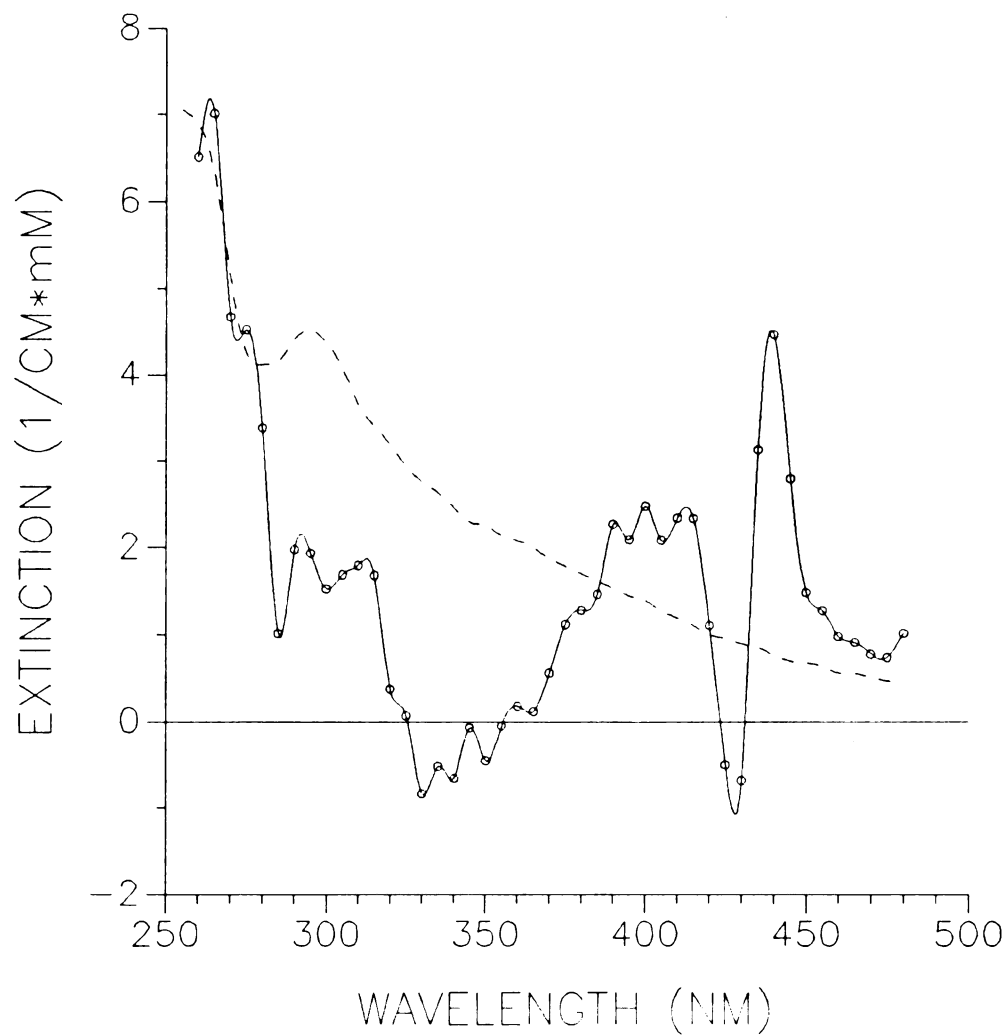


Figure 4-6 Absorption difference spectrum of the Y_2^+/Y_2 in tris-washed PSII. The spectrum is obtained by subtracting the Q_A^-/Q_A contributions from the spectrum in Figure 4-5 (open circle). The overlaid spectrum (dashed line) is the absorption difference spectrum of the phenoxy radical $TyrO\cdot$ in water.

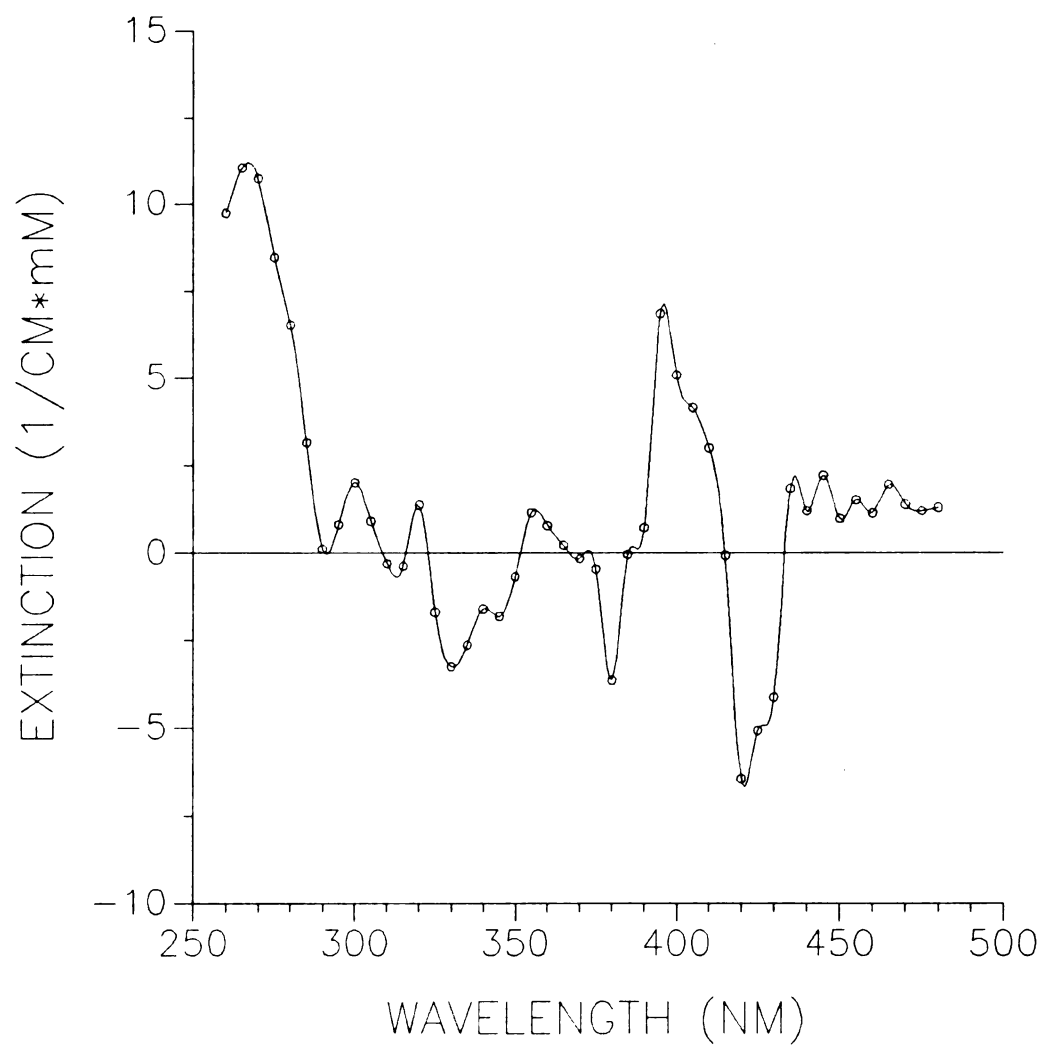


Figure 4-7 Absorption difference spectrum of the millisecond decay phase in NH_2OH treated tris-PSII after subtracting Q_A^-/Q_A spectrum from the spectrum in Figure 4-5 (open triangle).

2

h

m

e.

co

sp

sub

spe

ban

arou

shar

The

very

cowor

peaks

resolv

in try

Renger

Discussions

Monitoring the decay of the charge separated state Q_A^-/P^+680 provides a direct way to determine the $P^+680/P680$ absorption difference spectrum. This method uses tris inhibition to extend the lifetime of P^+680 into the microsecond range so that the charge recombination reaction between Q_A^- and P^+680 can be observed. The advantages of the method are that the decay pathway is relatively simple, fewer electron transfer reactions are involved, and the various components involved can be relatively easily separated spectrally and kinetically.

The $P^+680/P680$ absorption difference spectrum obtained by subtracting Q_A^-/Q_A contributions from the $Q_A^-P^+680/Q_A P680$ spectrum is shown in Figure 4-3. The spectrum has positive bands around 310, 345, 400 and 470 nm, and negative bands around 290, 375 and 430 nm. The bleaching at 430 nm is very sharp with an extinction coefficient of about $28.5 \text{ cm}^{-1}\text{mM}^{-1}$. The $P^+680/P680$ absorption difference spectrum we obtained is very similar to the spectrum recently reported by Gerken and coworkers [1] in cyanobacterium except that they observed two peaks at 400 nm and 415 nm, whereas only one peak at 400 nm is resolved in our spectrum. The spectrum is different from that in trypsinized and NH_2OH treated PSII obtained by Weiss and Renger [18], which might be caused by the different method

s
s
i
P
d
Q
s
r
s
n
sp
d.
[1
p*
ou
th

employed to subtract Q_A^-/Q_A contributions. Compared to the in vitro spectrum of $Chla^+/Chla$ (Figure 4-3, dashed line), there is a red shift of the 400 nm peak of the $P^*680/P680$ spectrum in tris-washed PSII, the bleaching at 430 nm is much sharper, the extinction coefficient at 430 nm is smaller [19,32]. These differences can be explained in terms of the aggregation of the reaction center chlorophyll (presumably a dimer [33]) that lowers the excited state energy and results in a red shift of the spectrum. In addition, the presence of charged species near the reaction center P680 might also play an important role in the modification of the spectrum.

Although Brudvig and coworkers [10,43] have suggested the possibility that a nearby chlorophyll, rather than P^*680 , is detected in various of the systems designed to monitor Q_A^-/P^*680 recombination, the results we obtained here strongly suggest that the reaction is indeed the charge recombination reaction from the state Q_A^-/P^*680 . This conclusion is supported by the decay kinetics of Q_A^- and P^*680 , which show nearly identical decay halftimes. Moreover, the difference spectrum we obtained here is very similar to the $P^*680/P680$ difference spectrum recently reported by Gerken and coworkers [1], which indicates that the reaction center chlorophyll P^*680 , rather than the auxiliary chlorophyll, is observed in our experiments. Finally, the similar kinetic behavior and the narrower EPR linewidth of the transient species observed

by Hoganson and Babcock [44] by using time resolved EPR technique is also consistent with this assumption.

The absorption difference spectrum of $P^+680/P680$ in NH_2OH treated tris-PSII shows near identically features to that in tris-washed PSII (Figure 4-4). The detection of the photo-induced charge separated state Q_A^-/P^+680 at 325 nm and 820 nm (Figure 3-6 and 3-7 in the chapter III) indicates that the reaction center P680 is still fully functional in NH_2OH treated samples. The NH_2OH treatment does not change the difference spectrum of $P^+680/P680$. This suggests that NH_2OH is not involved in direct interaction with the reaction center chlorophylls P680, since modification to the micro-environment should affect the difference spectrum of $P^+680/P680$.

Our results show that the NH_2OH inhibition site is more likely located near Y_2 . The reasoning that underlies this conclusion is the following: (1) NH_2OH has no effect on the absorption difference spectrum of reaction center P680, nor on the formation of the charge separated state Q_A^-/P^+680 . (2) the difference spectrum in the millisecond time scale, which arises from the charge recombination reaction between Q_A^- and Y_2^+ , is modified by the NH_2OH treatment. (3) EPR data [23] show that Y_2^+ can not be generated in NH_2OH treated samples.

The spectrum in Figure 4-5 shows the 45 ms decay phase (open circle) in tris-washed PSII, which arises from the charge recombination between Q_A^- and Y_2^+ [3]. Upon NH_2OH

.
o
s
t
i
re
pa
in
dor

Y₂

treatment, the amplitude of the spectrum is reduced, and the shape of the spectrum is altered as well. This implies that the electron transfer from Y_2 to P^+680 is inhibited and that the electron transfer pathway is modified in NH_2OH treated tris-PSII. Figure 4-6 shows the spectrum (open circle) after subtraction of the Q_A^-/Q_A contribution from the spectrum in Figure 4-5 (open circle) in tris-washed PSII. The spectrum has positive bands around 260, 300, 400, and 440 nm, and a negative band at 430 nm. It is similar to the Y_2^+/Y_2 absorption difference spectrum obtained by Dekker and coworkers [3] and has features similar to that of tyrosine radical in water in the UV region (Figure 4-6). This supports the conclusion that the 45 ms decay phase arises from charge recombination between Q_A^- and Y_2^+ . However, in NH_2OH treated tris-PSII, the spectrum after subtraction of the Q_A^-/Q_A contribution (Figure 4-7) is different from the Y_2^+/Y_2 spectrum, especially in the visible region. The components that contribute to this spectrum are not known yet, although it seems that some contributions may arise from the oxidized reaction center P^+680 . Other electron donors/acceptors may participate in the electron transfer reactions in NH_2OH inhibited tris-PSII, but the nature of these electron donors/acceptors were not identified in our experiments.

The possibility that NH_2OH inhibition takes place near the Y_2 site rather than at the reaction center $P680$ raises an

interesting question as to how NH_2OH reacts with Y_2 and prevents it from being oxidized. The chemistry of tyrosine in water [34,35] shows that the pK value for H^+ release from Tyr-OH is 10.1 and the value decreases to -1.6 upon the oxidation of the tyrosine (Tyr-OH^+). Thus it is likely that deprotonation of Y_2 occurs with electron extraction by P^+680 in PSII. The EPR data support this supposition as the EPR signal of Y_2^+ is characteristic of a neutral rather than a cation radical [8]. We expect, then, that protonation/deprotonation reaction of the tyrosine phenol oxygen will occur during the oxidation and reduction of Y_2 during the electron transfer reaction in PSII. Optical evidence to support this model has been observed in inactivated PSII [36,37]. Figure 4-8 shows the scheme of the hydrogen shift during the oxidation and reduction reactions.

The results of Eckert and Renger [38] suggest that the hydrogen bond shift, rather than proton release and re-uptake, occurs within a double well potential in intact PSII membrane preparations because the observed 10 kJ/mol activation energy of the electron transfer reaction from Y_2 to P^+680 is smaller than typical average energies of 20-25 kJ/mol for hydrogen bonds in proteins [39]. However in tris-washed PSII, which lacks oxygen evolution capacity, the activation energy is found to be about 45 kJ/mol [40]. This change of the activation energy can play an important role for the

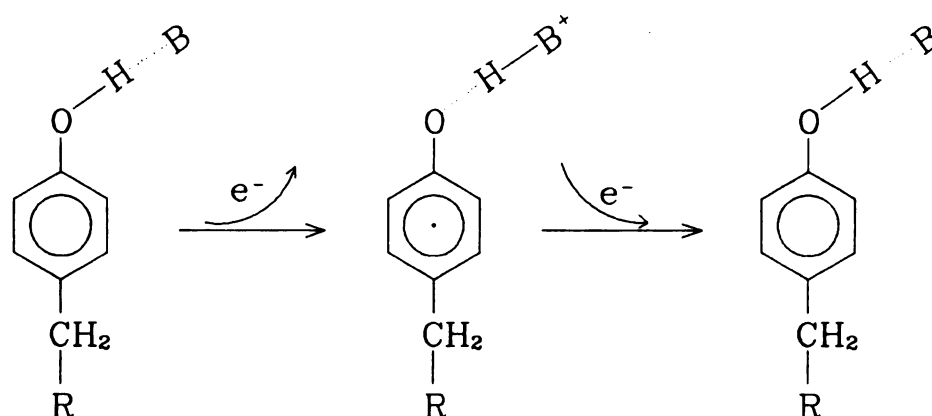


Figure 4-8 The electron transfer and hydrogen shift of the electron donor Y_2 during the electron transfer reactions in PSII. Here B represents an amino acid residue that forms a hydrogen bond with the tyrosine.

retardation of electron transfer from Y_2 to P^+680 , which is significantly slowed upon tris inhibition [38].

The inhibition of NH_2OH may be the results of a chemical reaction between the NH_2OH and the phenol group of the tyrosine residue. The phenol is nucleophilic and may react at oxygen or carbon centers that are neutral or positively charged electrophiles [41]. NH_2OH undergoes hydrolysis in aqueous solution to yield $\text{N}^+\text{H}_3\text{OH}$ [42]. Since the NH_2OH inhibition is reversible [23], covalent bond formation is unlikely during a chemical reaction of NH_2OH with Y_2 . One

possible reaction that fulfills these criteria is presented in Figure 4-9. In the scheme, the hydroxyl proton of the phenol group of Y_2 is shifted upon the extraction of an electron by P^+680 . When it is re-reduced in the presence of protonated NH_2OH , an ionic bond between the oxygen and the nitrogen is formed instead of the normal protonation reaction. The formation of the ionic bond inhibits the normal hydrogen bond shift and changes the redox potential of Y_2 so that the electron transfer from Y_2 to P^+680 can not proceed. The light requirement of the NH_2OH inhibition in PSII can be explained by the light induced hydrogen bond shift of the phenol group of Y_2 that results in the reaction with NH_2OH to form the O^-N^+ ionic bond.

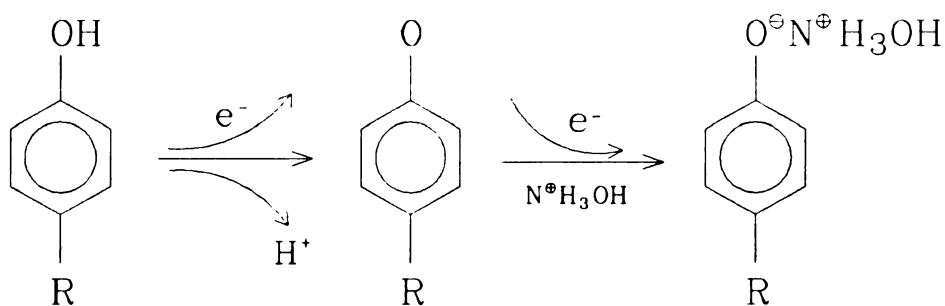


Figure 4-9 The possible chemical reactions of NH_2OH with the phenol group of the tyrosine residue of Y_2 in PSII.

Conclusion

The absorption difference spectrum of different decay phases can be used to identify components participating in photosynthetic reactions as well as the changes of their micro-environments under different treatments. Our results in tris-washed PSII show that the difference spectrum of the 230 μ s decay phase of the charge separated state Q_A^-/P^+680 arises from the contributions of Q_A^-/Q_A and $P^+680/P680$; the spectrum of the 45 ms decay phase arises from the contributions of Q_A^-/Q_A and Y_2^+/Y_2 . NH_2OH treatment has no effect on the spectrum of the microsecond decay phase, but the spectrum of the millisecond decay phase is altered and diminished. We conclude that the 230 μ s decay phase arises from the charge recombination reaction of the state Q_A^-/P^+680 and the 45 ms decay phase comes from the charge recombination reaction between Q_A^- and Y_2^+ in tris-washed PSII. Because NH_2OH treatment has no effect on the $P^+680/P680$ absorption difference spectrum, the inhibition site of NH_2OH is more likely to be near the Y_2 site rather than near the reaction center P680. The inhibition of the electron transfer capability of Y_2 under NH_2OH treatments is proposed to involve the reactions of NH_2OH with the phenol group of the tyrosine residue. This reaction either prevents the hydrogen shift that is required for the electron transfer to take place or

changes the redox potential and electron coupling between Y_2 and P^+680 so that Y_2 can no longer donate electrons to P^+680 .

References

1. Gerken, S., Dekker, J.P., Schlodder, E. and Witt, H.T. Biochim. Biophys. Acta 1989, 977, 52
2. Dekker, J.P., Van Gorkom, H.J., Wensink, J. and Ouwehand, L. Biochim. Biophys. Acta 1984, 767, 1
3. Dekker, J.P., Van Gorkom, H.J., Brok, M. and Ouwehand, L. Biochim. Biophys. Acta 1984, 764, 301
4. Van Gorkom, H.J., Pulles, M.P.J. and Wessels, J.S.C. Biochim. Biophys. Acta 1975, 408, 331
5. Van Gorkom, H.J. Biochim. Biophys. Acta 1974, 347, 439
6. Lavergne, J. FEBS Lett. 1984, 173, 9
7. Diner, B. and Völker, M. (1984) in Advances in Photosynthesis Research (Sybesma, C., ed.) Vol. I. page 407, Martinus Nijhoff/Dr. W. Junk Publishers, Dordrecht, The Netherlands
8. Barry, B.A. and Babcock, G.T. Proc. Natl. Acad. Sci. USA 1987, 84, 7099
9. Debus, R.J., Barry, B.A., Babcock, G.T. and McIntosh, L. Proc. Natl. Acad. Sci. USA 1988, 85, 427
10. Metz, J.G., Nixon, P.J., Rögner, M., Brudvig, G.W. and Diner, B.A. Biochemistry 1989, 28, 6960
11. Vermaas, W.F.J., Rutherford, A.W. and Hansson, O. Proc. Natl. Acad. Sci. USA 1988, 85, 8477

12. Bent, D.V. and Hayon, E. J. Am. Chem. Soc. 1975, 97, 2599
13. Bensasson, R.V., Land, E.J. and Truscott, T.G. (1983) Flash Photolysis and Pulse Radiolysis page 93, Pergamon, Oxford
14. Gerken, S., Brettel, K., Schlodder, E. and Witt, H.T. FEBS Lett. 1988, 237, 69
15. Ghanotakis, D.F., O'Malley, P.J., Babcock, G.T. and Yocum, C.F. (1983) in Oxygen Evolving Systems of Plant Photosynthesis (Inoue, Y., ed.) page 91, Academic Press Japan Inc., Tokyo
16. Babcock, G.T., Buttner, W.J., Ghanotakis, D.F., O'Malley, P.J., Yerkes, C.T. and Yocum, C.F. (1984) in Proceedings of the 6th International Congress on Photosynthesis (Sybesma, C., ed.) Nijhoff/Junk, The Hague
17. Brok, M., De Groot, A. and Hoff, A.J. (1984) in Proceedings of the 6th International Congress on Photosynthesis (Sybesma, C., ed.) Nijhoff/Junk, The Hague
18. Weiss, W. and Renger, G. Biochim. Biophys. Acta 1986, 850, 173
19. Borg, D.C., Fajer, J., Felton, R.H. and Dolphin, D. Proc. Natl. Acad. Sci. USA 1970, 67, 813
20. Berthold, D.A., Babcock, G.T. and Yocum, C.F. FEBS Lett. 1981, 134, 231
21. Ghanotakis, D.F., Babcock, G.T. and Yocum, C.F. Biochim. Biophys. Acta 1984, 765, 388
22. Ford, R.C. and Evans, M.C.W. Biochim. Biophys. Acta 1985, 807, 1
23. Ghanotakis, D.F. and Babcock, G.T. FEBS Lett. 1983, 153, 231

24. Stiehl, H.H and Witt, H.T. Z. Naturforsch 1968, 23b, 220
25. Stiehl, H.H and Witt, H.T. Z. Naturforsch 1968, 24b, 1588
26. Wasielewski, M.R., Johnson, D.G., Seibert, M. and Govindjee, Proc. Natl. Acad. Sci. USA, Vol. 86, 524-528, January 1989
27. Eckert, H.-J, Wiese, N., Bernarding, J., Eichler, H.-J. and Renger, G. FEBS Lett. 1988, 240, 153
28. Ghanotakis, D.F. and Babcock, G.T. FEBS Lett. 1983, 153, 231
29. Ford, R.C. and Evans, M.C.W. FEBS Lett. 1983, 160, 159
30. Vermeglio, A. and Mathis, P. Biochim. Biophys. Acta 1973, 314, 57
31. Haganason, C.W., Babcock, G.T. and Yocum, C.F. Photosyn. Res. 1989, 22, 285
32. Davis, M.S., Forman, A. and Fajer, J. Proc. Natl. Acad. Sci. USA, 1979, 76, 4170
33. R. Van Grondelle (1985), Biochim. Biophys. Acta, 811, 147
34. Dixon, W.T. and Murphy, D. J. Chem. Soc. Faraday Trans.2 1976, 72, 1221
35. Barker, R. Organic Chemistry of Biological Compounds (1971) Prentice-Hall, Inc., Englewood Cliffs, New Jersey
36. Renger, G. and Völker, M. FEBS Lett. 1982, 149, 203
37. Förster, V. and Junge, W. (1984) in Advances in Photosynthesis Research (Sybesma, C. ed.) Vol. II, 305, Nijhoff/Junk, The Hague
38. Eckert, H.J. and Renger, G. FEBS Lett. 1988, 236, 425

39. Stearn, A.E. (1949) Adv. Enzymol. 9, 25
40. Reinman, S. and Mathis, P. Biochim. Biophys. Acta 1981, 635, 249
41. Whiting, D.A. in Comprehensive Organic Chemistry (Barton, S.D. et. al. ed.) 1979, Vol 1, page 714
42. Jones, K. in Comprehensive Inorganic Chemistry (Bailar, J.C. ed.) 1973, Vol 2, page 265
43. Thompson, L.K. and Brudvig, G.W. Biochemistry 1988, 27, 6653
44. Hoganson, C.W. and Babcock, G.T. Biochemistry 1989, 28, 1448-1454

CHAPTER V

SUMMARY AND FUTURE WORK

Summary

The charge separated state Q_A^-/P^+680 is created within 300 ps following the excitation of the reaction center chlorophyll P680 by light in photosystem II in higher plants [1,2]. In intact PSII membrane preparations or chloroplasts, this charge separated state decays on the nanosecond time scale by a rapid electron donation by the physiological donor Y_2 [3,4]. Certain chemical treatments that inhibit oxygen evolution or electron transfer reactions on the donor side of PSII stabilize P^+680 so that the lifetime of the state Q_A^-/P^+680 is extended into the microsecond time range. The time evolution of Q_A^-/P^+680 is highly dependent on the micro-environments of the electron carriers and the presence of inhibitors. Studies of the decay kinetics of Q_A^-/P^+680 can provide us with valuable information about the mechanism of the inhibition reactions as well as the modifications of the micro-environments under different treatments.

In the experiments described in this dissertation, we investigated the kinetic and spectroscopic properties of the

reaction center P680, primary donor Y_2 , and acceptor Q_A in tris-washed, NaCl washed, and NH_2OH treated PSII by monitoring the decay of the charge separated state Q_A^-/P^+680 with transient absorption spectroscopy. The results we obtained can be summarized as follows: (1) The charge recombination reaction between Q_A^- and P^+680 occurs in the microsecond time range in tris-washed and NaCl-washed PSII under high flash repetition rate. NH_2OH treatment removes the high flash repetition rate requirement for observing Q_A^-/P^+680 recombination. (2) The rate of the charge recombination reaction between Q_A^- and P^+680 in NaCl washed PSII (halftime $\approx 130 \mu s$) is about twice as fast as that in tris-washed PSII (halftime $\approx 230 \mu s$). (3) The secondary plastoquinone acceptor Q_B is not directly involved during the charge recombination reactions. The Q_A to Q_B electron transfer reaction, which presumably has a halftime of $200 \mu s$, was not observed. (4) In tris-washed PSII, the absorption difference spectrum of the $230 \mu s$ decay phase of the charge separated state Q_A^-/P^+680 arises from the contributions from Q_A^-/Q_A and $P^+680/P680$; the spectrum of the $45 ms$ decay phase arises from contributions from Q_A^-/Q_A and Y_2^+/Y_2 . (5) NH_2OH treatment has no effect on the absorption difference spectrum of the microsecond decay phase, but the absorption difference spectrum of the millisecond decay phase is altered and diminished.

Based on the above results, as well as on observations

re
Ca
Y.
(
t
n
a

from other laboratories [4-11], we conclude the following:

- (1) The mode of tris inhibition is distinct from that of NH_2OH treatment. Tris washing inhibits the re-reduction of Y_2^+ by its physiological donor, whereas the electron transfer from Y_2 to P^+680 is not affected greatly. NH_2OH treatment greatly retards the electron transfer from Y_2 to P^+680 and keeps Y_2 in its reduced state.
- (2) The difference in the decay rate of the charge recombination reaction between Q_A^- and P^+680 in NaCl washed PSII and in tris-PSII probably arise from different micro-environments of reaction center P680 in the two preparations.
- (3) The absence of direct involvement of the secondary plastoquinone acceptor Q_B in oxidizing Q_A^- in the Q_A^-/P^+680 state may be attributed to the effects of the positive charge on the reaction center P^+680 or to the removal of Q_B molecules during sample preparation.
- (4) In tris-washed PSII, the 230 μs decay phase arises from charge recombination between Q_A^- and P^+680 , and the 45 ms decay phase arises from charge recombination involving Q_A^- and Y_2^+ .
- (5) The Soret band absorption red shift in the difference spectrum of $P^+680/P680$ relative to that of in vitro $\text{Chla}^+/\text{Chla}$ presumably arises from the aggregation state of the reaction center chlorophylls.
- (6) The inhibitory site of NH_2OH is more likely located near Y_2 than near P680. The inhibition of the electron transfer capability of Y_2 under NH_2OH treatments may involve reversible reaction of NH_2OH with the phenol group of the tyrosine

residue to form an O^--N^+ ionic bond. In such scenario this reaction would disrupt the network of covalent and hydrogen bonds and change the redox properties of Y_2 so that electron transfer from Y_2 to P^*680 can no longer be carried out effectively in competition with recombination.

Future Work

Transient absorption spectroscopy has been a very useful technique for studying electron transfer reactions that occur in photosynthesis. Almost all electron transfer components of photosystem II exhibit absorption changes upon oxidation or reduction following flash excitation. Thus, they are detectable by transient absorption spectroscopy. The studies presented in this dissertation show that we are able to obtain kinetic and spectroscopic information of individual electron transfer components in PSII by using the transient absorption technique. Spectral overlap of different components, which causes difficulties in interpreting the results, can be reduced by carefully preparing the reaction assay so that the oxidation or reduction of different components take place on different time scales.

Our results show that the charge recombination reaction between Q_A^- and P^*680 occurs when the physiological electron transfer reactions is inhibited by tris, NaCl, or NH_2OH treatment. However, there have been suggestions that other

1
R
w
e
m
no

alternative donors, besides the Y_2 , may exist and donate electrons to P^+680 when the physiological electron transfer reactions are inhibited. There have been many reports that non-physiological electron donors, such as chlorophylls [12-15], cytochrome b_{559} [16,17], and carotenoid [18], can be oxidized by P^+680 under certain conditions. It is worthwhile to investigate further these reactions by using transient absorption technique. By monitoring the charge recombination and absorption difference spectra in PSII membrane preparations under different inhibitory treatments, we should achieve a better understanding as to how these alternate donors participate in the electron transfer reactions under certain conditions.

The micro-environment plays a very important role in the electron transfer reactions in PSII. This has been observed in our experiments and in several other laboratories [5,6]. The Q_A^- to Q_B electron transfer is greatly modified in tris-washed PSII. The charge recombination reaction between Q_A^- and P^+680 in NaCl washed PSII is faster than that in tris-washed PSII because of the effects of the micro-environment. However, no extensive studies have been performed in such a way that allow us to obtain detailed information about how the electron transfer reactions are affected by the changes of the micro-environment. Mutagenesis techniques, which have become more and more important in photosynthesis research, may be

employed to address these reactions in greater detail. By selectively replacing certain redox active amino acid residues in PSII membrane polypeptides, and by monitoring the reaction rate and by measuring the induced free energy changes, we should be able to establish correlations between the function of individual components and the rate of electron transfer.

Protonation and deprotonation of the phenol head group have been suggested to be essential in the electron transfer reactions of Y_2 in PSII [19,20]. The results presented in chapter IV suggest that NH_2OH inhibition may be the result of the inhibition of the protonation/deprotonation reaction of Y_2 . Since protonation/deprotonation is directly affected by the pH value of the solution, the charge recombination in tris-washed PSII should be strongly depend on pH, and this pH dependence may be modified in NH_2OH treated PSII. Thus, studying the pH dependence of the charge recombination in tris-washed PSII and NH_2OH treated tris-PSII may provide useful information on the importance of protonation/deprotonation reactions that may occur during electron transfer and the mode of NH_2OH inhibition in blocking this proton motion.

References

1. M.R. Wasielewski, D.G. Johnson, M. Seibert, and Govindjee, Proc. Natl. Acad. Sci. USA, Vol. 86, 524-528, January 1989
2. Eckert, H.-J., Wiese, N., Bernarding, J., Eichler, H.-J. and Renger, G. FEBS Lett. 1988, 240, 153
3. Brettel, K., Schlodder, E., and Witt, H.T. Biochim. Biophys. Acta 766, 1984, 403
4. Gerken, S., Brettel, K., Schlodder, E., and Witt, H.T. FEBS Lett. 1988, 237, 69
5. Gerken, S., Dekker, J.P., Schlodder, E. and Witt, H.T. Biochim. Biophys. Acta 1989, 977, 52
6. Ford, R.C. and Evans, M.C.W. Biochim. Biophys. Acta 1985, 807, 1
7. Hoganson, C.W. and Babcock, G.T. Biochemistry 1988, 27, 5848
8. Ghanotakis, D.F. and Babcock, G.T. FEBS Lett. 1983, 153, 231
9. Dekker, J.P., Van Gorkom, H.J., Brok, M. and Ouwehand, L. Biochim. Biophys. Acta 1984, 764, 301
10. Weiss, W. and Renger, G. Biochim. Biophys. Acta 1986, 850, 173
11. Eckert, H.J. and Renger, G. FEBS Lett. 1988, 236, 425
12. Visser, J.W.M., Rijersberg, C.P. and Gast, P. Biochim. Biophys. Acta 460, 1977, 36
13. De Paula, J.C., Innes, J.B. and Brudvig, G.W. Biochemistry Vol. 24, 1985, 8114
14. Thompson, L.K. and Brudvig, G.W. Biochemistry 1988, 27, 6653

15. Metz, J.G., Nixon, P.J., Rögner, M, Brudvig, G.W. and Diner, B.A. Biochemistry 1989, 28, 6960
16. Vermeglio, A. and Mathis, P. Biochim. Biophys. Acta 314, 1973, 57
17. Malkin, R. and Vänngård, T. FEBS Lett. 111, 1980, 228, 16. Mathis, P. and Rutherford, A.W. Biochim. Biophys. Acta 767, 1984, 217
18. Mathis, P. and Rutherford, A.W. Biochim. Biophys. Acta 767, 1984, 217
19. Renger, G. and Völker, M. FEBS Lett. 1982, 149, 203
20. Förster, V. and Junge, W. (1984) in Advances in Photosynthesis Research (Sybesma, C. ed.) Vol. II, 305, Nijhoff/Junk, The Hague

APPENDICES

```
*****  
|  
|  
|  
| PROGRAM TASCI  
|  
| By Xingmin Liu  
| Dept. of Chemistry  
| Michigan State University  
|  
| April 5, 1988  
|  
|  
| PROGRAM TASCI (TRANSIENT ABSORPTION SPECTROMETER  
| COMPUTER INTERFACE) CONTROLS THE DATA ACQUISITION,TIMING  
| SEQUENCES AND INSTRUMENT INTERFACE. IT WAS DESIGNED TO  
| OPERATE THE TRANSIENT ABSORPTION SPECTROMETER BUILT BY  
| D. LILLIE AND XINGMIN LIU FOR STUDIES OF THE ELECTRON  
| TRANSFER REACTIONS IN PHOTOSYNTHESIS.  
|  
| *****  
100 '---- PARAMETER INPUT ----  
110 A% = 16000  
120 DIM DAT!(A%)  
140 CLS  
200 WA$ = "WAVELENGTH (nm)" "  
210 PRINT WA$; : INPUT WAVL%  
220 SR$ = "SAMPLING RATE (us)" "  
230 PRINT SR$; : INPUT SR!  
240 IF SR! < .05 OR SR! > 80000.1 THEN  
PRINT " ***** BAD SAMPLING RATE *****"  
GOTO 230  
ELSE  
GOTO 250  
END IF  
250 NS$ = "NUMBER OF SAMPLES" "  
260 PRINT NS$; : INPUT ; NS%
```

```

270 IF (.001 * SR! * NS%) > 8000.1 OR NS% > 16000 THEN
    PRINT "          TOO MANY SAMPLES"
    GOTO 230
ELSE
    GOTO 280
END IF
280 PRINT USING "          t = ####.### ms"; .001 * SR * NS%
290 NA$ = "NUMBER OF AVERAGES"
300 PRINT NA$; : INPUT NA%
310 IF NA% = 0 THEN NA% = 1
315 NA1% = NA%
320 INPUT "NUMBER OF SCANS TO BE DISPLAYED ON SCREEN "; SCR%
330 IF SCR% = 0 THEN SCR% = 1
340 DC$ = "DC OFFSET (v)"
350 PRINT DC$; : INPUT DC!
360 CT1$ = "TRIGGERING THE LASER (ms)"
370 GAN$ = "GAIN OF THE PRE-ADC AMPLIFIER"
380 PMT$ = "THE PMT VOLTAGE (v)"
390 CT4$ = "TIME DELAY OF COUNTER 4 (ms)"
400 PRINT GAN$; : INPUT GAN%
410 PRINT PMT$; : INPUT PMT%
420 PRINT CT1$; : INPUT CT1!
430 CT1P! = CT1!
440 CT1& = 1000 * CT1!
450 CT2& = SR! * CLNG(NS%) + 100 'SAMPLING TRIGGER DELAY
460 CT3& = CT1& / 4 'HOLDING TRIGGER DELAY
470 PRINT CT4$; : INPUT CT4!
480 CT4P! = CT4!
490 CT4& = 1000*CT4!
500 '
510 '----- INPUT END -----
520 '
530 GOTO 1000 'SET TIMER AND ADC BOARD, START MEASUREMENT
540 '
600 '----- COMMAND INPUT -----
610 '
620 LOCATE 25, 1: COLOR 12
630 PRINT "COMMAND:  Save  Reset  Do  Continue  Again
    Plot  View  Window  Exit";
640 COLOR 15, 9: LOCATE 1, 1
700 KEY$ = INKEY$
710 SELECT CASE KEY$
    CASE "S", "s"
        GOTO 3000
    CASE "R", "r"
        FOR I = 0 TO NS%
            DAT!(I) = 0
        NEXT I
        GOTO 200
    CASE "D", "d"

```

```

        FOR I = 0 TO NS%
        DAT!(I) = 0
        NEXT I
        L% = 0
        GOTO 2030
    CASE "C", "c"
        GOTO 2030
    CASE "A", "a"
        NA% = NA% + NA1%
        GOTO 2030
    CASE "P", "p"
        GOTO 6000
    CASE "V", "v"
        GOTO 4000
    CASE "W", "w"
        GOTO 5000
    CASE "E", "e"
        SCREEN 0: STOP
    CASE ELSE
750 END SELECT
760 GOTO 700
800 END
900 '
1000 '***** SET THE TIMER *****
1010 '
1020 '----- SET THE MASTER MODE -----
1030 OUT 769, 23
1040 OUT 768, 0
1050 OUT 768, 145
1060 '
1100 '----- SET THE SOFTWARE TRIGGER -----
1110 OUT 769, 1
1120 OUT 768, 5
1130 OUT 768, 11
1140 OUT 769, 9
1150 OUT 768, 250 'A/D TRIGGER DELAY FOR DCR-1A
1160 OUT 768, 0
1170 '
1200 '----- SET THE TIMNE DELAY COUNTERS -----
1210 SELECT CASE CT1& 'SELECT THE CLOCK SPEED
        CASE 0 TO 50000
            M1% = 11
            CT1& = CT1&
        CASE 50001 TO 500000
            M1% = 12
            CT1& = .1 * CT1&
        CASE 500001 TO 5000000
            M1% = 13
            CT1& = .01 * CT1&
        CASE 5000001 TO 50000000

```

```

        M1% = 14
        CT1& = .001 * CT1&
        CASE 50000001 TO 60000000
            M1% = 15
            CT1& = .0001 * CT1&
        CASE ELSE
            PRINT "THE LASER TRIGGER OUT OF THE RANGE"
            GOTO 420
1250 END SELECT
1260 OUT 769, 2
1270 OUT 768, 1
1280 OUT 768, M1%
1300 SELECT CASE CT2&
        CASE 0 TO 10000
            M2% = 11
            CT2& = CT2&
        CASE 10001 TO 100000
            M2% = 12
            CT2& = .1 * CT2&
        CASE 100001 TO 1000000
            M2% = 13
            CT2& = .01 * CT2&
        CASE 1000001 TO 10000000
            M2% = 14
            CT2& = .001 * CT2&
        CASE 10000001 TO 60000000
            M2% = 15
            CT2& = .0001 * CT2&
        CASE ELSE
            PRINT "THE SAMPLING TRIGGER OUT OF THE RANGE "
            GOTO 420
1350 END SELECT
1360 OUT 769, 3
1370 OUT 768, 5
1380 OUT 768, M2%
1400 SELECT CASE CT3&
        CASE 0 TO 10000
            M3% = 11
            CT3& = CT3&
        CASE 10001 TO 100000
            M3% = 12
            CT3& = .1 * CT3&
        CASE 100001 TO 1000000
            M3% = 13
            CT3& = .01 * CT3&
        CASE 1000001 TO 10000000
            M3% = 14
            CT3& = .001 * CT3&
        CASE 10000001 TO 60000000
            M3% = 15

```



```

        CT3& = .0001 * CT3&
    CASE ELSE
        PRINT "THE HOLDING TRIGGER OUT OF THE RANGE"
        GOTO 420
1450 END SELECT
1460 OUT 769, 4
1470 OUT 768, 5
1480 OUT 768, M3%
1500 SELECT CASE CT4&
        CASE 0 TO 10000
            M4% = 11
            CT4& = CT4&
        CASE 10001 TO 100000
            M4% = 12
            CT4& = .1 * CT4&
        CASE 100001 TO 1000000
            M4% = 13
            CT4& = .01 * CT4&
        CASE 1000001 TO 10000000
            M4% = 14
            CT4& = .001 * CT4&
        CASE 10000001 TO 60000000
            M4% = 15
            CT4& = .0001 * CT4&
        CASE ELSE
            CLS
            PRINT "COUNTER 4 OUT OF THE RANGE"
            GOTO 470
1550 END SELECT
1560 OUT 769, 5
1570 OUT 768, 5
1580 OUT 768, M4%
1590 '
1600 '----- LOAD THE TIME DELAY COUNTERS -----
1610 CT1H% = INT(CT1& / 256)
1620 CT1L% = INT(CT1& - 256 * CLNG(CT1H%))
1630 OUT 769, 10
1640 OUT 768, CT1L%
1650 OUT 768, CT1H%
1700 CT2H% = INT(CT2& / 256)
1710 CT2L% = INT(CT2& - 256 * CLNG(CT2H%))
1720 OUT 769, 11
1730 OUT 768, CT2L%
1740 OUT 768, CT2H%
1800 CT3H% = INT(CT3& / 256)
1810 CT3L% = INT(CT3& - 256 * CLNG(CT3H%))
1820 OUT 769, 12
1830 OUT 768, CT3L%
1840 OUT 768, CT3H%
1900 CT4H% = INT(CT4& / 256)

```

```

1910 CT4L% = INT(CT4% - 256 * CLNG(CT4H%))
1920 OUT 769, 13
1930 OUT 768, CT4L%
1940 OUT 768, CT4H%
1950 '
2000 '***** DATA ACQUISITION *****'
2010 '
2020 L% = 0
2030 SCREEN 9
2040 COLOR 15, 9
2050 WINDOW (-.05 * NS%, -145)-(1.05 * NS%, 145)
2060 MS% = INT(NS% / 1000)
2070 IF MS% = 0 THEN MS% = 1
2080 LOCATE 1, 1
2090 PRINT NA$; NA%
2100 SELECT CASE SR!           'SELECT SAMPLING RATE
      CASE .05
        CTRL% = 0
        DATMULP% = 1
      CASE .1
        CTRL% = 0
        DATMULP% = 2
      CASE .2
        CTRL% = 0
        DATMULP% = 4
      CASE .5
        CTRL% = 16
        DATMULP% = 1
      CASE 1
        CTRL% = 16
        DATMULP% = 2
      CASE 2
        CTRL% = 16
        DATMULP% = 4
      CASE 5
        CTRL% = 32
        DATMULP% = 1
      CASE 10
        CTRL% = 32
        DATMULP% = 2
      CASE 20
        CTRL% = 32
        DATMULP% = 4
      CASE 50
        CTRL% = 48
        DATMULP% = 1
      CASE 100
        CTRL% = 48
        DATMULP% = 2
      CASE 200

```

```

        CTRL% = 48
        DATMULP% = 4
CASE 500
        CTRL% = 64
        DATMULP% = 1
CASE 1000
        CTRL% = 64
        DATMULP% = 2
CASE 2000
        CTRL% = 64
        DATMULP% = 4
CASE 5000
        CTRL% = 64
        DATMULP% = 10
CASE 10000
        CTRL% = 64
        DATMULP% = 20
CASE 20000
        CTRL% = 64
        DATMULP% = 40
CASE 50000
        CTRL% = 64
        DATMULP% = 100
CASE 80000
        CTRL% = 64
        DATMULP% = 160
CASE ELSE
        CLS
        PRINT "NON-AVAILABLE SAMPLING RATE"
        GOTO 230
2120 END SELECT
2200 NSM% = NS% * DATMULP%
2210 SELECT CASE NSM%      'SELECT NUMBER OF SAMPLES
        CASE 100 TO 250
                NSH% = 254
                GOTO 2300
        CASE 251 TO 500
                NSH% = 253
                GOTO 2300
        CASE 501 TO 750
                NSH% = 252
                GOTO 2300
        CASE 751 TO 1000
                NSH% = 251
                GOTO 2300
        CASE 1001 TO 1250
                NSH% = 250
                GOTO 2300
        CASE 1251 TO 1500
                NSH% = 249

```

```

        GOTO 2300
    CASE 1501 TO 1750
        NSH% = 248
        GOTO 2300
    CASE 1751 TO 2000
        NSH% = 247
        GOTO 2300
    CASE 2001 TO 2500
        NSH% = 245
        GOTO 2300
    CASE 2501 TO 5000
        NSH% = 235
        GOTO 2300
    CASE 5001 TO 7500
        NSH% = 225
        GOTO 2300
    CASE 7501 TO 10000
        NSH% = 215
        GOTO 2300
    CASE 10001 TO 12500
        NSH% = 205
        GOTO 2300
    CASE 12501 TO 15000
        NSH% = 195
        GOTO 2700
    CASE 15001 TO 16000
        NSH% = 192
        GOTO 2700
    CASE ELSE
        CLS
        PRINT"SAMPLING RATE OR NNMBER OF SAMPLES TOO LARGE"
        GOTO 230
2250 END SELECT
2260 '
2300 '----- BEGINING SAMPLING -----
2310 'FOR 100 TO 12500 SAMPLES
2320     L% = L% + 1
        DEF SEG = &HD000           'BACKGROUND SCAN
        POKE &HC002, 99
        POKE &HC000, 0             'LOAD THE COUNTER
        POKE &HC001, NSH%
        POKE &HC000, 0
        POKE &HC001, NSH%
        POKE &HC002, CTRL%
        OUT 769, 125
2330     IF PEEK(&HC002) AND 1 THEN 2340 ELSE GOTO 2330
2340     POKE &HC002, 99
        N% = 256 * PEEK(&HC001) + PEEK(&HC000)
        FOR I = 0 TO NS%           'TRANSFER THE
            DAT!(I) = DAT!(I) - PEEK(N%) 'COLLECTED DATA INTO

```

```

      N% = N% + DATMULP%           'COMPUTER MEMORY
      NEXT I                       'AS BACKGROUND DATA
2400  DEF SEG = &HD000             'SIGNAL SCAN
      POKE &HC002, 99
      POKE &HC000, 0               'LOAD THE COUNTER
      POKE &HC001, NSH%
      POKE &HC000, 0
      POKE &HC001, NSH%
      POKE &HC002, CTRL%
      OUT 769, 127
2410  IF PEEK(&HC002) AND 1 THEN 2420 ELSE GOTO 2410
2420  POKE &HC002, 99
      N% = 256 * PEEK(&HC001) + PEEK(&HC000)
      FOR I = 0 TO NS%             'TRANSFER THE DATA
      DAT!(I) = DAT!(I) + PEEK(N%) 'COLLECTED INTO
      N% = N% + DATMULP%           'COMPUTER MEMORY
      NEXT I                       'AS REAL DATA
      IF INKEY$ = "S" THEN 2600    'CHECK THE INTERRUPT
      IF INKEY$ = "s" THEN 2600
      IF INT(L% / SCR%) = L% / SCR% OR L% = NA% THEN 2500
      ELSE 2300
2430  '
2500  '----- GRAPHIC DISPLAY (REAL TIME) -----
      CLS
      LOCATE 5, 58: PRINT "CYCLES ="; L%;
      LOCATE 14, 65: PRINT "t =";
      PRINT USING "####.###";.001 * SR * NS%;:PRINT "ms";
      FOR I = 0 TO NS% STEP MS%
      Y = DAT!(I) / L%
      PSET (I, Y)
      NEXT I
      IF L% < NA% GOTO 2300
      LINE (0, 0)-(NS%, 0), 12, , &HCCCC
      LINE (0, 40)-(NS%, 40), 9, , &HCCCC
      LINE (0, 80)-(NS%, 80), 9, , &HCCCC
      LINE (0, 120)-(NS%, 120), 9, , &HCCCC
      LINE (0, -40)-(NS%, -40), 9, , &HCCCC
      LINE (0, -80)-(NS%, -80), 9, , &HCCCC
      LINE (0, -120)-(NS%, -120), 9, , &HCCCC
      GOTO 600
2510  '
2600  '----- GRAPHIC DISPLAY (FINAL) -----
      CLS
      LOCATE 5, 58: PRINT "CYCLES ="; L%
      LOCATE 14, 65: PRINT "t =";
      PRINT USING "####.###";.001 * SR * NS%;:PRINT "ms";
      FOR I = 0 TO NS% STEP MS%
      Y = DAT!(I) / L%
      PSET (I, Y)
      NEXT I

```

```

LINE (0, 0)-(NS%, 0), 12, , &HCCCC
LINE (0, 40)-(NS%, 40), 9, , &HCCCC
LINE (0, 80)-(NS%, 80), 9, , &HCCCC
LINE (0, 120)-(NS%, 120), 9, , &HCCCC
LINE (0, -40)-(NS%, -40), 9, , &HCCCC
LINE (0, -80)-(NS%, -80), 9, , &HCCCC
LINE (0, -120)-(NS%, -120), 9, , &HCCCC
GOTO 600

2610 '
2700 '----- FOR 12501 TO 16000 SAMPLES -----
2710     L% = L% + 1
        DEF SEG = &HD000             'BACKGROUND SCAN
        POKE &HC002, 99
        POKE &HC000, 0               'LOAD THE COUNTER
        POKE &HC001, NSH%
        POKE &HC000, 0
        POKE &HC001, NSH%
        POKE &HC002, CTRL%
        OUT 769, 125
2720     IF PEEK(&HC002) AND 1 THEN 2630 ELSE GOTO 2620
2730     POKE &HC002, 99
        N% = 256 * PEEK(&HC001) + PEEK(&HC000)
        FOR I = 0 TO NS%
        DAT!(I) = DAT!(I) - PEEK(N%)
        N% = N% + DATMULP%
        IF N% > 16383 THEN N% = 0
        NEXT I
2800     DEF SEG = &HD000             'SIGNAL SCAN
        POKE &HC002, 99
        POKE &HC000, 0               'LOAD THE COUNTER
        POKE &HC001, NSH%
        POKE &HC000, 0
        POKE &HC001, NSH%
        POKE &HC002, CTRL%
        OUT 769, 127
2810     IF PEEK(&HC002) AND 1 THEN 2820 ELSE GOTO 2810
2820     POKE &HC002, 99
        N% = 256 * PEEK(&HC001) + PEEK(&HC000)
        FOR I = 0 TO NS%
        DAT!(I) = DAT!(I) + PEEK(N%)
        N% = N% + DATMULP%
        IF N% > 16383 THEN N% = 0
        NEXT I
2830 '
2900 '----- GRAPHIC DISPLAY -----
        CLS
        LOCATE 5, 58: PRINT "CYCLES ="; L%
        LOCATE 14, 65: PRINT "t =";
        PRINT USING "####.###";.001 * SR * NS%;:PRINT "ms";
        FOR I = 0 TO NS% STEP MS%

```

```

      Y = DAT!(I) / L%
      PSET (I, Y)
      NEXT I
      IF L% < NA% GOTO 2700
      LINE (0, 0)-(NS%, 0), 12, , &HCCCC
      LINE (0, 40)-(NS%, 40), 9, , &HCCCC
      LINE (0, 80)-(NS%, 80), 9, , &HCCCC
      LINE (0, 120)-(NS%, 120), 9, , &HCCCC
      LINE (0, -40)-(NS%, -40), 9, , &HCCCC
      LINE (0, -80)-(NS%, -80), 9, , &HCCCC
      LINE (0, -120)-(NS%, -120), 9, , &HCCCC
      GOTO 600
2910 '
3000 '***** SAVE THE DATA *****'
3010 '
3020 INPUT "ENTER DATA FILE NAME  ", N$
3030 N$ = N$ + ".DAT"
3040 OPEN "O", #1, N$
3050 PRINT #1, "*****"
3060 PRINT #1, " "
3070 PRINT #1, DATE$, TIME$      'SAVE THE PARAMETERS
3080 PRINT #1, " "
3090 PRINT #1, "EXPERIMENTAL PARAMETERS"
3100 PRINT #1, " "
3110 PRINT #1, WA$; WAVL%
3120 PRINT #1, SR$; SR!
3130 PRINT #1, NS$; NS%
3140 PRINT #1, NA$; L%
3150 PRINT #1, DC$; DC!
3160 PRINT #1, GAN$; GAN%
3170 PRINT #1, PMT$; PMT%
3180 PRINT #1, "(SOFTWARE TRIGGER DELAY  250 us)"
3190 PRINT #1, CT1$; CT1P!
3200 PRINT #1, CT4$; CT4P!
3210 PRINT #1, " "
3220 PRINT #1, "*****"
3230 PRINT #1, " "
3240 PRINT #1, "DATA"
3250 PRINT #1, " "
3260 PRINT #1, WAVL%
3270 PRINT #1, SR!
3280 PRINT #1, NS%
3290 PRINT #1, L%
3300 PRINT #1, DC!
3310 PRINT #1, GAN%
3320 PRINT #1, PMT%
3330 PRINT #1, CT1P!
3340 PRINT #1, CT4P!
3350 PRINT #1, "DATA BEGINS HERE"
3360 '

```

```

3400 FOR I = 0 TO NS%                                'SAVE THE DATA
3410 PRINT #1, .005 * (DAT!(I) / L%)
3420 NEXT I
3500 CLOSE #1
3510 PRINT "DATA HAVE BEEN SAVED IN FILE           "; N$
3520 GOTO 600
3600 '
4000 '***** VIEW DATA *****
4010 '
4020 LOCATE 1, 1
4030 INPUT "SELECT VIEW WINDOW           [t1,t2]      ", X1!, X2!
4040 WN! = X2! - X1!
4050 SCREEN 9
4060 COLOR 15, 9
4070 WINDOW ((X1! - .05 * WN), -.74)-((X2! + .05 * WN), .8)
4080 CLS
4100 TO = X1: TM = X2
4110 LINE (X1!, 0)-(X2!, 0), 12, , &HCCCC
4120 LINE (X2!, 0)-(X2!, .04), 12
4130 LINE ((X1! + WN / 2), 0)-((X1! + WN / 2), .04), 12
4140 LOCATE 14, 70: PRINT USING "####.### ms"; TM;
4150 LOCATE 14, 5: PRINT USING "t =###.### ms"; X1;
4160 LOCATE 14, 36: PRINT USING "####.### ms"; X1 + WN / 2;
4170 LOCATE 10, 4: PRINT "  + 0.2 v";
4180 LOCATE 7, 4: PRINT "  + 0.4 v";
4190 LOCATE 4, 4: PRINT "  + 0.6 v";
4200 LOCATE 17, 4: PRINT "  - 0.2 v";
4210 LOCATE 20, 4: PRINT "  - 0.4 v";
4220 LOCATE 23, 4: PRINT "  - 0.6 v";
4230 LINE (X1!, -.64)-(X1!, .64)
4240 LINE ((X1! + .12 * WN), .2)-(X2!, .2), 9, , &HCCCC
4250 LINE ((X1! + .12 * WN), .4)-(X2!, .4), 9, , &HCCCC
4260 LINE ((X1! + .12 * WN), -.2)-(X2!, -.2), 9, , &HCCCC
4270 LINE ((X1! + .12 * WN), -.4)-(X2!, -.4), 9, , &HCCCC
4280 LINE ((X1! + .12 * WN), .6)-(X2!, .6), 9, , &HCCCC
4290 LINE ((X1! + .12 * WN), -.6)-(X2!, -.6), 9, , &HCCCC
4300 '
4400 B% = 1000 * X1! / SR!: E% = 1000 * X2! / SR!
4410 NSL% = 1000 * WN! / SR!: XINC! = WN! / NSL%: XL! = X1!
4420 FOR I = B% TO E%
4430 Y! = .005 * (DAT!(I) / L%)
4440 PSET (XL!, Y!)
4450 XL! = XL! + XINC!
4460 NEXT I
4470 '
4500 LOCATE 4, 50
4510 PRINT "WAVELENGTH (nm)           "; WAVL%
4520 LOCATE 5, 50
4530 PRINT "SAMPLING RATE (us)       "; SR!
4540 LOCATE 6, 50

```



```

4550 PRINT "NUMBER OF AVERAGES "; L%
4560 LOCATE 7, 50
4570 PRINT "DC OFFSET (v) "; DC!
4600 GOTO 600
4700 '
5000 '***** WINDOW *****
5010 '
5020 LOCATE 1, 1
5030 INPUT "SELECT WINDOW [t1,t2,V(min),V(max)] ",
X1!, X2!, Y1!, Y2!
5040 WN! = X2! - X1!: YM! = Y2! - Y1!
5050 SCREEN 9
5060 COLOR 15, 9
5070 WINDOW ((X1! - .05 * WN), Y1! - .05 * YM!)-(X2! + .05
* WN), Y2! + .05 * YM!)
5080 CLS
5100 T0 = X1!: TM = X2!
5120 LINE (X2!, 0)-(X2!, .03 * YM!), 12
5130 LINE ((X1! + WN / 2), 0)-((X1! + WN / 2), .03 * YM!), 12
5140 IF Y1! < 0 AND Y2! > 0 THEN
    CSL% = 1 + Y2! * 25 / YM!
    LINE (X1!, 0)-(X2!, 0), 12, , &HCCCC
    LINE (X2!, 0)-(X2!, .03 * YM!), 12
    LINE ((X1! + WN/2), 0)-((X1! + WN / 2), .03 * YM!), 12
ELSE
    CSL% = 23
    YL! = Y1! + .01 * YM!
    LINE (X1!, YL!)-(X2!, YL!), 12, , &HCCCC
    LINE (X2!, YL!)-(X2!, YL! + .05 * YM!), 12
    LINE ((X1! + WN / 2), YL!)-((X1! + WN / 2), YL! +
.05 * YM!), 12
5150 END IF
5160 LOCATE CSL%, 70: PRINT USING "####.### ms"; TM;
5170 LOCATE CSL%, 1: PRINT USING "####.### ms"; X1;
5180 LOCATE CSL%, 36: PRINT USING "####.### ms"; X1 + WN / 2;
5200 LINE (X1!, Y1!)-(X1!, Y2!)
5210 LINE (X1!, .1)-(X2!, .1), 9, , &HCCCC
5220 LINE (X1!, .2)-(X2!, .2), 9, , &HCCCC
5230 LINE (X1!, .3)-(X2!, .3), 9, , &HCCCC
5240 LINE (X1!, .4)-(X2!, .4), 9, , &HCCCC
5250 LINE (X1!, .5)-(X2!, .5), 9, , &HCCCC
5260 LINE (X1!, .6)-(X2!, .6), 9, , &HCCCC
5270 LINE (X1!, -.1)-(X2!, -.1), 9, , &HCCCC
5280 LINE (X1!, -.2)-(X2!, -.2), 9, , &HCCCC
5290 LINE (X1!, -.3)-(X2!, -.3), 9, , &HCCCC
5300 LINE (X1!, -.4)-(X2!, -.4), 9, , &HCCCC
5310 LINE (X1!, -.5)-(X2!, -.5), 9, , &HCCCC
5320 LINE (X1!, -.6)-(X2!, -.6), 9, , &HCCCC
5330 '
5400 B% = 1000 * X1! / SR!: E% = 1000 * X2! / SR!

```

```

5410 NSL% = 1000 * WN! / SR!: XINC! = WN! / NSL%: XL! = X1!
5420 FOR I = B% TO E%
5430 Y! = .005 * (DAT!(I) / L%)
5440 PSET (XL!, Y!)
5450 XL! = XL! + XINC!
5460 NEXT I
5470 '
5500 LOCATE 3, 5
5510 PRINT USING " +##.### v"; Y2!;
5520 LOCATE 23, 5
5530 PRINT USING " +##.### v"; Y1!;
5540 '
5600 GOTO 600
5700 '
6000 '***** PLOT DATA *****
6010 '
6020 SCREEN 9
6030 COLOR 15, 9
6040 WINDOW (-.05 * NS%, -.74)-(1.05 * NS%, .8)
6050 CLS
6100 LINE (0, 0)-(NS%, 0), 12, , &HCCCC
6110 LINE (NS%, 0)-(NS%, .04), 12
6120 LINE (NS% / 2, 0)-(NS% / 2, .04), 12
6130 LOCATE 14,70:PRINT USING "###.### ms";.001 * SR! * NS%;
6140 LOCATE 13, 8:PRINT "0.0 v";
6150 LOCATE 14,36:PRINT USING "###.### ms";.0005 * SR! * NS%
6160 LOCATE 10, 4:PRINT " + 0.2 v";
6170 LOCATE 7, 4:PRINT " + 0.4 v";
6180 LOCATE 4, 4:PRINT " + 0.6 v";
6190 LOCATE 17, 4:PRINT " - 0.2 v";
6200 LOCATE 20, 4:PRINT " - 0.4 v";
6210 LOCATE 23, 4:PRINT " - 0.6 v";
6220 LINE (0, -.64)-(0, .64)
6230 LINE (.12 * NS%, .2)-(NS%, .2), 9, , &HCCCC
6240 LINE (.12 * NS%, .4)-(NS%, .4), 9, , &HCCCC
6250 LINE (.12 * NS%, -.2)-(NS%, -.2), 9, , &HCCCC
6260 LINE (.12 * NS%, -.4)-(NS%, -.4), 9, , &HCCCC
6270 LINE (.12 * NS%, .6)-(NS%, .6), 9, , &HCCCC
6280 LINE (.12 * NS%, -.6)-(NS%, -.6), 9, , &HCCCC
6290 '
6300 IF NS% > 640 THEN MP% = INT(NS% / 640) ELSE MP% = 1
6310 FOR I = 0 TO NS% STEP MP%
6320 Y! = .005 * (DAT!(I) / L%)
6330 PSET (I, Y!)
6340 NEXT I
6350 '
6400 LOCATE 4, 50
6410 PRINT "WAVELENGTH (nm)          "; WAVL%
6420 LOCATE 5, 50
6430 PRINT "SAMPLING RATE (us)       "; SR!

```

156

```
6440 LOCATE 6, 50
6450 PRINT "NUMBER OF AVERAGES "; L%
6460 LOCATE 7, 50
6470 PRINT "DC   OFFSET   (v)   "; DC!
6480 '
6500 GOTO 600
```

APPENDIX B
SOURCE CODES OF PROGRAM DTDSP

```

*****
PROGRAM DTDSP

By Xingmin Liu
  Dept. of Chemistry
  Michigan State University

April 10, 1988

PROGRAM DTDSP RETRIEVES THE DATA SAVED BY THE PROGRAM
TASCI FROM DISK, TRANSFERS THE DATA INTO ABSORBANCE UNITS,
DISPLAYS THE DATA ON THE COMPUTER MONITOR, AND TRANSFERS
THE DATA INTO KFIT, PLOTIT, AND PFF FORMATS.
*****
100 'RETRIEVE THE DATA
110 A% = 8000
120 DIM DAT!(A%): DIM BDAT!(A%)
130 CLS
140 LOCATE 4, 1: SHELL "DIR *.DAT/W "
150 LOCATE 1, 1: PRINT "
160 LOCATE 1, 1: INPUT "DATA FILE NAME "; N$
170 DTN$ = N$ + ".DAT"
180 CLS : PRINT "DATA FILE TO BE LOADED "; DTN$
190 OPEN "I", #1, DTN$
200 FOR PR% = 1 TO 21
210 INPUT #1, PR$
220 PRINT PR$
230 NEXT PR%
250 INPUT #1, WAVL%
260 INPUT #1, SR!
270 INPUT #1, NS%
280 INPUT #1, NA%
290 INPUT #1, DC!

```

```

300 INPUT #1, GAN%
310 INPUT #1, PMT%
320 INPUT #1, CT1!
330 INPUT #1, CT4!
340 INPUT #1, MS$
350 '
400 I = 0
410 INPUT #1, DAT!(I)
420 DAT!(I) = -.4343 * LOG(1 - (DAT!(I) / DC!))
430 I = I + 1
440 IF EOF(1) THEN 500 ELSE GOTO 410
450 '
500 PRINT "NUMBER OF SAMPLES BE TAKEN", NS%
510 PRINT "NUMBER OF DATA BE READ", I - 1;
520 CLOSE #1
530 '
600 LOCATE 25, 1: COLOR 12
610 PRINT "COMMAND: Plot View Window Kfit Lpt plotiT
      pfF New Smooth BC Exit";
620 COLOR 15, 9
630 KEY$ = INKEY$
640 SELECT CASE KEY$
      CASE "P", "p"
        GOTO 1000
      CASE "V", "v"
        GOTO 2000
      CASE "W", "w"
        GOTO 3000
      CASE "K", "k"
        GOTO 6000
      CASE "N", "n"
        CLOSE #1
        GOTO 130
      CASE "L", "l"
        GOTO 4000
      CASE "S", "s"
        GOTO 7000
      CASE "B", "b"
        GOTO 8000
      CASE "T", "t"
        GOTO 9500
      CASE "F", "f"
        GOTO 9000
      CASE "E", "e"
        SCREEN 0: STOP
      CASE ELSE
650 END SELECT
660 GOTO 630
700 END
800 '

```

```

1000 '***** PLOT *****
1010 '
1020 SCREEN 9
1030 COLOR 15, 9
1040 WINDOW (-.05 * NS%, -.004)-(1.05 * NS%, .004)
1050 CLS
1060 TM = .001 * NS% * SR
1070 LINE (0, 0)-(NS%, 0), 12, , &HCCCC
1080 LINE (NS%, 0)-(NS%, .0002), 12
1090 LINE (NS% / 2, 0)-(NS% / 2, .0002), 12
1100 LOCATE 14, 70: PRINT USING "####.### ms"; TM;
1110 LOCATE 14, 36: PRINT USING "####.### ms"; TM / 2;
1200 LINE (0, -.004)-(NS%, -.004), 13, , &H8080
1210 LINE (0, -.002)-(NS%, -.002), 13, , &H8080
1220 LINE (0, .002)-(NS%, .002), 13, , &H8080
1230 LINE (0, .004)-(NS%, .004), 13, , &H8080
1240 LINE (0, .003)-(NS%, .003), 13, , &H8080
1250 LINE (0, .001)-(NS%, .001), 13, , &H8080
1260 LINE (0, -.003)-(NS%, -.003), 13, , &H8080
1270 LINE (0, -.001)-(NS%, -.001), 13, , &H8080
1300 '
1310 IF NS% > 640 THEN MP% = INT(NS% / 640) ELSE MP% = 1
1320 FOR I = 0 TO NS% STEP MP%
1330 PSET (I, DAT!(I))
1340 NEXT I
1350 '
1360 LOCATE 4, 50
1370 PRINT "WAVELENGTH      (nm)      "; WAVL%
1380 LOCATE 5, 50
1390 PRINT "SAMPLING RATE (us)      "; SR!
1400 LOCATE 6, 50
1410 PRINT "NUMBER OF AVERAGES      "; NA%
1420 LOCATE 2, 2: PRINT "0.004"
1430 LOCATE 23, 2: PRINT "-0.004"
1440 CLOSE #1
1450 LKEY$="P"
1500 GOTO 600
1600 '
2000 '***** VIEW DATA *****
2010 '
2020 LOCATE 1, 1
2030 INPUT "SELECT VIEW WINDOW      [t1,t2]      ", X1!, X2!
2040 WN! = X2! - X1!
2050 SCREEN 9
2060 COLOR 15, 9
2070 WINDOW ((X1! - .05 * WN), -.004)-((X2! + .05 * WN),
      .004)
2080 CLS
2100 T0 = X1: TM = X2
2110 LINE (X1!, 0)-(X2!, 0), 12, , &HCCCC

```

```

2120 LINE (X2!, 0)-(X2!, .0002), 12
2130 LINE ((X1! + WN / 2), 0)-((X1! + WN / 2), .0002), 12
2140 LOCATE 14, 70: PRINT USING "####.### ms"; TM;
2150 LOCATE 14, 5: PRINT USING "t =####.### ms"; X1;
2160 LOCATE 14, 36: PRINT USING "####.### ms"; X1 + WN / 2;
2200 LINE (X1!, -.005)-(X1!, .005)
2210 LINE (X1!, -.004)-(X2!, -.004), 13, , &H8080
2220 LINE (X1!, -.002)-(X2!, -.002), 13, , &H8080
2230 LINE (X1!, .002)-(X2!, .002), 13, , &H8080
2240 LINE (X1!, .004)-(X2!, .004), 13, , &H8080
2250 LINE (X1!, .001)-(X2!, .001), 13, , &H8080
2260 LINE (X1!, .003)-(X2!, .003), 13, , &H8080
2270 LINE (X1!, -.001)-(X2!, -.001), 13, , &H8080
2280 LINE (X1!, -.003)-(X2!, -.003), 13, , &H8080
2300 '
2400 B% = 1000 * X1! / SR!: E% = 1000 * X2! / SR!
2410 NSL% = 1000 * WN! / SR!: XINC! = WN! / NSL%: XL! = X1!
2420 FOR I = B% TO E%
2430 PSET (XL!, DAT!(I))
2440 XL! = XL! + XINC!
2450 NEXT I
2500 LOCATE 4, 50
2510 PRINT "WAVELENGTH      (nm)      "; WAVL%
2520 LOCATE 5, 50
2530 PRINT "SAMPLING RATE (us)      "; SR!
2540 LOCATE 6, 50
2550 PRINT "NUMBER OF AVERAGES      "; NA%
2560 '
2570 LKEY$="V"
2600 GOTO 600
2700 '
3000 '***** WINDOW *****
3010 '
3020 LOCATE 1, 1
3030 INPUT "SELECT WINDOW      [t1,t2,V(min),V(max)]      ",
      X1!, X2!, Y1!, Y2!
3040 WN! = X2! - X1!: YM! = Y2! - Y1!
3050 SCREEN 9
3060 COLOR 15, 9
3070 WINDOW ((X1! - .05 * WN), Y1! - .05 * YM!)-((X2! + .05
      * WN), Y2! + .05 * YM!)
3080 CLS
3100 T0 = X1!: TM = X2!
3110 LINE (X1!, 0)-(X2!, 0), 12, , &HCCCC
3120 LINE (X2!, 0)-(X2!, .03 * YM!), 12
3130 LINE ((X1! + WN / 2), 0)-((X1! + WN / 2), .03 * YM!),
      12
3150 IF Y1! < 0 AND Y2! > 0 THEN
      CSL% = 1 + Y2! * 25 / YM!
      LINE (X1!, 0)-(X2!, 0), 12, , &HCCCC

```

```

        LINE (X2!, 0)-(X2!, .03 * YM!), 12
        LINE ((X1! + WN / 2), 0)-((X1! + WN / 2), .03 *
YM!), 12
    ELSE
        CSL% = 23
        YL! = Y1! + .01 * YM!
        LINE (X1!, YL!)-(X2!, YL!), 12, , &HCCCC
        LINE (X2!, YL!)-(X2!, YL! + .05 * YM!), 12
        LINE ((X1! + WN / 2), YL!)-((X1! + WN / 2), YL! +
.05 * YM!), 12
3160 END IF
3170 LOCATE CSL%, 70: PRINT USING "####.### ms"; TM;
3180 LOCATE CSL%, 1: PRINT USING "####.### ms"; X1;
3190 LOCATE CSL%, 36: PRINT USING "####.### ms"; X1 + WN / 2;
3200 LINE (X1!, Y1!)-(X1!, Y2!)
3210 LINE (X1!, .001)-(X2!, .001), 13, , &H8080
3220 LINE (X1!, .002)-(X2!, .002), 13, , &H8080
3230 LINE (X1!, .003)-(X2!, .003), 13, , &H8080
3240 LINE (X1!, .004)-(X2!, .004), 13, , &H8080
3250 LINE (X1!, .005)-(X2!, .005), 13, , &H8080
3260 LINE (X1!, .006)-(X2!, .006), 13, , &H8080
3270 LINE (X1!, -.001)-(X2!, -.001), 13, , &H8080
3280 LINE (X1!, -.002)-(X2!, -.002), 13, , &H8080
3290 LINE (X1!, -.003)-(X2!, -.003), 13, , &H8080
3300 LINE (X1!, -.004)-(X2!, -.004), 13, , &H8080
3310 LINE (X1!, -.005)-(X2!, -.005), 13, , &H8080
3320 LINE (X1!, -.006)-(X2!, -.006), 13, , &H8080
3400 '
3500 B% = 1000 * X1! / SR!
3510 E% = 1000 * X2! / SR!
3520 NSL% = 1000 * WN! / SR!
3530 XINC! = WN! / NSL%
3540 XL! = X1!
3550 FOR I = B% TO E%
3560 PSET (XL!, DAT!(I))
3570 XL! = XL! + XINC!
3580 NEXT I
3590 '
3600 LOCATE 3, 5
3610 PRINT USING " +##.### "; Y2!;
3620 LOCATE 23, 5
3630 PRINT USING " +##.### "; Y1!;
3640 LOCATE 4, 50
3650 PRINT "WAVELENGTH      (nm)      "; WAVL%
3660 LOCATE 5, 50
3670 PRINT "SAMPLING RATE (us)      "; SR!
3680 LOCATE 6, 50
3690 PRINT "NUMBER OF AVERAGES      "; NA%
3700 '
3750 LKEY$="W"

```



```

3800 GOTO 600
3900 '
4000 '***** PRINT OUT *****
4010 '
4020 SELECT CASE LKEY$
      CASE "P"
        GOTO 4500
      CASE "W"
        GOTO 5000
      CASE "V"
        GOTO 5500
      CASE ELSE
        PRINT "NON AVAILABLE FUNCTION"
4030 END SELECT
4100 '
4500 '----- PRINT PLOT -----
4510 '
4520 SCREEN 2
4530 WINDOW (-.05 * NS%, -.005)-(1.05 * NS%, .005)
4540 CLS
4550 TM = .001 * NS% * SR
4560 LINE (0, 0)-(NS%, 0), 7, , &HAAAA
4570 LINE (NS%, 0)-(NS%, .0005), 7
4580 LINE (NS% / 2, 0)-(NS% / 2, .0005), 7
4590 LOCATE 14, 70: PRINT USING "####.### ms"; TM;
4600 LOCATE 14, 36: PRINT USING "####.### ms"; TM / 2;
4610 LINE (0, -.005)-(0, .005)
4620 LINE (.12 * NS%, .002)-(NS%, .002), 7, , &H8080
4630 LINE (.12 * NS%, .004)-(NS%, .004), 7, , &H8080
4640 LINE (.12 * NS%, -.002)-(NS%, -.002), 7, , &H8080
4650 LINE (.12 * NS%, -.004)-(NS%, -.004), 7, , &H8080
4660 '
4700 IF NS% > 640 THEN MP% = INT(NS% / 640) ELSE MP% = 1
4710 FOR I = 0 TO NS% STEP MP%
4720 PSET (I, DAT!(I))
4730 NEXT I
4740 '
4750 LOCATE 4, 50
4760 PRINT "WAVELENGTH      (nm)      "; WAVL%
4770 LOCATE 5, 50
4780 PRINT "SAMPLING RATE (us)      "; SR!
4790 LOCATE 6, 50
4800 PRINT "NUMBER OF AVERAGES      "; NA%
4810 CLOSE #1
4820 '
4830 FOR I = 1 TO 17
4840     LPRINT CHR$(10)
4850 NEXT I
4860 LPRINT "DATA FILE NAME      "; N$
4870 LPRINT ""

```

```

4880 LPRINT "WAVELENGTH      (nm)      "; WAVL%
4881 LPRINT "SAMPLING RATE  (us)      "; SR!
4882 LPRINT "NUMBER OF SAMPLES      "; NS%
4883 LPRINT "NUMBER OF AVERAGES      "; NA%
4884 LPRINT "DC   OFFSET    (v)      "; DC!
4885 LPRINT "GAIN OF PRE-ADC AMP      "; GAN%
4886 LPRINT "PMT VOLTAGE    (v)      "; PMT%
4887 LPRINT "TIME OF TRIGGERING THE LASER    (ms)      "; CT1!
4888 LPRINT "TIME DELAY OF COUNTER  4      (ms)      "; CT4!
4890 LPRINT CHR$(12)
4900 SHELL "GRAPHICS"
4910 LP$ = INKEY$
4920 SELECT CASE LP$
      CASE "R", "r"
        LPRINT CHR$(12)
        SCREEN 9
        GOTO 1000
      CASE ELSE
4930 END SELECT
4940 GOTO 4910
4950 '
5000 '----- PRINT WINDOW -----
5010 '
5020 SCREEN 2
5030 WINDOW ((X1! - .05 * WN), Y1! - .05 * YM!)-((X2! + .05
      * WN), Y2! + .05 * YM!)
5040 CLS
5050 T0 = X1!: TM = X2!
5060 LINE (X1!, 0)-(X2!, 0), 12, , &HAAAA
5070 LINE (X2!, 0)-(X2!, .03 * YM!), 12
5080 LINE ((X1! + WN/2), 0)-((X1! + WN / 2), .03 * YM!), 12
5090 IF Y1! < 0 AND Y2! > 0 THEN
      CSL% = 1 + Y2! * 25 / YM!
      LINE (X1!, 0)-(X2!, 0), 12, , &HAAAA
      LINE (X2!, 0)-(X2!, .03 * YM!), 12
      LINE ((X1! + WN / 2), 0)-((X1! + WN / 2), .03 *
        YM!), 12
      ELSE
        CSL% = 23
        YL! = Y1! + .01 * YM!
        LINE (X1!, YL!)-(X2!, YL!), 12, , &HAAAA
        LINE (X2!, YL!)-(X2!, YL! + .05 * YM!), 12
        LINE ((X1! + WN / 2), YL!)-((X1! + WN / 2), YL! +
          .05 * YM!), 12
5100 END IF
5110 LOCATE CSL%, 70: PRINT USING "####.### ms"; TM;
5120 LOCATE CSL%, 1: PRINT USING "####.### ms"; X1;
5130 LOCATE CSL%, 36: PRINT USING "####.### ms"; X1 + WN/2;
5140 LINE (X1!, Y1!)-(X1!, Y2!)
5141 LINE (X1!, .001)-(X2!, .001), 9, , &H8080

```

```

5142 LINE (X1!, .002)-(X2!, .002), 9, , &H8080
5143 LINE (X1!, .003)-(X2!, .003), 9, , &H8080
5144 LINE (X1!, .004)-(X2!, .004), 9, , &H8080
5145 LINE (X1!, .005)-(X2!, .005), 9, , &H8080
5146 LINE (X1!, .006)-(X2!, .006), 9, , &H8080
5147 LINE (X1!, -.001)-(X2!, -.001), 9, , &H8080
5148 LINE (X1!, -.002)-(X2!, -.002), 9, , &H8080
5149 LINE (X1!, -.003)-(X2!, -.003), 9, , &H8080
5150 LINE (X1!, -.004)-(X2!, -.004), 9, , &H8080
5151 LINE (X1!, -.005)-(X2!, -.005), 9, , &H8080
5152 LINE (X1!, -.006)-(X2!, -.006), 9, , &H8080
5160 '
5170 B% = 1000 * X1! / SR!
5180 E% = 1000 * X2! / SR!
5190 NSL% = 1000 * WN! / SR!
5200 XINC! = WN! / NSL%
5210 XL! = X1!
5220 FOR I = B% TO E%
5230 PSET (XL!, DAT!(I))
5240 XL! = XL! + XINC!
5250 NEXT I
5260 LOCATE 3, 5
5261 PRINT USING " +##.### "; Y2!;
5262 LOCATE 23, 5
5263 PRINT USING " +##.### "; Y1!;
5264 LOCATE 4, 50
5265 PRINT "WAVELENGTH      (nm)      "; WAVL%
5266 LOCATE 5, 50
5267 PRINT "SAMPLING RATE (us)      "; SR!
5268 LOCATE 6, 50
5269 PRINT "NUMBER OF AVERAGES      "; NA%
5270 CLOSE #1
5280 FOR I = 1 TO 17
5290 LPRINT CHR$(10)
5300 NEXT I
5301 LPRINT "DATA FILE NAME      "; N$
5302 LPRINT ""
5303 LPRINT "WAVELENGTH      (nm)      "; WAVL%
5304 LPRINT "SAMPLING RATE (us)      "; SR!
5305 LPRINT "NUMBER OF SAMPLES      "; NS%
5306 LPRINT "NUMBER OF AVERAGES      "; NA%
5307 LPRINT "DC   OFFSET      (v)      "; DC!
5308 LPRINT "GAIN OF PRE-ADC AMP      "; GAN%
5309 LPRINT "PMT VOLTAGE      (v)      "; PMT%
5310 LPRINT "TIME OF TRIGGERING THE LASER      (ms)      "; CT1!
5311 LPRINT "TIME DELAY OF COUNTER      4      (ms)      "; CT4!
5320 LPRINT CHR$(12)
5330 SHELL "GRAPHICS"
5340 LP$ = INKEY$
5350 SELECT CASE LP$

```

```

CASE "R", "r"
  LPRINT CHR$(12)
  SCREEN 9
  GOTO 3060
CASE ELSE
5360 END SELECT
5370 GOTO 5340
5400 '
5500 '----- PRINT VIEW -----
5510 '
5520 SCREEN 2
5530 WINDOW ((X1! - .05 * WN), -.74)-((X2! + .05 * WN), .8)
5540 CLS
5550 T0 = X1: TM = X2
5560 LINE (X1!, 0)-(X2!, 0), 12, , &HAAAA
5570 LINE (X2!, 0)-(X2!, .0004), 12
5580 LINE ((X1! + WN / 2), 0)-((X1! + WN / 2), .0004), 12
5590 LOCATE 14, 70: PRINT USING "####.### ms"; TM;
5600 LOCATE 14, 5: PRINT USING "t =###.### ms"; X1;
5610 LOCATE 14, 36: PRINT USING "####.### ms"; X1 + WN / 2;
5611 LINE (X1!, -.004)-(X1!, .004)
5612 LINE ((X1! + .12 * WN), .002)-(X2!, .002), 9, , &H8080
5613 LINE ((X1! + .12 * WN), .004)-(X2!, .004), 9, , &H8080
5614 LINE ((X1! + .12 * WN), -.002)-(X2!, -.002), 9, , &H8080
5615 LINE ((X1! + .12 * WN), -.004)-(X2!, -.004), 9, , &H8080
5620 '
5630 B% = 1000 * X1! / SR!: E% = 1000 * X2! / SR!
5640 NSL% = 1000 * WN! / SR!: XINC! = WN! / NSL%: XL! = X1!
5650 FOR I = B% TO E%
5660 PSET (XL!, DAT!(I))
5670 XL! = XL! + XINC!
5680 NEXT I
5690 LOCATE 4, 50
5700 PRINT "WAVELENGTH      (nm)          "; WAVL%
5710 LOCATE 5, 50
5720 PRINT "SAMPLING RATE (us)          "; SR!
5730 LOCATE 6, 50
5740 PRINT "NUMBER OF AVERAGES          "; NA%
5750 CLOSE #1
5760 FOR I = 1 TO 17
5770 LPRINT CHR$(10)
5780 NEXT I
5790 LPRINT "DATA FILE NAME      "; N$
5800 LPRINT ""
5801 LPRINT "WAVELENGTH      (nm)          "; WAVL%
5802 LPRINT "SAMPLING RATE (us)          "; SR!
5803 LPRINT "NUMBER OF SAMPLES          "; NS%
5804 LPRINT "NUMBER OF AVERAGES          "; NA%
5805 LPRINT "DC   OFFSET      (v)          "; DC!
5806 LPRINT "GAIN OF PRE-ADC AMP          "; GAN%

```

```

5807 LPRINT "PMT VOLTAGE      (v)          "; PMT%
5808 LPRINT "TIME OF TRIGGERING THE LASER      (ms)      "; CT1!
5809 LPRINT "TIME DELAY OF COUNTER  4          (ms)      "; CT4!
5810 LPRINT CHR$(12)
5820 SHELL "GRAPHICS"
5830 LP$ = INKEY$
5840 SELECT CASE LP$
      CASE "R", "r"
        LPRINT CHR$(12)
        SCREEN 9
        GOTO 2040
      CASE ELSE
5850 END SELECT
5860 GOTO 5830
5900 '
6000 '***** KFIT FILE OUTPUT *****
6010 '
6020 LOCATE 3, 3
6030 PRINT "      COMMENT      ?          ": INPUT ; "", COMT$
6040 BDP% = 1000 * X1! / SR!: EDP% = 1000 * X2! / SR!
6050 NDP% = EDP% - BDP% + 1
6060 KFN$ = N$ + ".FIT"
6070 KDPM! = NDP% / 1001
6080 SELECT CASE KDPM!
      CASE 0 TO 1
        KMULT% = 1
      CASE 1.0009 TO 2
        KMULT% = 2
      CASE 2.0009 TO 3
        KMULT% = 3
      CASE 3.0009 TO 4
        KMULT% = 4
      CASE 4.0009 TO 5
        KMULT% = 5
      CASE 5.0009 TO 6
        KMULT% = 6
      CASE 6.0009 TO 7
        KMULT% = 7
      CASE 7.0009 TO 8
        KMULT% = 8
      CASE 8.0009 TO 9
        KMULT% = 9
      CASE 9.0009 TO 10
        KMULT% = 10
      CASE ELSE
        PRINT "      TOO MANY DATA POINTS TO FIT      ": GOTO 600
6090 END SELECT
6100 '
6110 OPEN "O", #3, KFN$
6120 PRINT #3, COMT$

```

```

6130 PRINT #3, "ABSORBANCE"
6140 PRINT #3, INT(NDP% / KMULT%)
6150 PRINT #3, (SR! / 1000000) * KMULT%
6160 FOR I = BDP% TO EDP% STEP KMULT%
6170 PRINT #3, DAT!(I)
6180 NEXT I
6190 CLOSE #3
6200 GOTO 600
6300 '
7000 '***** SMOOTHING *****
7010 '
7020 BDP% = 1000 * X1! / SR!: EDP% = 1000 * X2! / SR!
7030 NDP% = EDP% - BDP% + 1
7040 LOCATE 1, 2
7050 INPUT " ENTER THE SMOOTHING WINDOW "; SMW%
7060 SMWM% = (SMW% - 1) / 2
7070 FOR I = BDP% TO (BDP% + SMWM%)
7080 FOR N = (I + 1) TO (I + SMWM%)
7090 DAT!(I) = DAT!(I) + DAT!(N)
7100 NEXT N
7110 DAT!(I) = DAT!(I) / (SMWM% + 1)
7120 NEXT I
7130 FOR I = (BDP% + (SMWM% + 1)) TO (EDP% - (SMWM% + 1))
7140 FOR N = (I - SMWM%) TO (I - 1)
7150 DAT!(I) = DAT!(I) + DAT!(N)
7160 NEXT N
7170 FOR N = (I + 1) TO (I + SMWM%)
7180 DAT!(I) = DAT!(I) + DAT!(N)
7190 NEXT N
7200 DAT!(I) = DAT!(I) / SMW%
7210 NEXT I
7220 FOR I = (EDP% - SMWM%) TO EDP%
7230 FOR N = (I - SMWM%) TO (I - 1)
7240 DAT!(I) = DAT!(I) + DAT!(N)
7250 NEXT N
7260 DAT!(I) = DAT!(I) / (SMWM% + 1)
7270 NEXT I
7300 PRINT " ***** DONE ***** "
7400 GOTO 600
7500 '
8000 '***** BACKGROUND CORRECTION *****
8010 '
8120 LOCATE 1, 1: PRINT " "
8130 LOCATE 1, 1: INPUT "BACKGROUND DATA FILE NAME "; B$
8140 BKN$ = B$ + ".DAT"
8150 OPEN "I", #2, BKN$
8200 FOR PR% = 1 TO 21
8210 INPUT #2, PR$
8230 NEXT PR%
8300 INPUT #2, WAVL%

```

```

8310 INPUT #2, SR!
8320 INPUT #2, NS%
8330 INPUT #2, NA%
8340 INPUT #2, DC!
8350 INPUT #2, GAN%
8360 INPUT #2, PMT%
8370 INPUT #2, CT1!
8380 INPUT #2, CT4!
8390 INPUT #2, MS$
8400 '
8500 I = 0
8510 INPUT #2, BDAT!(I)
8520 BDAT!(I) = LOG(1 + (BDAT!(I) / DC!))
8530 DAT!(I) = DAT!(I) - BDAT!(I)
8540 I = I + 1
8550 IF EOF(2) THEN 8600 ELSE GOTO 8510
8600 CLOSE #2
8700 PRINT "          ***** DONE ***** "
8800 GOTO 600
8900 '
9000 '***** WRITE PFT DATA FILE *****
9010 LOCATE 1, 1
9020 STN$ = N$ + ".SET"
9030 PRINT "DATA FILE NAME TO BE SENT      ", STN$
9040 OPEN "O", #1, STN$
9050 FOR I = 0 TO NS%
9060 X = CSNG(SR! * I): Y = 1000 * CSNG(DAT(I))
9070 PRINT #1, "RD";
9080 PRINT #1, X, Y
9090 NEXT I
9100 CLOSE #1
9200 PRINT "          ***** DONE ***** "
9300 GOTO 600
9400 '
9500 '***** WRITE PLOTIT DATA FILE *****
9510 LOCATE 1, 1
9520 STN$ = N$ + ".SET"
9530 PRINT "DATA FILE NAME TO BE SENT      ", STN$
9540 OPEN "O", #1, STN$
9550 FOR I = 0 TO NS%
9560 X = CSNG(SR! * I): Y = 1000 * CSNG(DAT(I))
9570 PRINT #1, X, Y
9580 NEXT I
9600 CLOSE #1
9700 PRINT "          ***** DONE ***** "
9800 GOTO 600

```

MICHIGAN STATE UNIV. LIBRARIES



31293009146055